

Lateral Systems for Tall Buildings

by

Kermin Chok

B.S., Civil and Environmental Engineering (2003)
Northwestern University

Submitted to the Department of Civil and Environmental Engineering
In Partial Fulfillment of the Requirements for the Degree of
Master of Engineering in Civil and Environmental Engineering

at the

Massachusetts Institute of Technology
June 2004

© 2004 Kermin Chok
All rights reserved

*The author hereby grants MIT permission to reproduce and to distribute publicly paper and
electronic copies of this thesis document in whole or in part*

Signature of Author

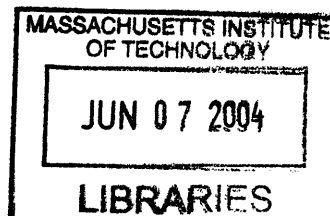
.....
Department of Civil and Environmental Engineering
May 7, 2004

Certified by.....

.....
/ Professor Jerome J. Connor
/ Professor of Civil and Environmental Engineering
Thesis Supervisor

Accepted by.....

.....
Heidi Nepf
Chairman, Committee For Graduate Students



BARKER

Lateral Systems for Tall Buildings

by

Kermin Chok

B.S., Civil and Environmental Engineering (2003)

Northwestern University

Submitted to the Department of Civil and Environmental Engineering on May 7, 2004

In Partial Fulfillment of the Requirements for the Degree of
Master of Engineering in Civil and Environmental Engineering

ABSTRACT

The advances in three-dimensional structural analysis and computing resources have allowed the efficient and safe design of increasingly taller structures. These structures are the consequence of increasing urban densification and economic viability. The modern skyscraper has and will thus continue to feature prominently in the landscape of urban cities. The trend towards progressively taller structures has demanded a shift from the traditional strength based design approach of buildings to a focus on constraining the overall motion of the structure. Structural engineers have responded to this challenge of lateral control with a myriad of systems that achieve motion control while adhering to the overall architectural vision. An investigation was carried out to understand the behavior of the different lateral systems employed in today's skyscrapers. The investigation examined the structural behavior of the traditional moment frame, the braced frame, the braced frame with outriggers and finally the tubular structure. The advantages and disadvantages of all schemes were explored from both an architectural and structural efficiency standpoint. Prior to the computer modeling of each lateral system, each scheme was understood from an analytical standpoint to both verify computer results and to illustrate the importance of hand calculations. The study repeatedly illustrated that motion was the governing condition and this led to the proposal of an approach for the design of braced frames.

Thesis Supervisor: Professor Jerome J. Connor
Professor of Civil and Environmental Engineering

ACKNOWLEDGEMENTS

I would like to thank my parents and family for always being unconditionally supportive of my education in the United States. The environment and knowledge gained at both Northwestern University and MIT has been invaluable and has allowed incredibly opportunity unforeseen a few years ago. Thank you.

I would also like to acknowledge the professors who have challenged and encouraged me throughout my academic career. Many thanks to Professor Jerome Connor and Professor Edwin Rossow for being the guiding force during my structural engineering studies. Their dedication to the advancement of the field and student focus has been resolute and my gratitude is immense.

Thanks to:

Tiffany for her sense of humor and going through the ups and downs of the year with me. I hope that I can have the positive impact on you as you had on me when your graduate studies come around.

Diego for being supportive and a great buddy. I have learnt many things from you besides that there is no such thing as hard tacos.

Midori for her patience and belief. You have broadened my horizons far beyond that of only architecture.

Mark Chang. Thanks for being a great friend and homework buddy. Our experiences at Northwestern will be with me for a long time to come.

Evan for personifying dedication and perseverance.

And of course all the M. Eng HPS people who have made the year a great experience. All the best to you all.

“Iteration is only for people who don’t know what they are doing.”

Professor Jerome Connor

Table of Contents

1 CHAPTER 1: OVERVIEW	15
1.1 INTRODUCTION	15
1.2 HISTORY OF THE SKYSCRAPER	16
1.2.1 <i>First Skyscraper Period</i>	16
1.2.2 <i>Second Skyscraper Period</i>	18
1.2.3 <i>Third and Fourth Skyscraper Period</i>	19
1.3 REFERENCES	20
2 CHAPTER 2: LOADING AND DESIGN CRITERIA.....	21
2.1 BUILDING TYPE AND DIMENSIONS	21
2.2 WIND LOADING.....	22
2.3 LIVE LOADING	23
2.4 MEMBER DESIGN CRITERIA	23
2.4.1 <i>Strength Based AISC Design Criteria</i>	23
2.4.2 <i>Displacement Criteria</i>	24
2.5 COLUMN SIZES.....	24
2.6 REFERENCES	24
3 CHAPTER 3: MOMENT FRAMES.....	25
3.1 MOMENT FRAME INTRODUCTION.....	25
3.2 STRUCTURAL ANALYSIS	25
3.2.1 <i>Portal Analysis</i>	26
3.2.2 <i>Drift Analysis</i>	28
3.3 COLUMN / GIRDER DESIGN	29
3.4 MOTION BASED DESIGN.....	29
3.4.1 <i>Virtual Work Displacement Optimization</i>	30
3.4.2 <i>Motion Based Column Design</i>	31
3.5 EFFICIENCY OF MOMENT FRAMES	32
3.6 CONCLUSION (MOMENT FRAME)	33
3.7 REFERENCES	34

4 CHAPTER 4: BRACED FRAMES.....	35
4.1 BRACED FRAME INTRODUCTION	35
4.2 STRUCTURAL ANALYSIS	38
4.2.1 Structural Analysis For Component Sizing.....	40
4.2.2 Drift Analysis	40
4.2.2.1 Virtual Work Drift Analysis	41
4.2.2.2 Approximate Drift Analysis.....	41
4.3 SAP MODEL (BRACED FRAME)	43
4.3.1 30 Story Braced Frame Models	44
4.3.1.1 Force Analysis (SAP Model).....	46
4.3.1.2 Structural Efficiency of Braced Frames.....	48
4.3.1.3 Virtual Work Drift Optimization	50
4.3.1.4 Displacement Profile.....	51
4.3.2 40 Story Braced Frame Models	52
4.3.2.1 SAP MODEL	54
4.3.2.2 Theoretical Shear Force Distributions	55
4.3.2.3 Optimization of Theoretical Shear Force Distributions.....	56
4.3.2.4 Optimized Shear Force Distribution (SAP Model).....	58
4.3.3 Virtual Work Drift Optimization.....	59
4.4 CONCLUSION (BRACED FRAME).....	61
4.5 REFERENCES	62
5 CHAPTER 5: BRACED FRAMES WITH OUTRIGGERS	63
5.1 BRACED FRAME WITH OUTRIGGERS.....	63
5.2 STRUCTURAL ANALYSIS	64
5.2.1 Governing Equations	65
5.2.2 Optimum Location of Outriggers.....	67
5.3 SAP MODELS (BRACED FRAME WITH OUTRIGGERS)	68
5.3.1 Optimum Location	69
5.3.2 Structural Efficiency	71
5.3.3 Deformed Shape and Design Issues.....	73

5.4 CONCLUSION (BRACED FRAME WITH OUTRIGGERS)	77
5.5 REFERENCES	78
6 CHAPTER 6: TUBULAR STRUCTURES	79
6.1 TUBULAR STRUCTURES INTRODUCTION.....	79
6.2 STRUCTURAL ANALYSIS	81
6.2.1 <i>Shear Lag</i>	82
6.2.1.1 Positive Shear Lag	83
6.2.1.2 Negative Shear Lag.....	84
6.2.2 <i>Quantification of Shear Lag</i>	85
6.2.2.1 Variation of Shear Lag with Height.....	87
6.2.2.2 Shear Lag Variation with Base Dimensions	88
6.3 SAP MODELS (TUBULAR STRUCTURES)	91
6.3.1 <i>Shear Lag Coefficients</i>	92
6.3.2 <i>SAP Model Results</i>	94
6.3.2.1 Variation of Flange and Web Shear with H/F and H/W.....	95
6.3.2.2 Variation of Flange and Web Shear Lag with Height.....	97
6.3.2.3 Variation of Flange Shear Lag with F/W.....	98
6.3.2.4 Effect of Increased Girder Stiffness on Flange Shear Lag	99
6.3.2.5 Braced Tube Structures.....	100
6.4 CONCLUSION (TUBULAR STRUCTURES)	102
6.5 REFERENCES	103
7 CHAPTER 7: STIFFNESS DISTRIBUTION FOR BRACED FRAMES.....	105
7.1 INTRODUCTION	105
7.2 METHODOLOGY FOR ANALYZING STIFFNESS DISTRIBUTIONS.....	105
7.3 RESULTS OF PARAMETRIC STUDY	107
7.4 IMPLICATIONS FOR DESIGN	109
7.5 CONCLUSION.....	109
7.6 REFERENCES	110
APPENDIX A.....	111

APPENDIX B.....115

APPENDIX C.....121

APPENDIX D.....137

APPENDIX E.....145

APPENDIX F.....153

APPENDIX G.....173

List of Figures

Figure 1 - 1: Evolution of Skyscraper Form	17
Figure 1 - 2: Chrysler Building (New York) [1].....	19
Figure 1 - 3: Woolworth Building (New York).....	19
Figure 2 - 1: Typical Structure (Elevation View)	21
Figure 2 - 2: Typical Structure (Plan View)	21
Figure 3 - 1: Portal Frame Deflected Shape.....	26
Figure 3 - 2: Portal Frame Moment Diagram Under Lateral Loads	28
Figure 3 - 3 : Virutal Work Optimization	30
Figure 3 - 4: Normalized Amount of Steel Required.....	33
Figure 4 - 1: Empire State Building (New York) [1].....	36
Figure 4 - 2: John Hancock Center (Chicago) [2].....	37
Figure 4 - 3: Bank of China Tower (Hong Kong) [2].....	37
Figure 4 - 4: John Hancock Center Interior Space (Chicago) [3]	38
Figure 4 - 5: Flexural Deformation Mode.....	39
Figure 4 - 6: Braced Frame Deformation Mode	40
Figure 4 - 7: 3 Bay Braced Frame.....	45
Figure 4 - 8: Single Bay Braced Frame	46
Figure 4 - 9: Comparison of Steel Volume Required	49
Figure 4 - 10: 3 Bay Bracing Virtual Work Drift Optimization	51
Figure 4 - 11: Displacement Profile (Braced Frame).....	52
Figure 4 - 12: 40 Story Integrated Model	53
Figure 4 - 13: 40 Story Separated Model.....	54
Figure 4 - 14: Theoretical Shear Force Distribution.....	57
Figure 4 - 15: Shear Force Distribution	59
Figure 4 - 16: Virtual Work Diagram (Separated Model)	60
Figure 4 - 17: Virtual Work Diagram with Increased Bracing Cross Sectional Area	61

Figure 5 - 1: US Bank Center (Milwaukee) [1]	64
Figure 5 - 2: Vila Olimpica (Barcelona, Spain) [1]	64
Figure 5 - 3: Structural Model	65
Figure 5 - 4: Optimum location of outrigger [2].....	68
Figure 5 - 5: SAP Outrigger Model	69
Figure 5 - 6: Deformed Outrigger Shape	70
Figure 5 - 7: Braced Frame with Single Outrigger	71
Figure 5 - 8: Braced Frame with 2 Outriggers.....	72
Figure 5 - 9: Graph of Steel Volume Required.....	73
Figure 5 - 10: Deformed Shape (Braced Frame with 2 Outriggers)	74
Figure 5 - 11: Virtual Work Diagram (Braced Frame with 2 Outriggers).....	75
Figure 5 - 12: Location of Inflexion point in a Braced Frame with 2 Outriggers.....	76
Figure 6 - 1: World Trade Center (New York) [1]	81
Figure 6 - 2: Sears Tower (Chicago) [1].....	81
Figure 6 - 3: Axial Stress with Shear Lag [3].....	83
Figure 6 - 4: Deformation Resulting in Positive Shear Lag [4].....	84
Figure 6 - 5: Deformation Resulting in Negative Shear Lag [4]	85
Figure 6 - 6: Quantification of Web Shear Lag [5].....	86
Figure 6 - 7: Quantification of Flange Shear Lag [5]	86
Figure 6 - 8: Variation of Shear Lag with Height [6]	87
Figure 6 - 9: Variation of Shear Lag with Height [4]	88
Figure 6 - 10: Variation of Shear with Base Dimensions [5]	89
Figure 6 - 11: Structural Model [5].....	89
Figure 6 - 12: Plot of Shear Lag Coefficients with Varying H/a and H/b [5].....	90
Figure 6 - 13: Flange Axial Force Distribution for Model 1	93
Figure 6 - 14: Web Axial Force Distribution for Model 1.....	94
Figure 6 - 15: Variation of Flange Shear Lag with H/F.....	96
Figure 6 - 16: Variation of Web Shear Lag with H/W	97
Figure 6 - 17: Variation of Flange Shear Lag with F:W.....	99

Figure 6 - 18: Tubular Structure with Bracing..... 101

Figure 7 - 1: Variation of “s” with Aspect Ratios..... 109

List of Tables

Table 1 - 1: List of Buildings for Figure 1-1	19
Table 2 - 1: Wind Point Loads.....	23
Table 3 - 1: Top Story Drift Using Strength Based Column Design	29
Table 3 - 2: Volume of Steel Required for Strength and Motion Based Design	31
Table 3 - 3: Normalized Steel Volumes.....	32
Table 4 - 1: Shear Rigidity of Different Bracing Schemes	43
Table 4 - 2: Distribution of Lateral Forces in Braced Frames	47
Table 4 - 3: Comparison of Steel Volumes Required	49
Table 4 - 4: Theoretical Average Frame Shear Force and Standard Deviation	58
Table 4 - 5: Average Shear Force and Standard Deviation	59
Table 5 - 1: Comparison of Top Story Drift with Outrigger Placement.....	71
Table 5 - 2: Comparison of Steel Volume Required.....	73
Table 5 - 3: Comparison of Base Moments	77
Table 6 - 1: SAP Models Analyzed	92
Table 6 - 2: Flange Axial Forces for Model 1 (Bottom Column).....	93
Table 6 - 3: Computed Shear Lag Coefficients	95
Table 6 - 4: Variation of Flange Shear Lag with H/F	95
Table 6 - 5: Variation of Web Shear Lag with H/W	96
Table 6 - 6: Flange Shear Lag with Varying Girder Stiffness	99
Table 6 - 7: Shear Lag Coefficients with Bracing Introduced	102
Table 7 - 1: Braced Frame Models Analyzed	107

1 Chapter 1: Overview

1.1 Introduction

Mankind has always had a fascination for height and throughout our history, we have constantly sought to metaphorically reach for the stars. From the ancient pyramids to today's modern skyscraper, a civilization's power and wealth has been repeatedly expressed through spectacular and monumental structures. Today, the symbol of economic power and leadership is the skyscraper. There has been a demonstrated competitiveness that exists in mankind to proclaim to have the tallest building in the world.

This undying quest for height has laid out incredible opportunities for the building profession. From the early moment frames to today's ultra-efficient mega-braced structures, the structural engineering profession has come a long way. The recent development of structural analysis and design software coupled with advances in the finite element method has allowed the creation of many structural and architecturally innovative forms. However, increased reliance on computer analysis is not the solution to the challenges that lie ahead in the profession. The basic understanding of structural behavior while leveraging on computing tools are the elements that will change the way structures are designed and built.

The design of skyscrapers is usually governed by the lateral loads imposed on the structure. As buildings have gotten taller and narrower, the structural engineer has been increasingly challenged to meet the imposed drift requirements while minimizing the architectural impact of the structure. In response to this challenge, the profession has proposed a multitude of lateral schemes that are now expressed in tall buildings across the globe.

This thesis seeks to understand the evolution of the different lateral systems that have emerged and its associated structural behavior. For each lateral scheme examined, its advantages and disadvantages will be looked at. This investigation will rely on both analytical models and computer analysis and this dual exploration will serve to reiterate the importance of analytical solutions. The lateral schemes look looked at are the moment frame, the braced frame, the braced frame with outriggers and the tubular form.

1.2 History of the Skyscraper

Skyscrapers have a long history dating back to the early 1900s. The modern skyscraper movement has been widely regarded to have started in Chicago with the Home Life Insurance Company building which was the first building to utilize a metal skeleton as its load carrying structure. Up till 1900, buildings were predominantly constructed out of masonry which immediately limited the height of buildings through its relatively low strength (200psi).

As skyscraper design progressed and structural innovations occurred, the form and structural behavior evolved. The form and look of skyscrapers have been generally grouped into four periods.

1.2.1 First Skyscraper Period

With the construction of the Home Life Insurance Company in Chicago, the first skyscraper period began. The increase in steel availability in the late 1800s allowed engineers to design and propose new structural forms that allowed an economical progression towards taller structures. However, architects of the day struggled to find an acceptable geometric form for the new structures. They were bound to the historical styles which they had been familiar with. A compromise was sought between the styles of the past and the new urban landscape which was quickly taking form.

The first style adopted was the Renaissance Palazzo style that comprised a block and slab like form for the building which gave buildings a highly regular and repetitive form. As buildings got taller, architects sought to break this pattern approach by introducing different styles of palazzi on top of each other. For example, a building might be comprised of three different styles of palazzi stacked on top of each other with the base section designed in the Romanesque style, the middle section in the Classical style and the roof section with a Queen Anne inspired design [1]. This style generally dominated the first skyscraper period in the Chicago school.

As the Chicago school developed and refined their architectural ideas, the expression of a building's underlying structure began to take place. This was best demonstrated by the Carson Pirie Scott Department Store (Figure 1 - 1g) in 1904 whose spans and bay widths were determined by the underlying structural form and not the standard architectural rules of

regularity and symmetry. This expression of structural form was in clear contrast to the second skyscraper period which predominantly occurred in New York.

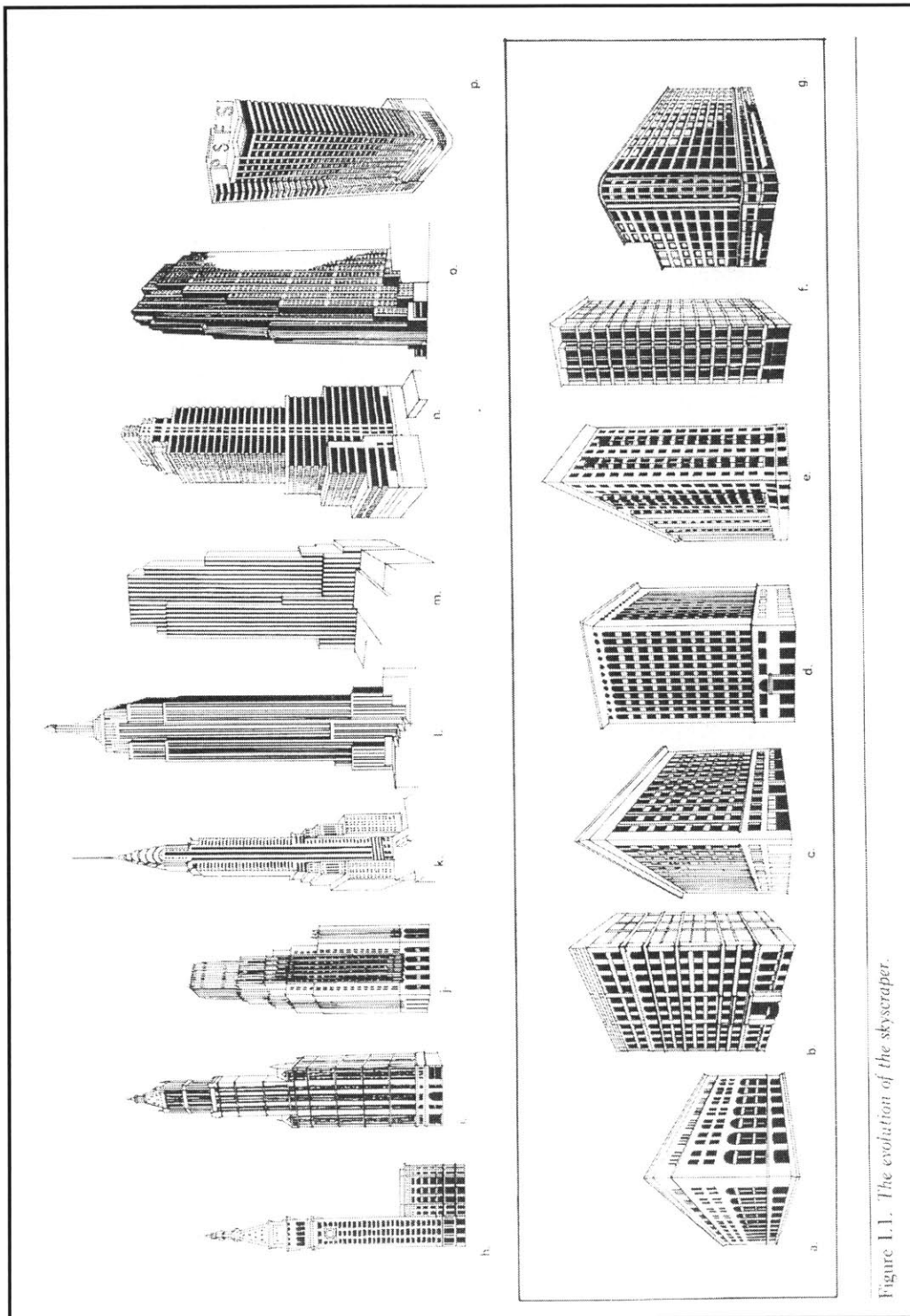


Figure 1.1. The evolution of the skyscraper.

Figure 1 - 1: Evolution of Skyscraper Form

1.2.2 Second Skyscraper Period

The completion of the 47 story 614 ft Singer Building in New York (1908) marked the movement in the race for height from Chicago to New York. One year later, the 50 story Metropolitan Life Insurance Tower topped out at 675ft. The race for vertical supremacy had clearly begun. Unlike their counterparts in Chicago, design in New York was still firmly rooted in the ornamentation and visual impact of a structure which inevitably resulted in hidden structural forms. As the palazzo style became increasingly unsuited for taller and taller structures, architects were challenged to find a new language to define the new quickly emerging towers.

New York skyscrapers generally fell into two styles, Classical/Gothic (Figure 1 - 1i) and Art Deco. The Classical/Gothic utilized an ornamental façade which miniature towers and buttresses were a predominant feature. This façade was subsequently attached to the steel skeleton beneath. These forms hid well the structural characteristics of the building.

The Art Deco design was brought about by the revision in the New York city building code which sought to limit the impact of skyscrapers on the lighting and ventilation of adjacent buildings and also the visual impact at the street level. Buildings were then forced to incorporate set backs which allowed more light at the street level. With the zoning requirements in place, tall buildings began to take the form of sculptures. This sculptural Art Deco style was best expressed by the Chrysler building which incorporates distinct set backs and a tall spire.

Towards the end of the 1920s, skyscrapers begun to take a more austere linear form that was the hallmark of the modernists. The expression of structural form and efficiency less the architectural ornamentation were distinctions of their designs.



Figure 1 - 2: Chrysler Building (New York) [1]



Figure 1 - 3: Woolworth Building (New York)

1.2.3 Third and Fourth Skyscraper Period

The third skyscraper period continued with modernism but with increasing focus and expression of technological innovation and structural form. The Sears Tower and John Hancock Center in Chicago clearly demonstrate the modernist style with distinct expression of the structural form. To this day, modernism continues to persist in the architectural language for tall structures as they continue to soar with increasing ambition.

Table 1 - 1: List of Buildings for Figure 1-1

Figure 1-1	Building	City	Year
a	Marshall Field Warehouse	Chicago	1887
b	Home Life Insurance Company	Chicago	1885

c	Wainwright Building	St Louis	1891
d	Guaranty Building	Buffalo	1895
e	Monadnock Building	Chicago	1891
f	Reliance Building	Chicago	1894
g	Carson Pirie Scott Department Store	Chicago	1904
h	Metropolitan Life Insurance	New York	1909
i	Woolworth Building	New York	1913
j	Elie Saarinén's Entry for Chicago Tribune Tower Competition	Chicago	1922
k	Chrysler Building	New York	1930
l	Empire State Building	New York	1931
m	Daily News Building	New York	1930
n	McGraw-Hill Building	New York	1931
o	RCA Building	New York	1933
p	PSFS Building	Philadelphia	1932

1.3 References

- [1] W. Schueller, The Vertical Building Structure, New York: Van Nostrand Reinhold, 1990.

2 Chapter 2: Loading and Design Criteria

2.1 Building Type and Dimensions

In order to give realism to this academic study, an office building steel structure of various heights was sited in Boston, MA with the following dimensions. The building is 35m x 35m in plan with columns spaced 7m on center. A floor to floor height of 3.5m was also assumed. This location and structure type allowed a definition of building type and basic wind velocities. An elevation and plan view of a typical structure is shown in Figure 2-1 and 2-2. Complete drawings are attached in Appendix B.

The façade system of the structure was also assumed to transfer the full wind loading applied to the main lateral load carrying system (e.g. moment frame, bracing) as point loads. This allowed the application of the wind loading to node points in the SAP model and eliminated local deformations that might occur at the windward face columns. This allowed a more accurate estimation of deflections and story shears.

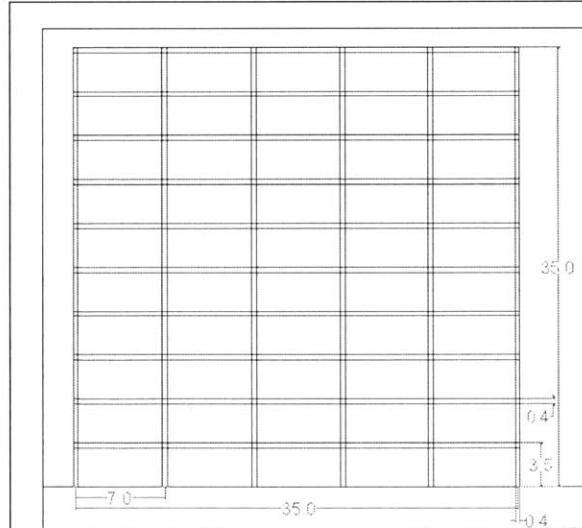


Figure 2 - 1: Typical Structure (Elevation View)

All units in meters

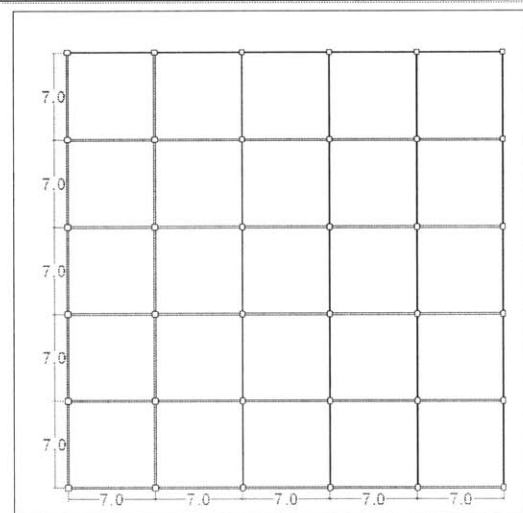


Figure 2 - 2: Typical Structure (Plan View)

2.2 Wind Loading

The wind loading in this study was established in accordance with ASCE Standard 7-95. From the code, the following equations were established and constants defined. For expediency, wind loads were only evaluated every 5 stories. A table of calculations and nodal forces are attached in Appendix B.

P	:	$qGC_p - q_h(GC_{pi})$
q	:	q_z (windward wall), q_h (leeward wall)
q	:	$0.613K_zK_{zt}V^2I$ (N/m ²)
q _h	:	q at roof height
G	:	Gust Effect Factor (0.8)
C _p	:	Wall Pressure Coefficients (0.8 Windward Wall, -0.5 Leeward Wall)
GC _{pi}	:	Internal Pressure Coefficient (+/- 0.18)
K _z	:	Velocity Pressure Coefficient ($2.01[z/z_g]^{2/\alpha}$)
z _g	:	457m (with exposure category A)
alpha	:	5.0 (with exposure category A)
K _{zt}	:	Topographic Factor $(1+K_1K_2K_3)^2$
K ₁	:	Factor to account for shape of topographic feature (1)
K ₂	:	Factor to account for reduction in speed up with distance with respect to crest (1)
K ₃	:	Factor to account for reduction in speed up with height above local terrain (0.14)
V	:	Basic Wind Speed (49m/sec for MA, USA)
I	:	Importance Factor (1.15 with Building Category III classification)

The following nodal forces Table 2-1 were established for the various structures of same plan dimension but of varying heights. For simplicity, nodal point forces were only computed every 5 stories, this allowed faster application of nodal loads.

Table 2 - 1: Wind Point Loads

Story	10 Story	20 Story	30 Story	40 Story
0-5	51	52	53	54
6-10	66	67	68	69
11-15		78	79	80
16-20		87	88	89
21-25			95	96
26-30			102	103
31-35				109
36-40				115

*nodal wind loads in kN

2.3 Live Loading

In accordance with ASCE 7-95, a uniform live loading of 2.4kN/m^2 (office use) was assumed for the sizing of columns. This was applied over the total floor area (1225m^2) of each story and distributed evenly among all 30 columns. This imposed an axial load of 82kN per column per story. Naturally, actual live loading imposed on the columns would depend greatly on the floor system but an even distribution was assumed to simplify the model.

2.4 Member Design Criteria

The primary area of study is the amount of steel dedicated to columns as structure height increases. In order to size the columns realistically, they were designed in accordance with LRFD recommendations. This equations used are illustrated below.

2.4.1 Strength Based AISC Design Criteria

The following equations were used in the proportioning the sizes of columns.

$$\frac{P_u}{\phi P_n} > 0.2$$

$$\frac{P_u}{\phi P_n} + \frac{8}{9} \frac{M_u}{\phi M_n} < 1.0$$

$$\frac{P_u}{\phi P_n} < 0.2$$

$$\frac{P_u}{2\phi P_n} + \frac{M_u}{\phi M_n} < 1.0$$

(2-1, 2-2)

Where:

P_u	:	Applied axial force (kN)
P_n	:	Nominal axial capacity (kN)
M_u	:	Applied moment (kN-m)
M_n	:	Nominal elastic moment capacity (kN-m)

2.4.2 Displacement Criteria

Standard design codes limit top story drift of a structure to 0.002H. This criteria was used throughout all models studied.

2.5 Column Sizes

An architectural constraint of 0.4m on column sizes was assumed for the purpose of this study. This was done to enforce that the only way to increase strength/stiffness properties was to increase the wall thickness. This would then be used to demonstrate the increase in amount of material as strength/stiffness requirements increased. Properties such as elastic moment and axial capacity of these square columns of varying wall thicknesses was computed and this is shown in Appendix B. These sections were used in designing in column and girder elements.

2.6 References

- [1] J. C. McCormac and J. K. Nelson, Structural Steel Design: LRFD Method, New Jersey: Prentice Hall, 2003
- [2] ASCE Standard, American Society of Civil Engineers: Minimum Design loads for Buildings and Other Structures 7-95, New York: American Society of Civil Engineers, 1996

3 Chapter 3: Moment Frames

3.1 Moment Frame Introduction

A moment frame is a structure that utilizes moment resisting connections between columns and girders throughout its perimeter to resist the lateral loads applied. These frame structures are characteristic of early skyscrapers where 3 dimensional structural analysis was still in its infancy. The repetitive pattern with small cross sectional changes from floor to floor allows simple construction. Moment frames also allows unobstructed bays that allows for flexibility in spatial programming and locations of openings. This feature is much desired by architects seeking flexibility in their design and also helps to introduce as much natural light into the space as possible.

However, as a result of the multitude of fixed connections that are required in moment frames, additional cost would be incurred due to field welding or additional bolting required. This was and still is a costly process. The load carrying behavior (through element bending) of moment frames also result in significant column and girder end moments. This immediately leads to larger designed sections than in a situation where a separate lateral system is employed. Another drawback of the moment frame is that the gravity system of the structure is coupled with the lateral system. In other words, the design of the perimeter frame and floor system has to occur concurrently. Furthermore, as a result of the significant column end moments, the floor system has to vary from story to story to account for end moments. This leads to a more tedious design process.

3.2 Structural Analysis

The structural analysis of any structure can be broken into a force analysis and a displacement analysis. For different structural forms, different methods need to be employed for both the force and displacement analysis. In moment frames, the force analysis can be done via the portal method and the displacement analysis can be performed by decomposing the drift into the contributions by column and girder deformation. The portal method and displacement analysis procedures are detailed below.

With rigid connections within the whole frame, the lateral loads are carried in the columns by shear action and as a result the columns deform in double curvature. This is

illustrated in Figure 3 - 1 where the deformed shape of a 10 story portal frame is shown. This shape is characteristic of a shear beam where most inter-story deformation occurs at the base and decreases as we move up the structure. This is attributed to the accumulation of shear forces towards the bottom of the structure where the base columns have to carry the entire lateral load applied to the structure. This gives rise to the relatively large inter-story displacement at this story.

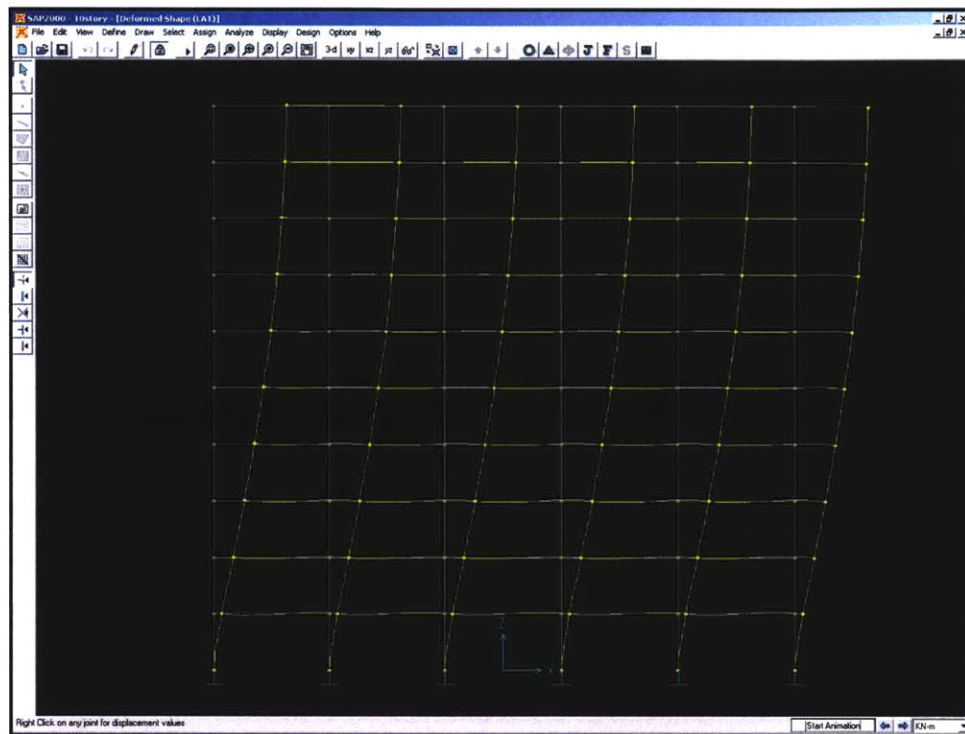


Figure 3 - 1: Portal Frame Deflected Shape

3.2.1 Portal Analysis

Analysis of moment frames can be easily carried out by one of the two popular methods, the portal method and the cantilever method. The portal method which was used in the preliminary analysis to obtain design loads will be described briefly. The portal analysis makes the following assumptions.

1. Story shears are carried by corner and interior columns in a 1 to 2 ratio.
2. An inflexion point is assumed in the middle of both beams and columns.

With these assumptions, a highly indeterminate frame can be easily analyzed. The portal analysis proceeds as following.

1. Compute story shears by summing the lateral forces at and above the current story.
2. Distribute story shear between interior and corner columns.
3. Compute column moments by multiplying the column shear by half the story height.
4. Compute associated beam moments by taking moment equilibrium at each joint.
5. Compute beam shears by dividing beam moments by half the span length.
6. Compute imposed column axial loads by summing beam shears at and above the current column.

This preliminary analysis was carried out in Excel which allowed sizing of columns on a strength basis. Figure 3 - 2 depicts the moment diagram obtained from SAP which result in a portal frame under lateral loads. From the diagram, it is observed that inflexion points are not exactly at the mid-points of columns but occur at approximately $2/3$ along its length. However for schematic purposes, the portal analysis is sufficiently accurate. The complete portal analysis for 10, 20, 30 and 40 story structure are detailed in Appendix C. In order the quickly size the columns for the portal frames under lateral loads, only the interior columns (which carry greater moment) were analyzed.

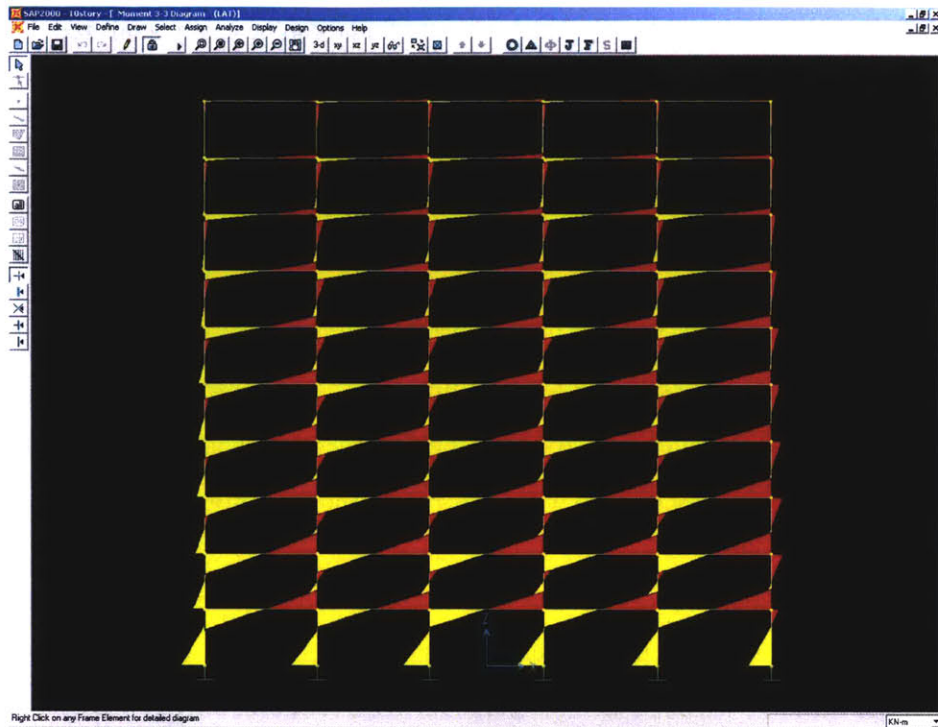


Figure 3 - 2: Portal Frame Moment Diagram Under Lateral Loads

3.2.2 Drift Analysis

The displacement of a portal frame can be accounted for by the two different modes of deformation (column rotation and girder rotation) that occurs. The two modes are analyzed separately and the total story drift is the sum of the two effects.

$$\Delta_{column} = \frac{Vh^3}{12EI_c}$$

$$\Delta_{girder} = \frac{Vh^2}{12E \sum \left(\frac{I_{bi}}{L_i} \right)} \quad (3-1, 3-2)$$

These equations [1] were used in estimating the drift of the various moment frames under the applied lateral loading. This estimation was checked against a SAP model and the percentage error was calculated. These values of each top story drift and its error are tabulated in Appendix C. It was noted that as the number of stories increased, the equations increasingly underestimated

the drift. This error is attributed to the assumption of inflexion at the middle of the column which gives rise to smaller column moments and thus smaller calculated drifts. A further error arises from the omission of column axial shortening/lengthening in the analysis. As the number of stories increase, this effect becomes more pronounced.

3.3 Column / Girder Design

Column design for strength proceeded as detailed in Chapter 2. Only columns every five stories were designed and that selected uniform section was carried throughout 5 stories. The same section was also employed in the girders of the associated 5 stories. This was done to simplify the design procedure and also provide sufficient rotational stiffness at the joints. This rotational stiffness will be illustrated to play a major role in the lateral deflection of moment frames.

3.4 Motion Based Design

Table 3 - 1 below illustrates that strength based design did not provide sufficient lateral stiffness to the moment frames to meet the H/500 drift criteria. The columns had to be redesigned with stiffer sections to meet the criteria.

Table 3 - 1: Top Story Drift Using Strength Based Column Design

No of Stories	Top Story Drift	Drift Criteria	% difference
10	0.09	0.07	+25.7
20	0.30	0.14	+114.3
30	0.54	0.21	+159.1
40	0.79	0.28	+182.1

An analysis procedure was required to determine the optimum location to add more material to the structure. It was important to determine the main sources of inter-story displacement and reduce its relative contribution. The virtual work approach was adopted for this task.

3.4.1 Virtual Work Displacement Optimization

The virtual work displacement optimization approach involves applying a unit load at the location at which displacement is sought to be calculated (the top story being the location in this situation). Routine structural analysis is then performed and the percentage contribution of each member can be computed. This procedure is performed succinctly in SAP2000. An example output of the relative contribution of each member is shown in Figure 3 - 3. This is illustrated for a fifteen story moment frame under lateral loads. Reducing top story drift was the goal of this exercise.

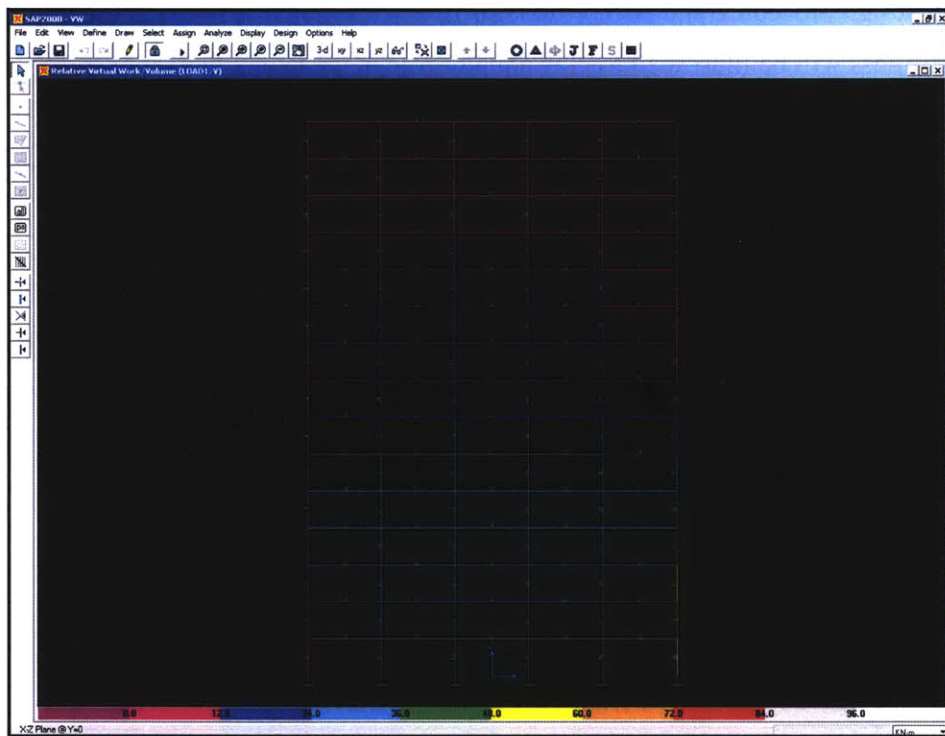


Figure 3 - 3 : Virtual Work Optimization

It is noted that the percentage contributions increase towards the bottom of the structure and this indicates that material allocated towards the bottom of the structure would be most efficient in reducing the top story displacement. The virtual work contributions of the girders are also noted to be significant where they make up almost an equal amount as the columns. Therefore, material should also be allocated to the girders to reduce the joint rotations which

would ultimately reduce top story drift. This insight is the basis for using the same sections for both the columns and girders in a particular story.

Another method to decide whether the girder or column sizes should be increased in a particular floor is the ratio of the column and girder's relative stiffness. This ratio [2] is given in Equation 3-2 and denoted by ψ .

$$\psi = \frac{\frac{I_c}{h}}{\sum \frac{I_g}{L}} \quad (3-2)$$

$\psi \gg 0.5$, adjust girder sizes

$\psi \ll 0.5$, adjust column sizes

$\psi = 0.5$, both girder and column sizes

This allows the control of each individual story's drift and could be used in reducing the drift contribution of the most flexible floors.

3.4.2 Motion Based Column Design

With the above displacement optimization insight, each moment frame was redesigned to meet the H/500 criteria. This significantly increased the required column sizes. The total steel volume required for both strength based and motion based design are tabulated in Table 3 - 2. It is clearly noted that the amount of steel required for motion control increases significantly as height increases.

Table 3 - 2: Volume of Steel Required for Strength and Motion Based Design

Story	Strength Based (m3)	Motion Based (m3)
10	8.74	8.74
20	17.02	60.59
30	65.30	219
40	133.73	336

3.5 Efficiency of Moment Frames

Moment frames of 10, 20, 30 and 40 stories was designed for both strength and displacement criteria. A total of 8 models were designed and the total steel volume incurred in each case tabulated and the normalized numbers are plotted in Figure 3 - 4.

It is immediately apparent that the amount of material required for deflection control increases much faster as the aspect ratio increases than the amount of material required for strength based design. Within the aspect ratios modeled, it is noted that moment frames are reasonably efficient up to the aspect ratio of 2. Beyond this point, the amount of material required for deflection control via curvature deformation of the columns and girders quickly outpaces the amount of material solely required for strength purposes.

With this realization and increasing demands for height, structural engineers are challenged to come up with forms that would provide lateral stiffness without the penalty of additional steel. Three more structurally efficient forms are examined in the proceeding chapters.

Table 3 - 3: Normalized Steel Volumes

Story	Height (m)	Aspect Ratio (H/Base)	Strength Based (normalized to 8.74)	Motion Based (normalized to 8.74)
10	35	1	1.00	1.00
20	70	2	1.95	6.93
30	105	3	7.47	25.06
40	140	4	15.30	38.44

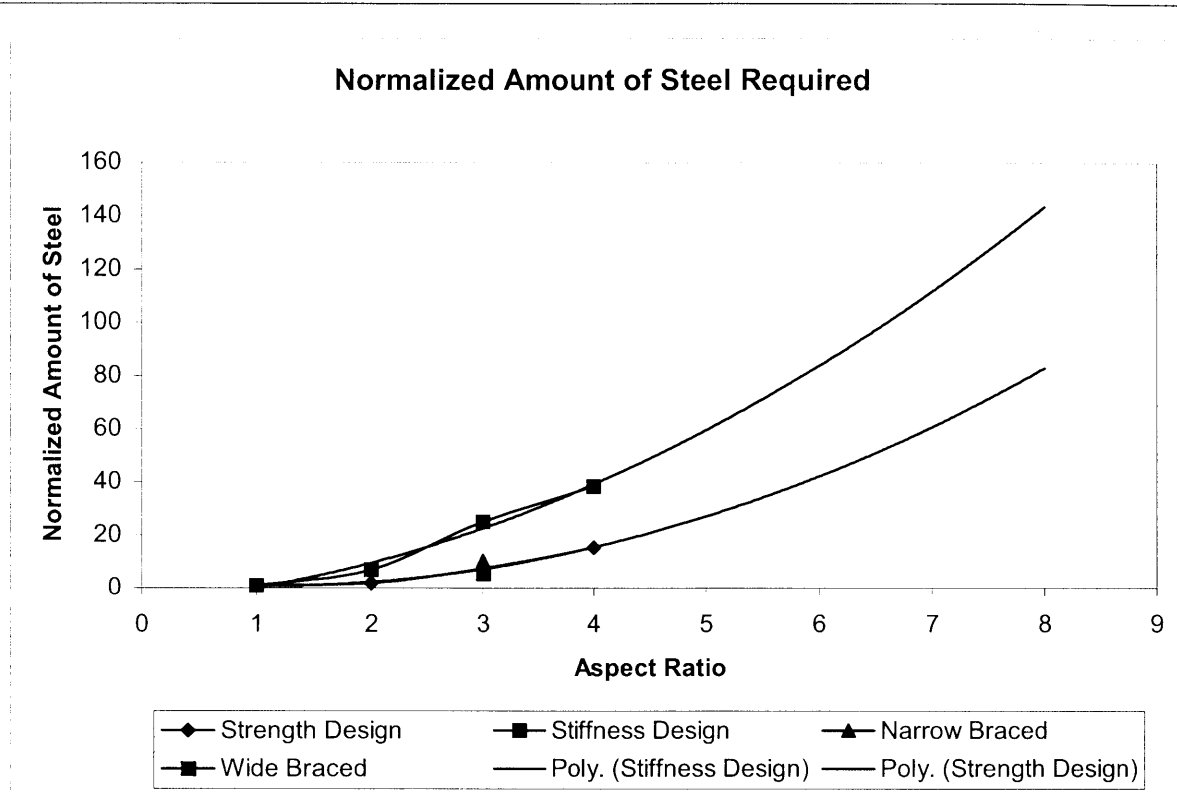


Figure 3 - 4: Normalized Amount of Steel Required

3.6 Conclusion (Moment Frame)

This chapter has surveyed the structural behavior of the moment frame. It has demonstrated how preliminary structural analysis and displacement analysis is carried out and also the assumptions used. It has also demonstrated the accuracy of the preliminary analysis decreases as the number of stories increase in a building. The basis for strength and stiffness design for each particular structure was also illustrated.

The efficiency of the moment frame was evaluated from a materials standpoint. It was demonstrated that due to drift requirements, the volume of materials required increased at an increasing rate. This was illustrated in Figure 3 - 4. With these insights, the following chapters will explore more structural efficient lateral schemes such as the braced frame, braced frame with outriggers and the tubular form.

3.7 References

- [1] B. Taranath, Structural Analysis & Design of Tall Buildings, New York: McGraw-Hill Book Company, 1988.
- [2] B. S. Smith and A. Coull, Tall Building Structures: Analysis and Design, New York: John Wiley & Sons Inc, 1991.
- [3] W. Schueller, The Vertical Building Structure, New York: Van Nostrand Reinhold, 1990.

4 Chapter 4: Braced Frames

4.1 Braced Frame Introduction

The braced frame is a common system employed to resist the significant lateral loads that exceptionally tall structures are subjected to. Bracing for the frames can occur within a single bay or can span the entire face of a structure. The Empire State Building is an early example of single bay bracing being employed in a structure to resist the lateral loads imposed. Other signature projects such as the Bank of China tower in Hong Kong and the John Hancock center in Chicago are examples of large scale bracing employed to resist lateral loading. These buildings and their bracing schemes are illustrated in Figure 4 - 1 to Figure 4 - 3. The diagonal elements that run across a bay or the face of a building “tie” the whole structure together and transform the building into a vertical cantilever beam. The diagonal braces are analogous to the webs that are found in truss structures.

The advantages of braced frames from a structural engineering standpoint are enormous. Braced frames carry the lateral forces in an axial manner (through the diagonal elements) rather than through the bending of elements which is highly inefficient. The separation of the lateral system from the gravity system gives further advantages during the design phase. This allows the lateral system to be designed separately from the gravity system which allows for repetition in floor systems and column sections. With minimal frame action and mostly axial deformation, minimal moments in the columns and girders result from the applied lateral loads compared to a moment frame. This in turn leads to cheaper girder-column connections.

The largest drawback for braced frames is that the scheme is obstructive and significantly reduces openings within bays. This can be seen from Figure 4 - 4 which shows an interior space in the John Hancock Center. The large bracing covers a significant part of the bay window. However, it should be noted that while the bracing element covers a significant portion in certain bays, the separation of the lateral system from vertical system leads to much large column spacing which allows more flexibility in programming of the interior space within those bays. Another issue with large scale bracing is that it must fit within the larger architectural concept and is often hard to implement if such structural expression was not considered during the competition stage of the project. Such architectural design is the pinnacle of function meeting

form and its practice is concentrated within a few firms such as SOM, Foster and Partners and the Richard Rogers Partnership.

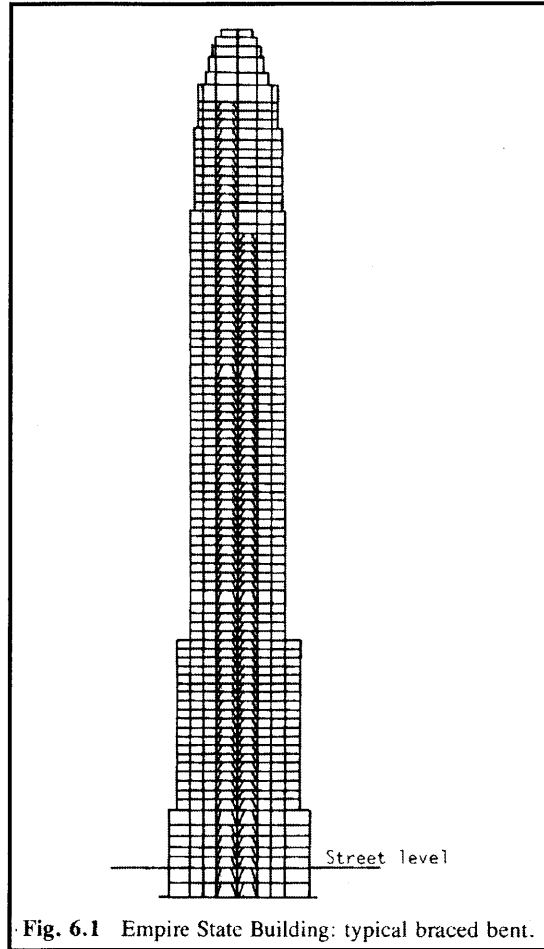


Figure 4 - 1: Empire State Building (New York) [1]



Figure 4 - 2: John Hancock Center (Chicago) [2]

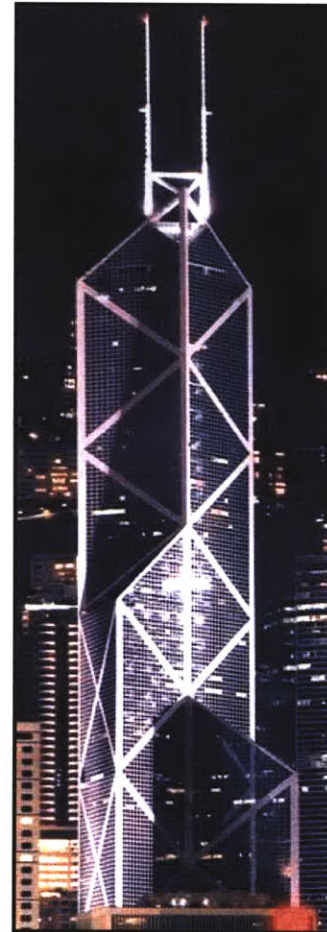


Figure 4 - 3: Bank of China Tower (Hong Kong) [2]



Figure 4 - 4: John Hancock Center Interior Space (Chicago) [3]

4.2 Structural Analysis

A braced frame is essentially a vertical cantilever truss structure where the columns in the structure acts as the chords of the truss and carry significant axial loads. The columns of the braced bay are then designed for these larger than usual axial loads. The other columns can generally be designed predominantly for gravity loads. The tension force in the windward column is a key design parameter as the condition of overturning in the structure is much sought to be avoided. The usual design situation is one in which the dead loads of the structure reduce this overturning force and results in a net compressive force in all the columns. In the event of uplift forces, the bracing scheme can be staggered across the bays of a structure engaging different sets of columns in different floors.

In the deformation of braced frames, two deformation modes are present, shear and bending. The braced bay (bay at which bracing is installed) deforms in flexural due to its high shear rigidity while the frame deforms in shear due to its low bending resistance. These two profiles are the direct opposite to each other. The flexural deformation mode results in axial lengthening/shortening in columns while the shear mode of deformation results in the extension of the diagonals. Compatibility between the two deformation modes are ensured through the rigid floors slabs in each floor. Illustrated in Figure 4 - 5 is the flexural deformation shape. The

shear deformation mode has been previously illustrated in Figure 3-1. It is noted that in the flexural mode, maximum curvature occurs towards the top of the structure. With the two modes of deformation combined, the resulting shape is usually one that is represented in Figure 4 - 6. As the aspect ratio of the structure increases, the flexural component mode of deformation tends to dominate.

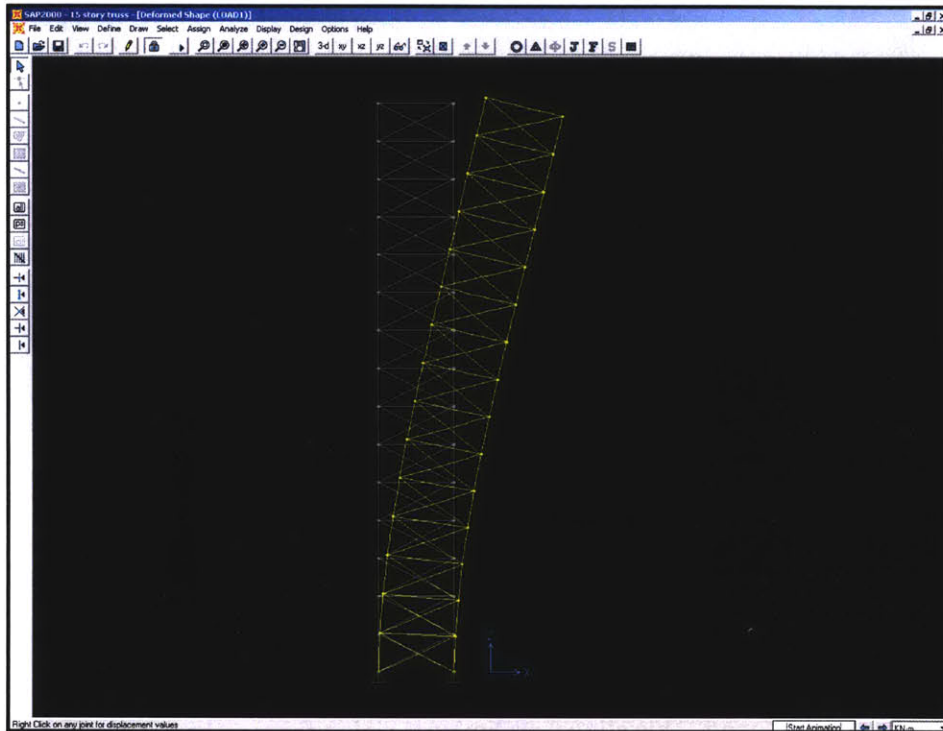


Figure 4 - 5: Flexural Deformation Mode

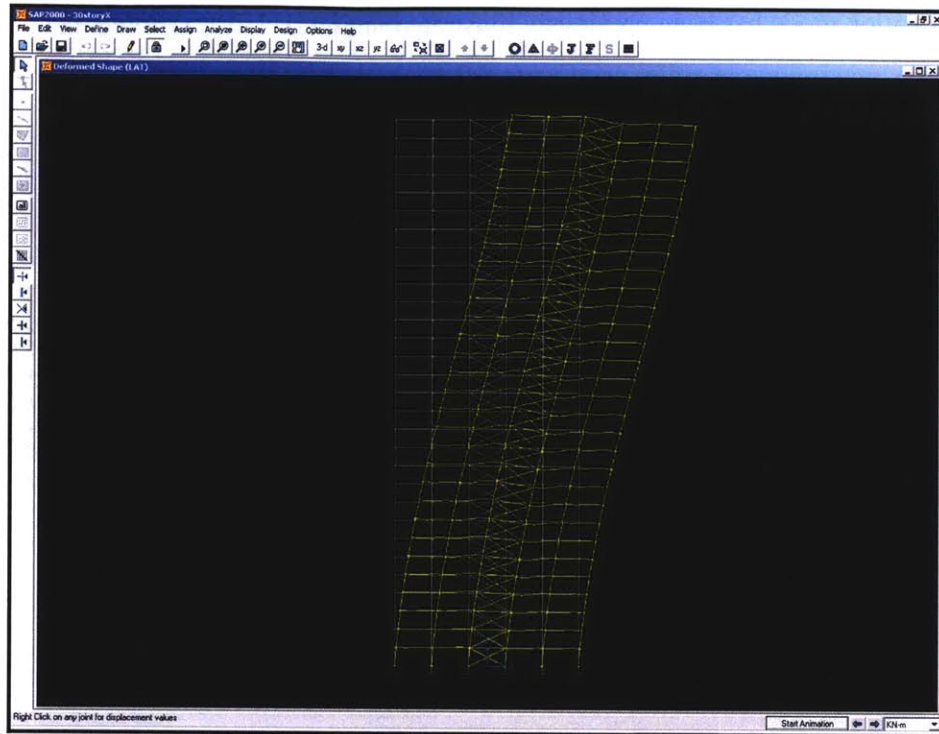


Figure 4 - 6: Braced Frame Deformation Mode

4.2.1 Structural Analysis For Component Sizing

In the preliminary structural analysis of braced frame, it is assumed that the braced bay carries all applied lateral load. This reduces the analysis to an analysis of structure illustrated in Figure 4 - 5. Through the method of joints or sections, the axial forces in the diagonal and vertical elements can be found. This allows preliminary sizing for members prior to complete analysis of the frame. However, in the detailed analysis of braced frame structures, one should look at the combined behavior of braced frame structures. The lateral resistance provided by the moment frame might be significant and could result in a more economical structure compared to one where the lateral stiffness of the moment frame is ignored. This combined behavior is studied later in the chapter.

4.2.2 Drift Analysis

As a result of the simplified structure, drift analysis can be conveniently carried out by either an exact virtual work method or an approximate method which separates the deformation components of shear and flexure.

4.2.2.1 Virtual Work Drift Analysis

The virtual work drift analysis requires two force analyses, one for the actual loading condition and another for a unit load (virtual load) applied at the position at which the drift is to be determined. This is given by the following equation [1].

$$\Delta = \sum_{j=1}^N \bar{p}_{jN} \left(\frac{PL}{EA} \right)_j + \sum_{j=1}^N \int \bar{m}_{xjN} \left(\frac{M_x}{EI} \right)_j dx \quad (4-1)$$

where:

Δ	-	deflection
P	-	axial force in element under applied loading
A	-	cross sectional area
M	-	moment from applied loading
I	-	moment of inertia
\bar{p}	-	axial force from virtual force
\bar{m}	-	moment in element from virtual force
N	-	no of elements

4.2.2.2 Approximate Drift Analysis

The approximate method of analysis breaks the drift at a particular story into its flexure and shear components which is similar to the approach in the drift analysis for moment frames except in this situation, the overall bending of the structure is accounted for.

The flexural component of drift is analyzed by considering the structure as a beam with an specific moment of inertia. This moment of inertia is dependent on the area of the chords (columns) and the width of the bracing. Reasonable of averaging of column cross sections should be done so as to reduce the number of cross sectional changes which have to be taken into account along the structure.

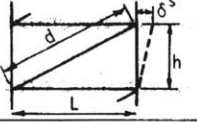
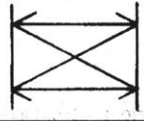
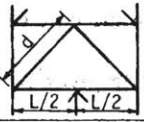
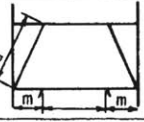
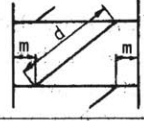
$$\begin{aligned}\delta_{iF} &= h_i \theta_{iF} \\ \Delta_{nF} &= \sum_1^N \delta_{iF}\end{aligned}\tag{4-2) [1]}$$

where:

- δ_{iF} - story drift due to flexure
- Δ_{nF} - deflection due to flexure
- h_i - story height
- θ_{iF} - rotation of story i which is equal to area under M/EI curve
(subscript F referring to terms related to flexure)

The shear component of deformation is a function of the type of bracing used and the shear carried in that story. This is given in Table 4 - 1 where the shear deflection of various bracing layouts are given. The top story drift, as a result of shear deflection, is thus the sum of all inter-story drifts beneath that floor.

Table 4 - 1: Shear Rigidity of Different Bracing Schemes

TABLE 6.1 Braced Bents: Shear Deflection per Story		
TYPE OF BRACING	DIMENSIONS	SHEAR DEFLECTION PER STORY
SINGLE DIAGONAL		$\delta^S = \frac{Q}{E} \left(\frac{d^3}{L^2 A_d} + \frac{L}{A_g} \right)$
DOUBLE DIAGONAL		$\delta^S = \frac{Q}{2E} \left(\frac{d^3}{L^2 A_d} \right)$
K-BRACE		$\delta^S = \frac{Q}{E} \left(\frac{2d^3}{L^2 A_d} + \frac{L}{4A_g} \right)$
STORY HEIGHT KNEE-BRACE		$\delta^S = \frac{Q}{E} \left(\frac{d^3}{2m^2 A_d} + \frac{m}{2A_g} + \frac{h^2 (L-2m)^2}{12I_g L} \right)$
OFFSET DIAGONAL		$\delta^S = \frac{Q}{E} \left(\frac{d^3}{(L-2m)^2 A_d} + \frac{(L-2m)}{A_g} + \frac{h^2 m^2}{3I_g L} \right)$

Q is the story shear
 A_d is the sectional area of a diagonal
 A_g and I_g are, respectively, the sectional area and inertia of the upper girder
 E is the elastic modulus

$$\Delta_{ns} = \sum_1^N \delta_{is} \quad (4-3) [1]$$

where:

Δ_{ns} - deflection due to shear

δ_{is} - story drift due to shear

4.3 SAP Model (Braced Frame)

Four braced frame models were studied in SAP, each illustrating a specific aspect of braced frame structural behavior. The four models comprised two thirty story models and two forty story models. The thirty story models were used to study the effects of different bracing schemes. In one model, bracing was only built in a single bay but in the other, bracing was installed across three bays. This gave rise to a much “deeper” vertical truss which gave the

structure significantly more stiffness. It is important to note that in this height/aspect ratio range, the key concern is no longer strength design but stiffness that resulted from the need to control top story drift.

The two forty story models were used to analyze the interaction between the moment frame and the braced frame. As previously mentioned, the two frames deform in different modes but compatibility is ensured due to rigid floor slabs. This different deformation modes result a distribution of lateral loads that is not immediately apparent.

4.3.1 30 Story Braced Frame Models

The two braced frame models considered are shown in Figure 4 - 7 and Figure 4 - 8. The columns were initially sized on a strength basis in sets of five stories. This was adapted from the strength design of columns conducted in Chapter 3 where columns were sized for strength capacity in moment frame action. The loadings on the structure were the nodal forces computed in Chapter 2 during the establishment of wind loading.

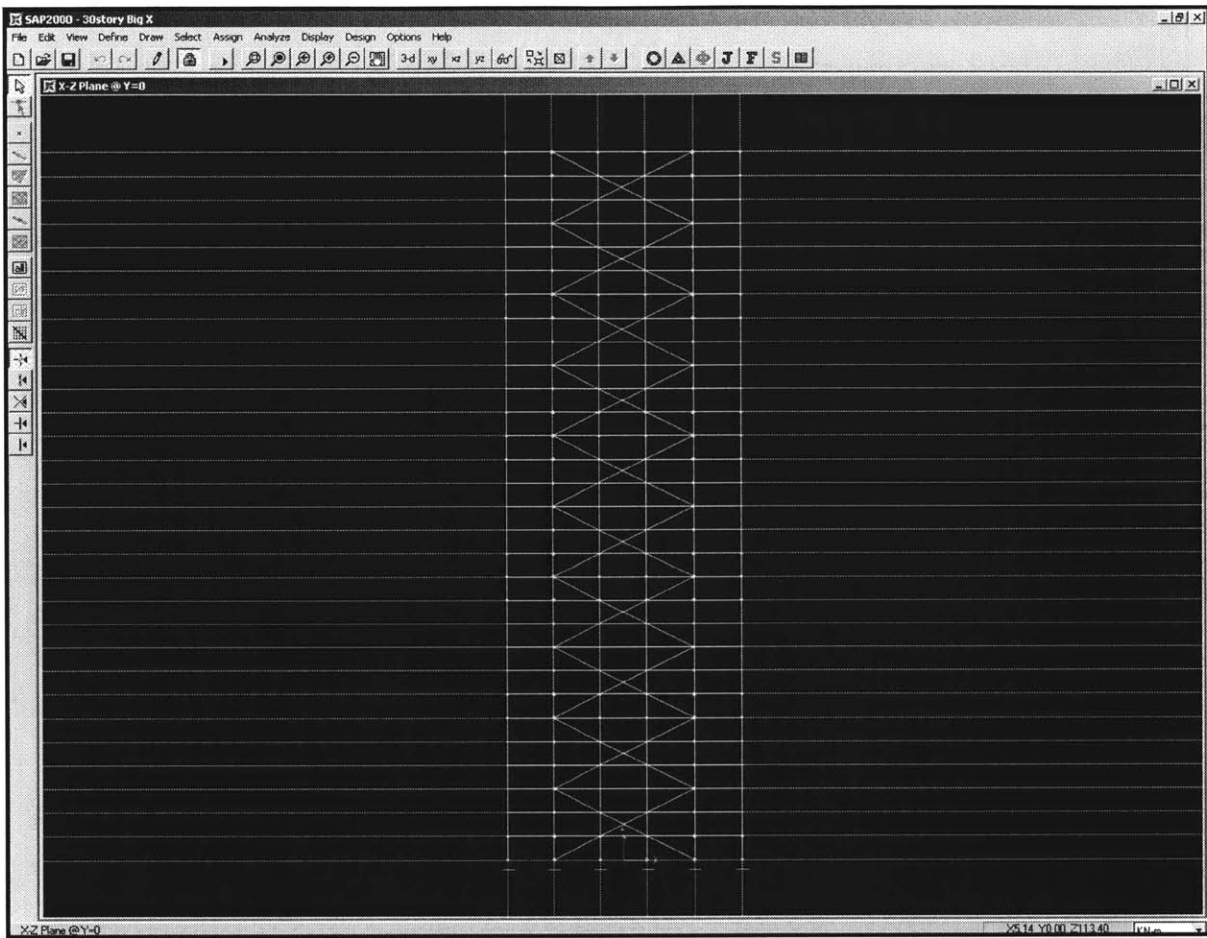


Figure 4 - 7: 3 Bay Braced Frame

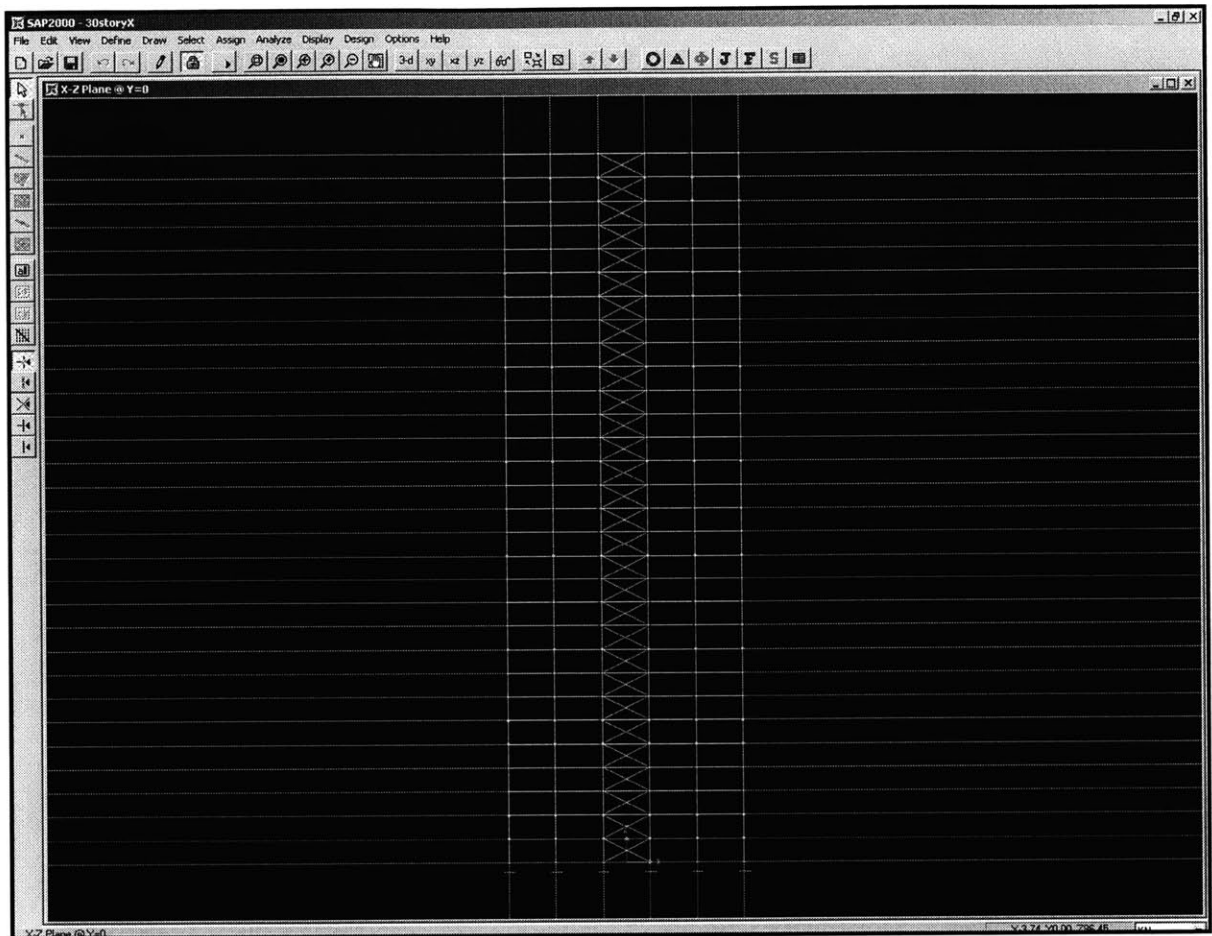


Figure 4 - 8: Single Bay Braced Frame

4.3.1.1 *Force Analysis (SAP Model)*

An analysis of how the lateral loads were carried in the structure was performed to investigate how the lateral forces were distributed between the bracing and frame elements. This was carried out at the base of the structure. This location allowed the verification of the SAP results against the expected base shear (2425kN) and also against the expected displacement and force distribution. This distribution is tabulated in Table 4 - 2. Three models were run. They were the models illustrated in Figure 4 - 7 and Figure 4 - 8. The single bay braced model (Figure 4 - 8) was run twice with the cross-sectional area of the base columns modified upwards (model 4). This was done to remove the presence of axial deformation which was speculated to cause the significant deviation from the theoretical results.

Table 4 - 2: Distribution of Lateral Forces in Braced Frames

Bracing Analysis (SAP Results)					
		Model 2	Model 3	Model 4	Model 1
		3 Bay Bracing	Single Bay Bracing	Single Bay Bracing 2	Moment Frame
Base Columns (Shear Force) (kN)	Column No. 1	82	61	54	336
	2	102	87	72	441
	3	97	72	66	439
	4	96	72	65	
	5	100	85	71	
	6	80	58	53	
Shear Total (kN)		557	435	381	2432
Bracing Diagonal (Axial) (kN)		1861	1984	2040	
Total Lateral Force (kN)		2418	2420	2421	
% resisted in shear action		23%	18%	16%	100%
% resisted in axial action		77%	82%	84%	
SAP Model Lateral Displacement (m)		3.49 E-3	4.06 E-3	3.26 E-3	
SAP Model Vertical Displacement (m)		-7.01 E-4	1.23 E-3	3.38 E-4	
% Difference from Theoretical (Displacement)			29.75	-0.29	
% Difference from Theoretical (Shear Dist)			-15.94	-13.64	
Theoretical Results (Single Bay Bracing)					
Base Shear (kN)		2425			
Bracing Shear Rigidity (kN/γ)		2.86E6			
Frame Shear Rigidity (kN/γ)		103,929			
Total Structure Shear Rigidity (kN/γ)		2.933 E6			
Expected Shear Deformation (γ)		8.27E-4			
Expected Shear Displacement (m)		2.89E-3			
Braced Bay Moment of Inertia (m ⁴)		1.47E8			
Expected Bending Displacement (m)		2.36E-4			
Total Expected Displacement (m)		3.13E-3			
Expected % of Shear Carried in Axial		98%			

It is expected that the diagonal elements should provide the same degree of shear rigidity regardless of location within the story. Thus, in the SAP models, the degree of shear carried by the bracing diagonals should be the same regardless of layout. However, as it is seen, this is not the case. A small variance in the distribution of shear force (between the diagonal and columns) and also the horizontal displacements was seen between the models. A variance was also seen between the theoretical shear force distribution (computed by calculating the shear rigidity of the columns and diagonals) and the results reported by SAP. This variance in results both between the models and from the theoretical results was speculated to be due to the omission of axial deformation that was assumed in the theoretical calculations. An indication of this was the magnitude of vertical displacements in Model 3 that was the same order of magnitude as the horizontal displacements. The assumption of small axial deformations in the theoretical calculations was thus not a good one. This was the basis of running Model 4 (refer Table 4 - 2) with the modified column cross sectional areas.

In Model 4 (refer Table 4 - 2), the axial stiffness of the columns was increased to remove the presence of axial deformation and it is noticed that the displacement results are closer to the expected theoretical displacements. This can be contrasted to Model 3 (refer Table 4 - 2) where the element's stiffness was unmodified and the force distributions and displacements differ more from the expected values. However, the distribution of shear forces between the columns and diagonals in both models was far from the expected theoretical results. It is thus imperative for the engineer to understand the limitations of hand calculations and the results obtained from computer analysis. As it is seen here, neither approach provides the perfect answer but rather serves as a guide for the engineer. Complete calculations of the structure's shear and bending rigidity are shown in Appendix D.

4.3.1.2 Structural Efficiency of Braced Frames

A steel volume comparison was done for the two thirty story structures modeled here and the two moment frames analyzed previously. The four models are the strength based and stiffness based moment frames and the two bracing schemes looked at in this chapter. The volume of steel in each situation was tabulated in Table 4 - 3 and plotted below in Figure 4 - 9. Results were similarly normalized to the ten story moment frame steel volume of 8.74m^3 .

It is immediately apparent that braced frames incur a small cost in terms of steel tonnage for additional height. This explains why large scale braced frames such as those illustrated in Figure 4 - 2 and Figure 4 - 2 were employed in those tall structures. For example, the John Hancock Center is an extremely efficient structure utilizing 29.7psf of steel and this is especially remarkable given its aspect ratio of 7.9.

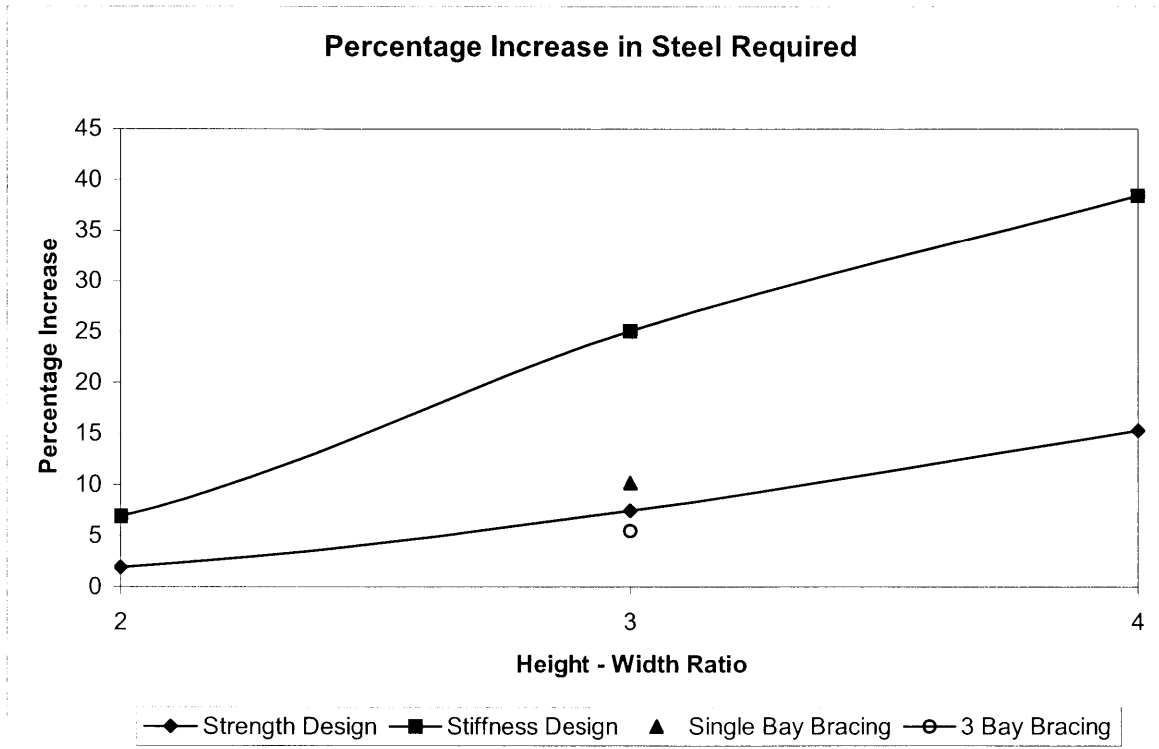


Figure 4 - 9: Comparison of Steel Volume Required

Table 4 - 3: Comparison of Steel Volumes Required

				Moment Frames		Braced Frames	
Stories	Height (m)	Aspect Ratio	Deflection Criteria (m)	Strength Based Steel Volume (m ³)	Stiffness Based Steel Volume (m ³)	Single Bay Bracing	3 Bay Wide Bracing
30	105	3	0.21	65.3	219	88.79	47.87
Normalized Steel Volume				7.47	25.06	10.16	5.48

4.3.1.3 Virtual Work Drift Optimization

With the members sized, the SAP model was run and the drift was analyzed. On the first run, drift in both models proved to be excessive and the virtual work optimization analysis as described in Chapter 3 was carried out. The output is shown in Figure 4 - 10. It is immediately observed that the diagonal bracing elements play a significant role in controlling the drift of the structure. Another observation from this diagram which is not readily apparent from cursory observation is the moment induced in the girders immediately adjacent to the braced bay.

From the virtual work diagram, three locations are identified to minimize top story drift. They are at the columns of the braced bay especially at the base where a large percentage of the resisting moment is generated and also within the webs of the braced bay. These two locations are seen to comprise a large percentage of the virtual work. The other location identified to minimize drift is the girders immediately adjacent to the braced bay. They are also seen to comprise a large percentage of the virtual work. Minimization of joint rotation at these locations is thus key in reducing the top story drift. These insights were used in the drift reduction of the structure after the strength based element design was carried out.

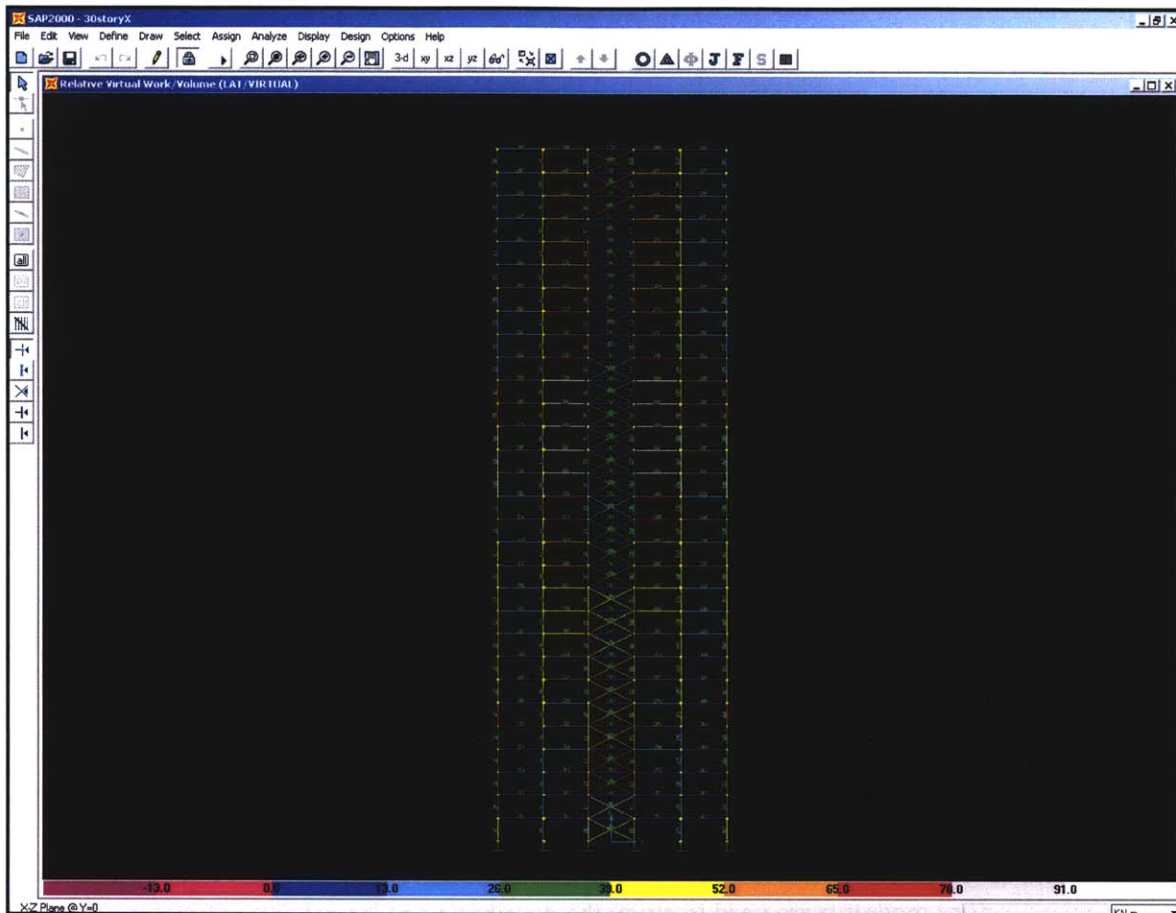


Figure 4 - 10: 3 Bay Bracing Virtual Work Drift Optimization

4.3.1.4 *Displacement Profile*

The displacement profile for the two braced frames are illustrated in Figure 4 - 11. They are contrasted against the moment frame displacement profile. It is immediately observed that the braced frames are stiffer than the stiffness designed moment frame. Another difference between the displacement profiles is the gradual decrease in inter-story drift towards the top of the moment frame. This gives the curve a concave shape and this is attributed to the reduction in story shear towards the top of the structure while a braced frame is observed to have a generally constant inter-story displacement.

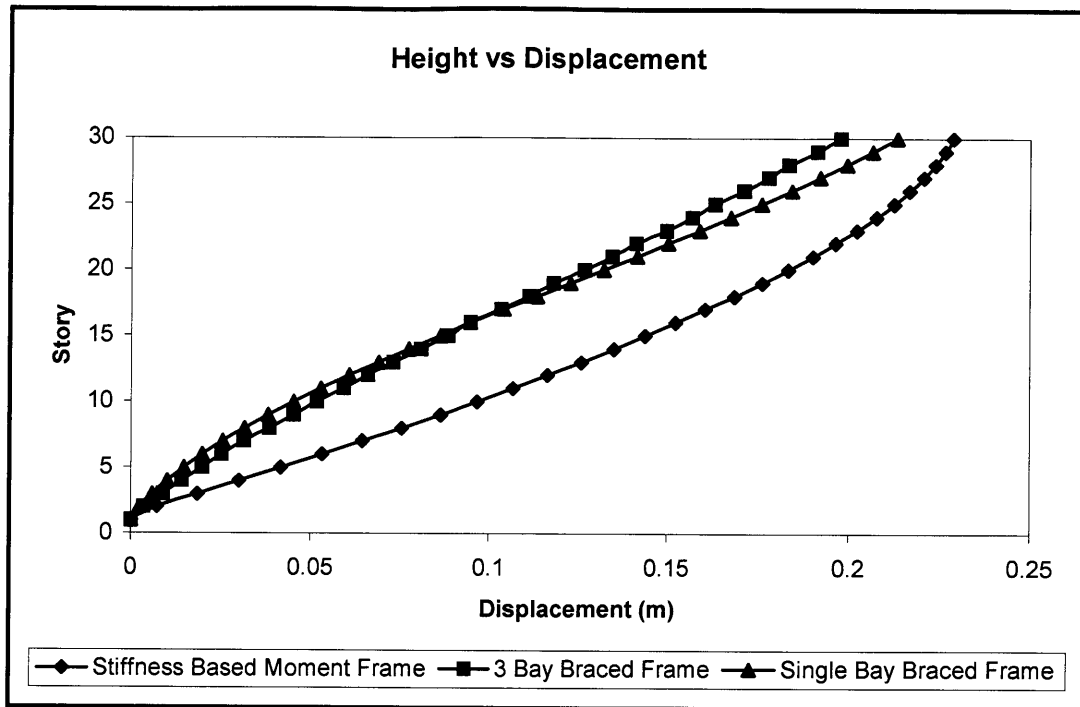


Figure 4 - 11: Displacement Profile (Braced Frame)

4.3.2 40 Story Braced Frame Models

Two 40 story models were used to study the distribution of lateral forces between the moment frame and the bracing. These models also provided a platform to analyze the distribution of shear forces across stories in a braced frame. This shear distribution differs from one of a moment frame due to the redistributive effects of the bracing elements.

As previously mentioned, the moment frame deforms in the shear mode of deflection while the bracing is assumed to deform in flexure only. Compatibility between the two modes at each story is ensured through the rigid floor slab. This behavior results in a distribution of lateral forces which is of interest in this section.

One model comprised of a complete moment frame with three bay wide bracing integrated into the model and the other was built with the moment frame separate from the braced bays. The purpose of this separated model was to isolate the individual deformation effects of each lateral system (moment frame and cantilever truss). These models are illustrated in Figure 4 - 12 and Figure 4 - 13. In the separated model, the elements connecting the moment

frame on the left and the braced bays on the right are pure axial members, which ensures no transfer of moment from one section to another.

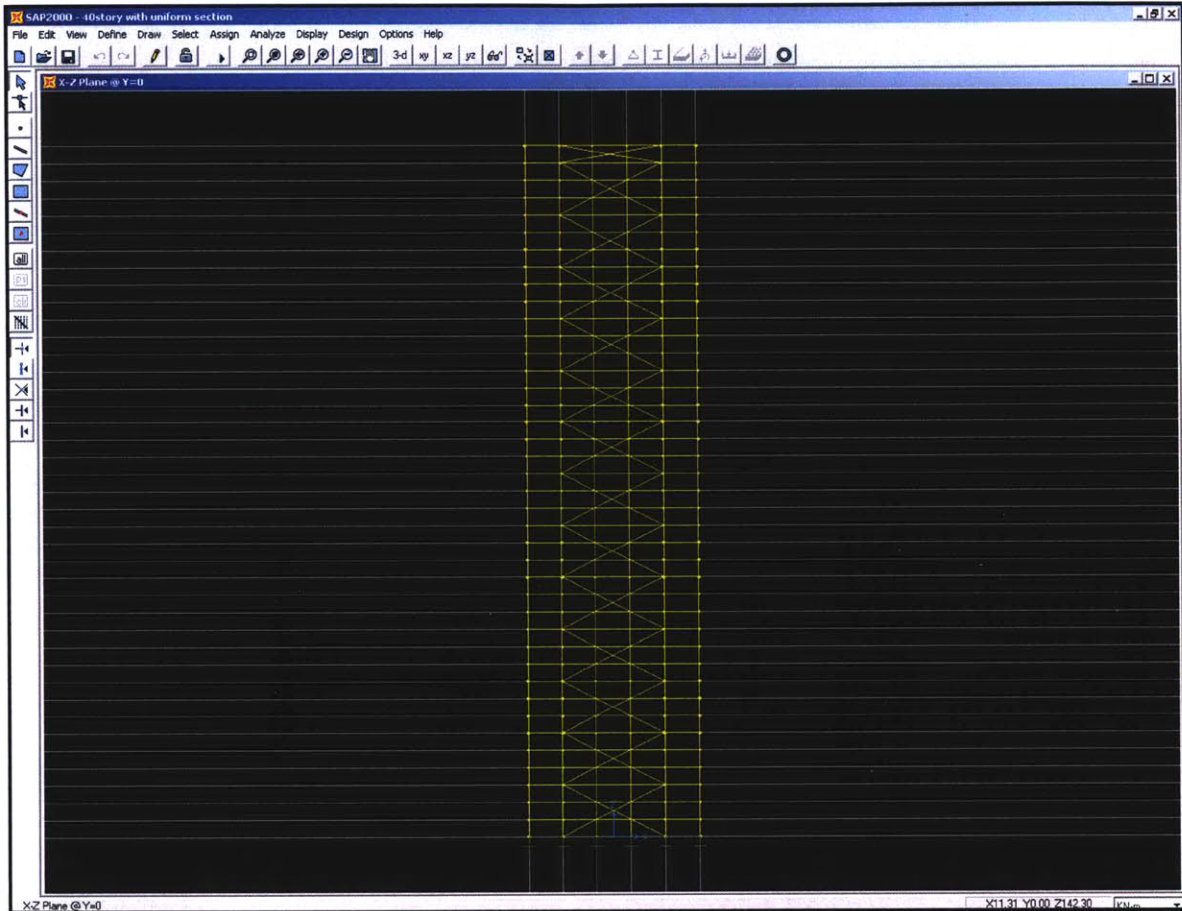


Figure 4 - 12: 40 Story Integrated Model

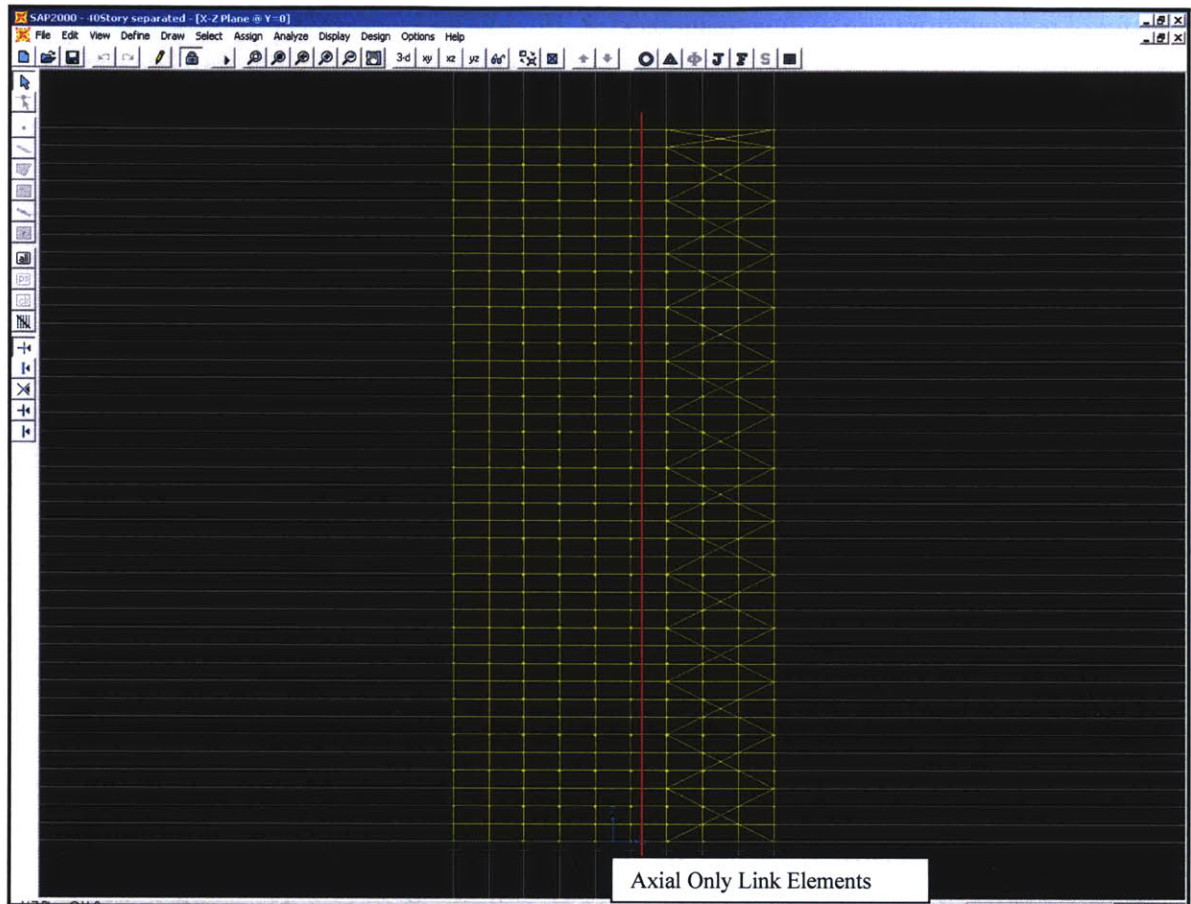


Figure 4 - 13: 40 Story Separated Model

4.3.2.1 *SAP MODEL*

The following assumptions were made in order to establish and follow previous studies on the interaction between moment frames and braced bays.

1. A uniform section for the moment frame and brace bays is present.
2. The moment frame deforms mainly in shear and the braced bays deforms mainly in flexure.
3. The connecting members transfer only axial forces.
4. The structure was laterally loaded uniformly.

In order to simplify the analysis, a uniform lateral load was assumed. The total lateral loads for a forty story structure was assumed to be uniformly distributed along the face of the structure. The loading value was found to be 26kN/m.

The line in Figure 4 - 13 denotes the axial only members which ensured only axial forces were transferred to the braced frame. This was accomplished by modifying downwards the moments of inertia of the link elements.

In the SAP models, the deformation modes of the moment frame and the braced bay were ensured to be bending and flexure respectively. It was sought that the moment frame deform only in the shear mode and this was achieved by the frame's inherent high shear rigidity and low flexural resistance. However, in order to ensure that the braced bay deformed only in flexure, the shear rigidity of the braced bay had to be modified downwards. The moment of inertias of the individual members was modified downwards to reduce the shear rigidity of the braced bay to ensure only flexural deformation.

4.3.2.2 Theoretical Shear Force Distributions

The equation for the shear force carried by the braced bay at any height (z) is given by equation 4-3 [1].

$$Q_b = -wH \left\{ \frac{1}{\alpha H} \left[\frac{(\alpha H \sinh(\alpha H) + 1)}{\cosh(\alpha H)} \sinh(\alpha z) - \alpha H \cosh(\alpha z) \right] \right\} \quad (4-3, 4-4)$$

$$Q_s = w(H - z) - Q_b(z)$$

where:

Q_b	-	Shear carried braced bay
Q_s	-	Shear carried in frame
w	-	Uniform external loading
α^2	-	(GA)/EI
z	-	Height along structure
H	-	Total height of structure
GA	-	Shear rigidity of frame
EI	-	Flexural rigidity of braced bay

The shear force carried by the moment frame is difference between the story shear and the shear force carried by the braced bay. These equations give the following insights into the distribution of shear forces in the structure.

The key parameters that determine the shear force in the braced bay is (αH) and (z/H) . Therefore, it is possible to manipulate the forces carried in the braced bay and moment frame by adjusting these parameters. An approximate constant story shear is sought for the moment frame as this allows small section changes from floor to floor and also the repetition of floor systems. This optimization is studied below.

The Equations in 4 - 3 and 4 - 4 allow for the following observations. At the top of the structure, although the applied lateral force is zero, the braced bay and moment frame carry a shear force that is equal and opposite to each other while being non-zero. This non-zero shear force at the top of the structure results from the non-zero deflected shape and gives rise to an associated shear in the braced bay. Because the external lateral load applied is zero, this shear has to be equilibrated by a shear force opposite in direction. In the SAP model, this is demonstrated by a non-zero axial force in the top most link element.

The theoretical lateral force carried by the moment frame at the base of the structure is zero. This arises from the zero slope at the base of the braced bay. However, it is known that this is not true because the first story is displaced and therefore shear forces must be present in the first set of columns. This is also verified in the SAP model.

4.3.2.3 Optimization of Theoretical Shear Force Distributions

With the above considerations, it is now possible to analyze the theoretical and SAP modeled shear force distributions. A graph of the theoretical shear force distributions obtained from the evaluation of Equations 4-3 and 4-4 is shown in Figure 4 - 14.

With the original element sections, it was possible to calculate the parameters GA and EI as defined before. The results as shown illustrate a high degree of non-uniformity and a point of inflexion in the graph.

A parametric study of the variation of αH had on the distribution was carried out. It was observed that as α decreased, the average frame shear force decreased and there was less variance in the distribution. However, this was found to be a continuously decreasing function

which implied the limit occurred when the frame had zero shear rigidity and all lateral load was carried by the braced bay. This is obviously unrealistic. However, this parametric study was not in vain. Given that decreasing α had a positive effect on the frame shear force distribution, the design process was then to decrease α until a reasonable distribution in frame shear forces was achieved.

With a value of $\alpha = 0.004$, the distribution shown by the blue graph was obtained. It is immediately observed that the average frame shear force had decreased and also had less variance in it. The average values of frame shear forces and its associated standard deviations are tabulated in Table 4 - 4. Complete calculations are shown in Appendix D.

It would be naturally more efficient to design the frame with fairly uniform sections throughout its height and the theoretical shear force distribution shown by the optimized graph is more likely to allow this than the unoptimized shear force distribution. The distributions are shown in Figure 4 - 14.

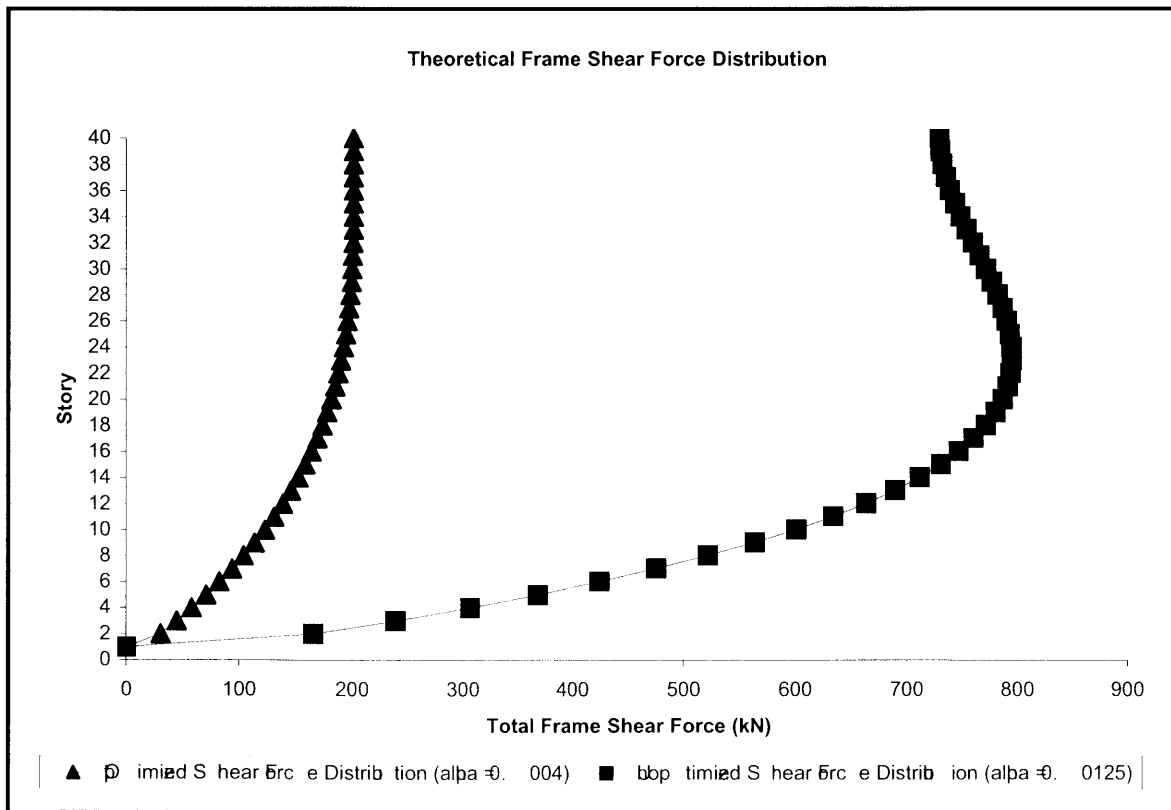


Figure 4 - 14: Theoretical Shear Force Distribution

Table 4 - 4: Theoretical Average Frame Shear Force and Standard Deviation

Model (Theoretical Calculations)	Average Shear Force (kN)	Standard Deviation
Unoptimized (alpha = 0.0125)	657	196
Optimized (alpha = 0.004)	157	56

4.3.2.4 *Optimized Shear Force Distribution (SAP Model)*

The theoretical frame behavior was carried over to the SAP model and a reduction of α was sought. This was achieved by decreasing the shear rigidity of the frame. The primary “most efficient” manner to do so was to reduce the moment of inertias of the frame girders as they have been demonstrated in Chapter 3 and earlier in this chapter to be the key parameter in affecting frame shear rigidity.

The results of this shear rigidity reduction are shown in Figure 4 - 15. Three graphs are plotted, the original complete braced frame model and the two separated models with and without optimization. The optimized model performed as anticipated with a reduction in the average frame shear carried with a smaller variance. Exact data of these distributions are shown in Table 4 - 5.

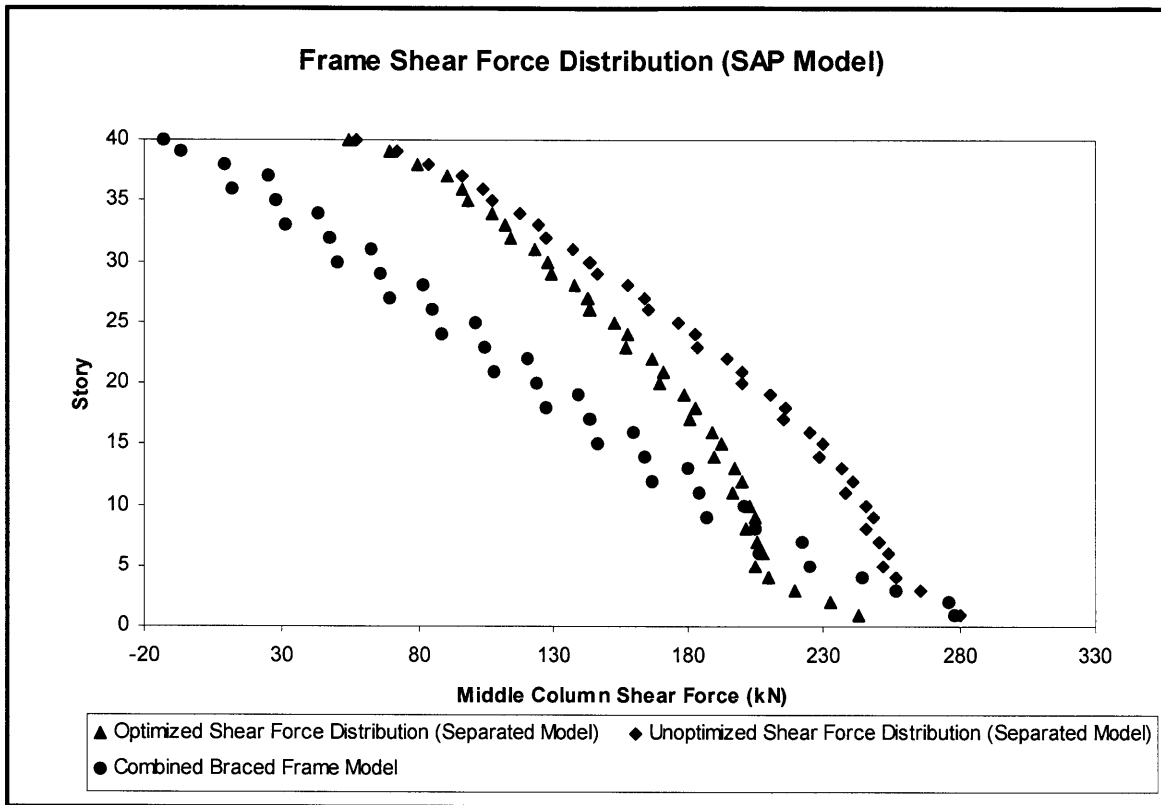


Figure 4 - 15: Shear Force Distribution

Table 4 - 5: Average Shear Force and Standard Deviation

Model (SAP Model)	Average Shear Force (kN)	Standard Deviation
Combined Braced Frame Model	124	81
Unoptimized Separated Model (alpha = 0.0125)	189	61
Optimized Separated Model (alpha = 0.004)	160	47

4.3.3 Virtual Work Drift Optimization

The SAP analysis was concluded with a virtual work drift optimization. This model, like before, illustrated the locations to add material in order to reduce top story drift. It is noticed from Figure 4 - 16 that the optimum locations to introduce material into the structure was in the diagonal elements of the braced bay. This is to be expected since loads are more efficiently carried axially than in bending and force should be “directed” to those elements.

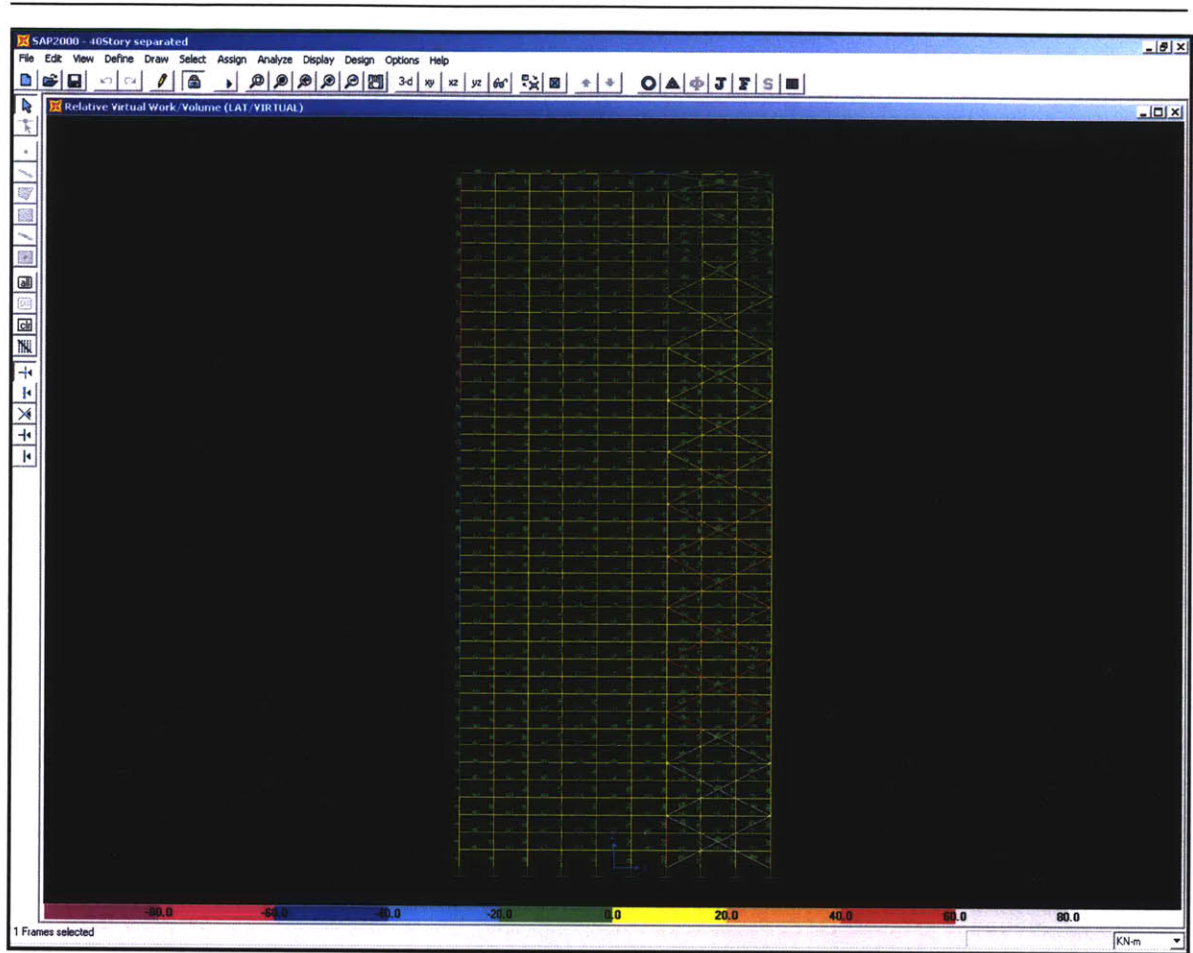


Figure 4 - 16: Virtual Work Diagram (Separated Model)

Upon increasing the cross sectional areas of the bracing elements, Figure 4 - 17 was obtained. It is immediately noticed that an almost uniform virtual work percentage is achieved. Larger images are shown in Appendix D.

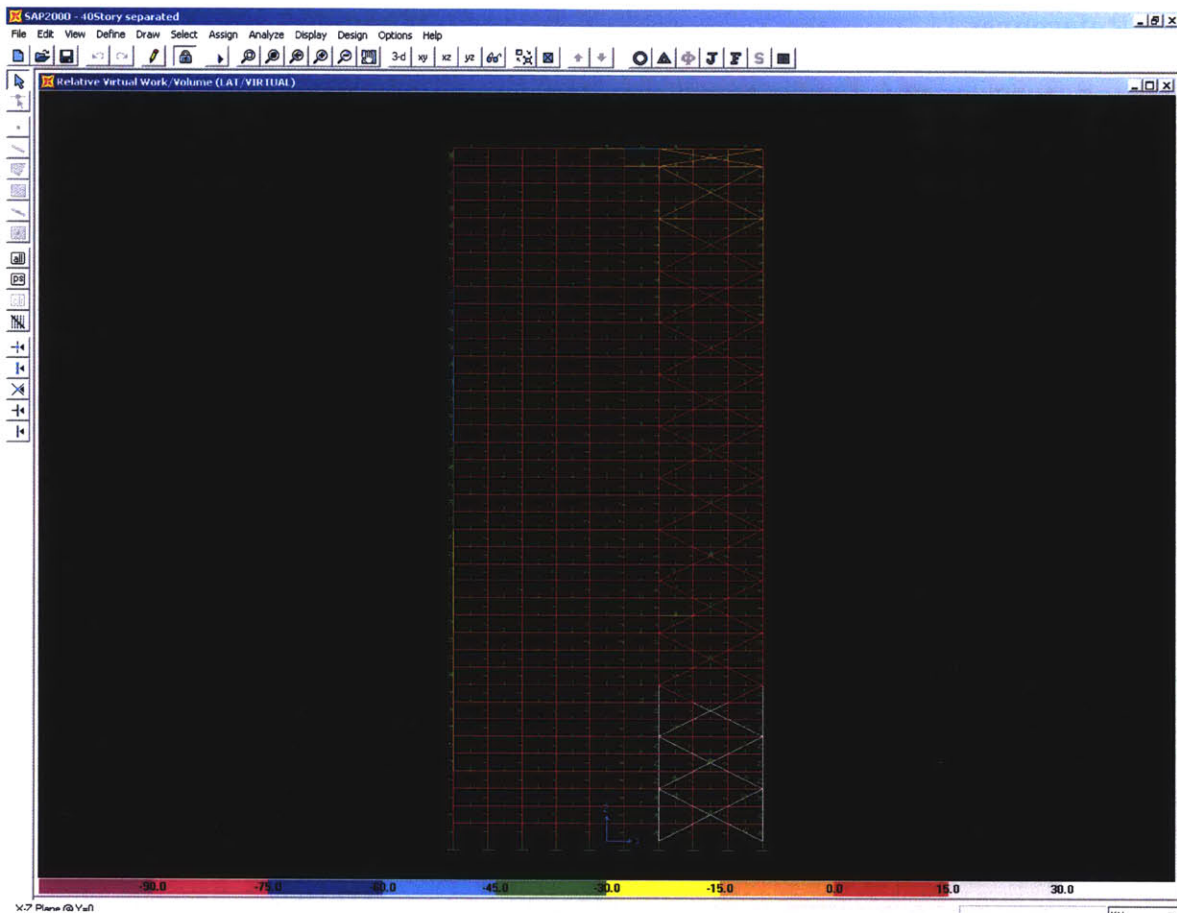


Figure 4 - 17: Virtual Work Diagram with Increased Bracing Cross Sectional Area

4.4 Conclusion (Braced Frame)

This chapter explored a lateral system greatly favored by structural engineers, the braced frame. The resistance of lateral loads through axial action as opposed to bending has been demonstrated to be significantly more efficient. With the introduction of diagonal elements, the braced bay analyzed was illustrated to be resisting the majority of the lateral loads. This was shown through the virtual work optimization process.

It was also illustrated that it is possible to calibrate the stiffness of the braced bay to allow for a fairly uniform story shear in the moment frame. Uniformity in forces allows a uniformity in sections selected and also corresponding gains in construction efficiency. In Chapter 5, an extension of the braced frame that is the braced frame with outriggers will be explored.

4.5 References

- [1] B. S. Smith and A. Coull, Tall Building Structures: Analysis and Design, New York: John Wiley & Sons, Inc, 1991.
- [2] www.emporis.com
- [3] www.som.com
- [4] B. Taranath, Structural Analysis & Design of Tall Buildings, New York: McGraw-Hill Book Company, 1988.
- [5] W. Schueller, The Vertical Building Structure, New York: Van Nostrand Reinhold, 1990.

5 Chapter 5: Braced Frames with Outriggers

5.1 Braced Frame with Outriggers

In the vein of trying to achieve structural efficiency for a building's lateral system, it is widely known that the larger the section of a building that can be mobilized for lateral resistance, the more efficient the building will be from a structural engineering standpoint. A scheme which is less architecturally intrusive than large scale bracing is a braced frame with outriggers.

A braced frame with outriggers consists of a rigid core or a braced bay with deep truss sections connecting the core to perimeter columns. Illustrated in Figure 5 - 1 and Figure 5 - 2 are two buildings which utilize outrigger schemes in its lateral system. The presence of this scheme is clearly evident to a structural engineer on observation of the "obstructed" story high sections that run around the perimeter of the building. These obstructions hint towards the presence of story deep sections which attach the core to the perimeter columns.

A clear advantage of an outrigger scheme is that the structure does not impose itself on spatial programming requirements. The only location where the structure affects the interior space is where the story deep truss sections are located. However, these sections are most often located at plant levels and thus have minimal impact on the interior space. Early co-ordination between the HVAC team and the structural engineering team is thus critical for optimization of the structure. It will be illustrated later that the relative stiffness of the outrigger and core is a critical parameter in its location.

Another advantage of this scheme that is common to all designs where the lateral system is isolated from the gravity system is that it allows relative separation of design between the gravity and lateral system. This also allows repetition in floor framing which is a feature much desired by contractors and engineers. Repetition allows simplified analysis and ease of construction.

This chapter will study the optimum location of outriggers along the height of the structure, the efficiency of the scheme from a steel volume standpoint and also the displacement profile which is expected.



Figure 5 - 1: US Bank Center (Milwaukee) [1]



Figure 5 - 2: Villa Olimpica (Barcelona, Spain) [1]

5.2 Structural Analysis

The key structural feature of an outrigger braced frame is that the perimeter columns are engaged in resisting the lateral loads applied to the structure. This engagement significantly increases the effective width of the structure and therefore results in large increases in the structure's stiffness. The extent to which the perimeter columns are engaged depends highly on the outrigger's flexural and shear stiffness. In essence, the less deformation the outrigger undergoes during lateral loading the more compositely the structure will behave. In full composite structural behavior, the stresses in the columns parallel to the loading (webs) are proportionate to its distance from the structure's center of mass.

5.2.1 Governing Equations

For simplicity during the preliminary structural analysis of the building, the following assumptions are made.

1. Sectional properties of the core, columns and outriggers are uniform throughout the height of the structure.
2. The outriggers are rigidly attached to the core and the core is rigidly attached to the foundation. This implies a transfer of moment at these locations.
3. Only axial forces are induced in the perimeter columns.

The following equations [2] 5-1 to 5-4 result from compatibility applied at the core outrigger joint. The structure has been solved for a two outrigger system ignoring the shear deformation of the outrigger. Hoenderkamp and Bakker (2003) solved for the optimum location of outriggers taking into account the shear deformation of the outriggers.

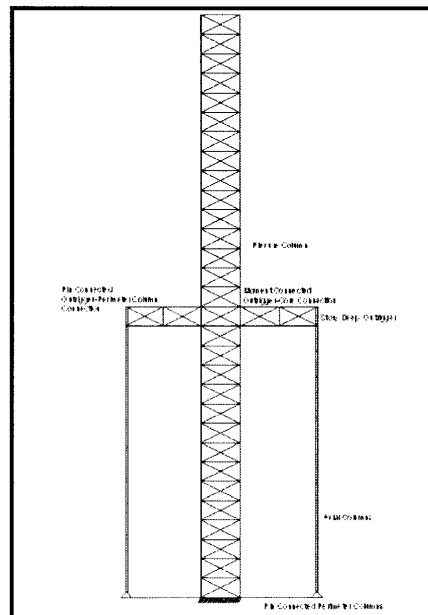


Figure 5 - 3: Structural Model

$$M_1 = \frac{w}{6EI} \left[\frac{S_1(H^3 - x_1^3) + S(H - x_2)(x_2^3 - x_1^3)}{S_1^2 + S_1S(2H - x_1 - x_2) + S^2(H - x_2)(x_2 - x_1)} \right] \quad (5-1)$$

$$M_2 = \frac{w}{6EI} \left[\frac{S_1(H^3 - x_2^3) + S \left[(H - x_1)(H^3 - x_2^3) - (H - x_2)(H^3 - x_1^3) \right]}{S_1^2 + S_1 S (2H - x_1 - x_2) + S^2 (H - x_2)(x_2 - x_1)} \right] \quad (5-2)$$

$$M_x = \frac{wx^2}{2} - M_1 - M_2 \quad (5-3)$$

$$\Delta_o = \frac{wH^4}{8EI} - \frac{1}{2EI} \left[M_1(H^2 - x_1^2) + M_2(H^2 - x_2^2) \right] \quad (5-4)$$

where:

w = uniform lateral loading applied on structure

$$S = \frac{1}{EI} + \frac{2}{d^2(EA)_c}$$

$$S_1 = \frac{d}{12(EI)_o}$$

$$EI_o = \left(1 + \frac{a}{b}\right)^3 (EI')$$

EI' = flexural rigidity of outrigger

a = half width of braced bay

b = distance from end of braced bay to perimeter column

d = distance from perimeter column to centroid of braced bay

With the above equations, it is possible to minimize the top story drift in the structure by maximizing the second term in equation 5-4 with respect to x_1 and x_2 . The minimization can be simplified and found to depend on the following parameters [2].

$$\alpha = \frac{EI}{(EA)_c \left(\frac{d^2}{2} \right)} \quad (5-5)$$

$$\beta = \frac{EI}{(EI)_o} \frac{d}{H} \quad (5-6)$$

$$\omega = \frac{\beta}{12(1 + \alpha)} \quad (5-7)$$

where:

- α - represents ratio of the core to column rigidities
- β - represents ratio of the core to outrigger rigidities
- ω - characteristic structural parameter for uniform structure with flexible outriggers

The term ω is a dimensionless parameter that captures the structural characteristic of a uniform core with flexible outriggers installed and its value determines the optimum location for a outrigger braced frame structure. Two general trends are observed. The value of ω decreases as the outrigger's flexural stiffness increases and increases as the axial stiffness of the perimeter columns increases. The optimum location of the outriggers for drift control is thus found to depend on these two factors.

5.2.2 Optimum Location of Outriggers

The graph in Figure 5 - 4 allows the easy identification of the optimum locations of single and double outrigger structures for drift reduction. For a single relatively stiff outrigger, the optimum location for drift reduction is approximately at mid-height of the structure. This is not readily apparent from inspection where it might be expected that the optimum location of a single outrigger to be at the top of the structure.

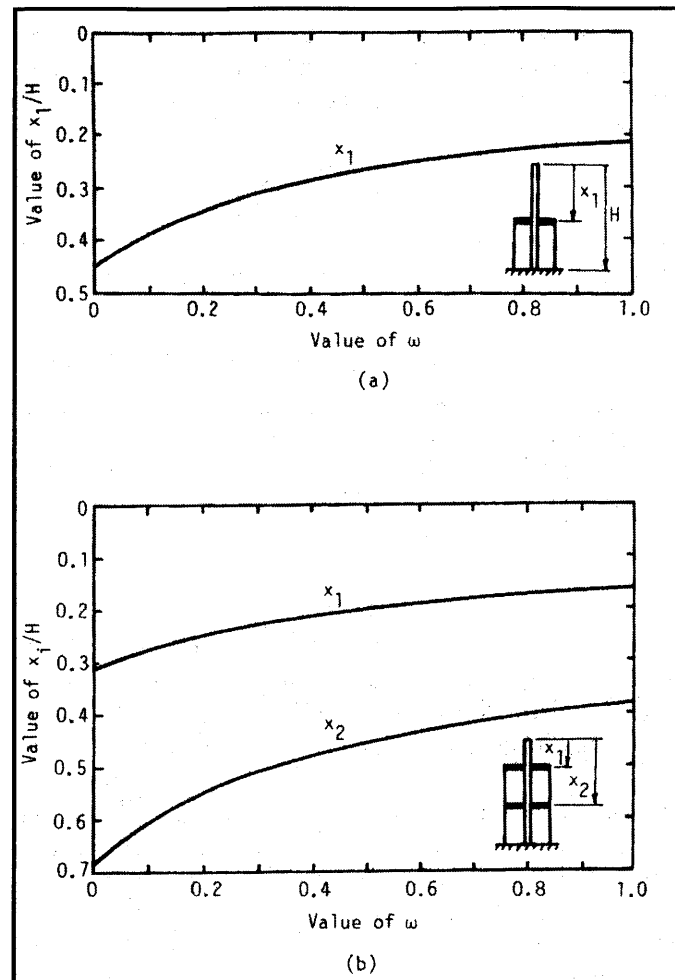


Figure 5 - 4: Optimum location of outrigger [2]

5.3 SAP Models (Braced Frame with Outriggers)

Forty story planar SAP models were built to study the optimum locations of outrigger structures. The design criteria in these models similar to those in tall braced frames was top story drift. The structural efficiency of scheme was also studied and the steel volume required was compared against volumes required for other lateral schemes.

The initial element dimensions were taken from the strength based braced frame design with a loading of 26kN/m applied uniformly over the core.

5.3.1 Optimum Location

A simplified SAP model was used to study the results of the proposed structural model. The model comprised only the perimeter columns and the braced core. The SAP model is illustrated in Figure 5 - 5. In order to accurately model the theoretical structural model proposed before, the bases of the perimeter columns were pin supported. Also, the outer connection between the perimeter column and outrigger truss was pin connected. This ensured no moment was created in the columns. The inner connections between the outrigger truss and core was moment connected. This causes the outrigger to bend in double curvature illustrated in Figure 5 - 6. This moment connection leads to a reduction in the moments at the base of the core structure which will be analyzed later.

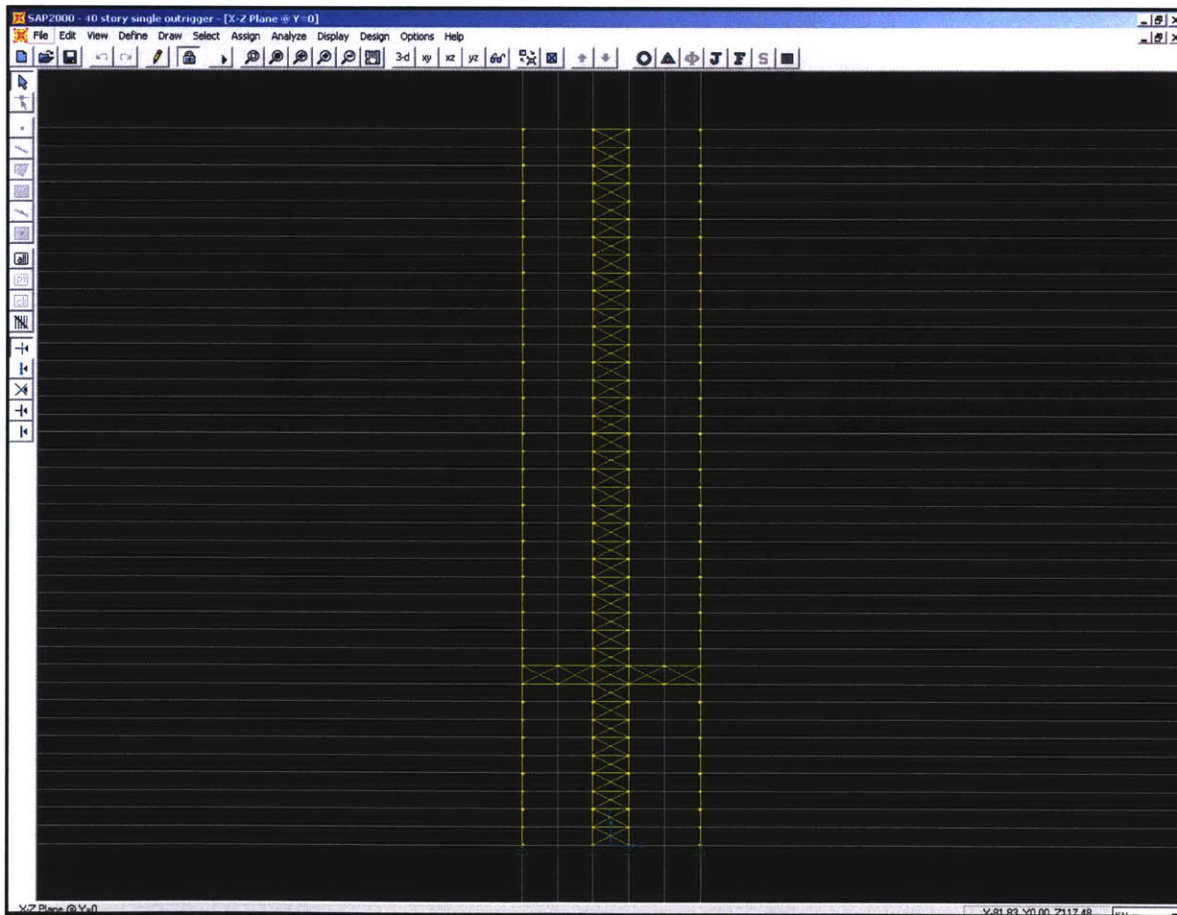


Figure 5 - 5: SAP Outrigger Model

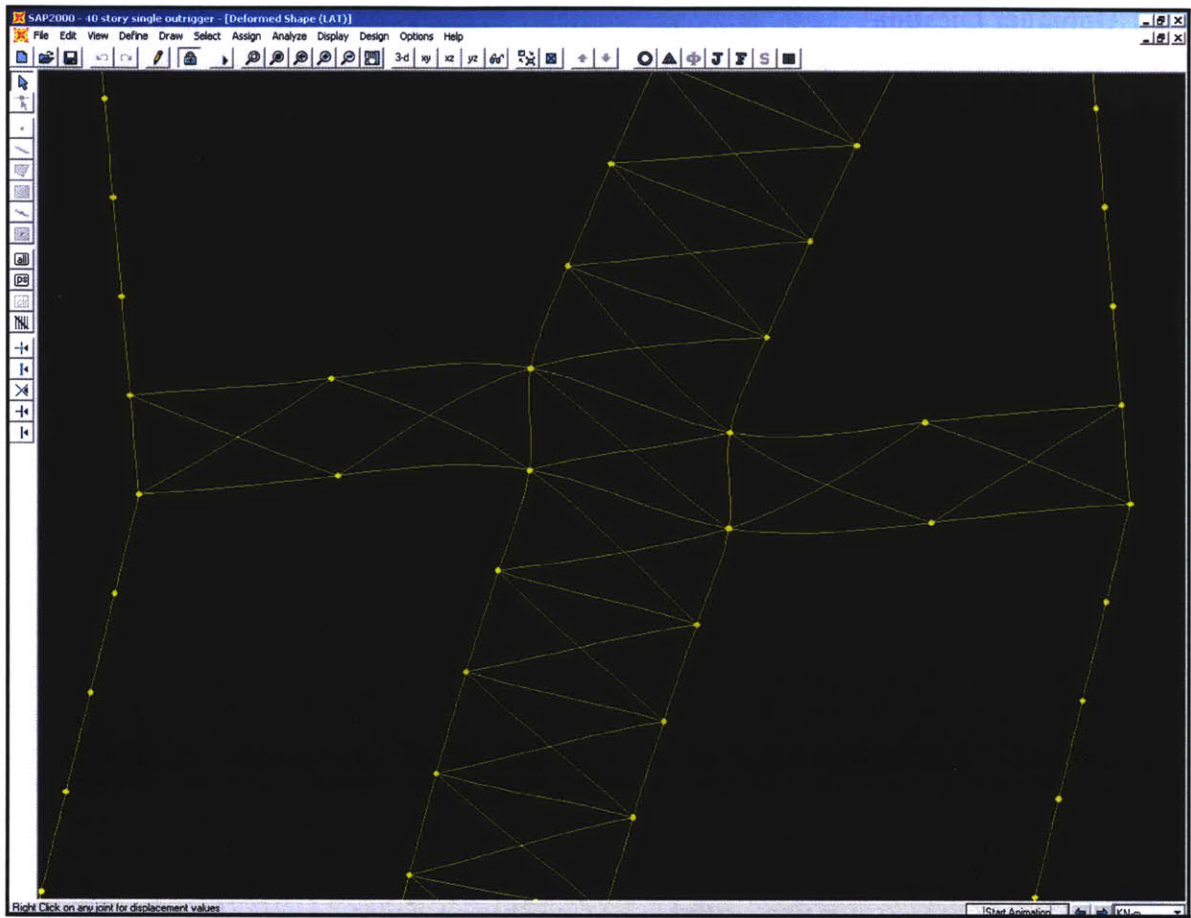


Figure 5 - 6: Deformed Outrigger Shape

Included in appendix E are the calculations of the various parameters needed to compute ω in order to determine the optimum location of the outrigger. For the SAP model with the strength based design sections, the value of ω was found to be 0.034. This implied that the optimum location of the outrigger should be at mid-height of the structure. In studying the optimum location for a single outrigger, outriggers were located at three locations along the structure, mid-height, top and bottom quarter of the structure.

The results of varying the location of the outrigger on top story drifts for the three situations modeled are tabulated in Table 5-1. This correlates well with the optimum location that is expected with the value of ω and Figure 5-4. It is noticed that the smallest drift was obtained with the outrigger placed at mid-height. Deflected shapes for these models are shown in Appendix E.

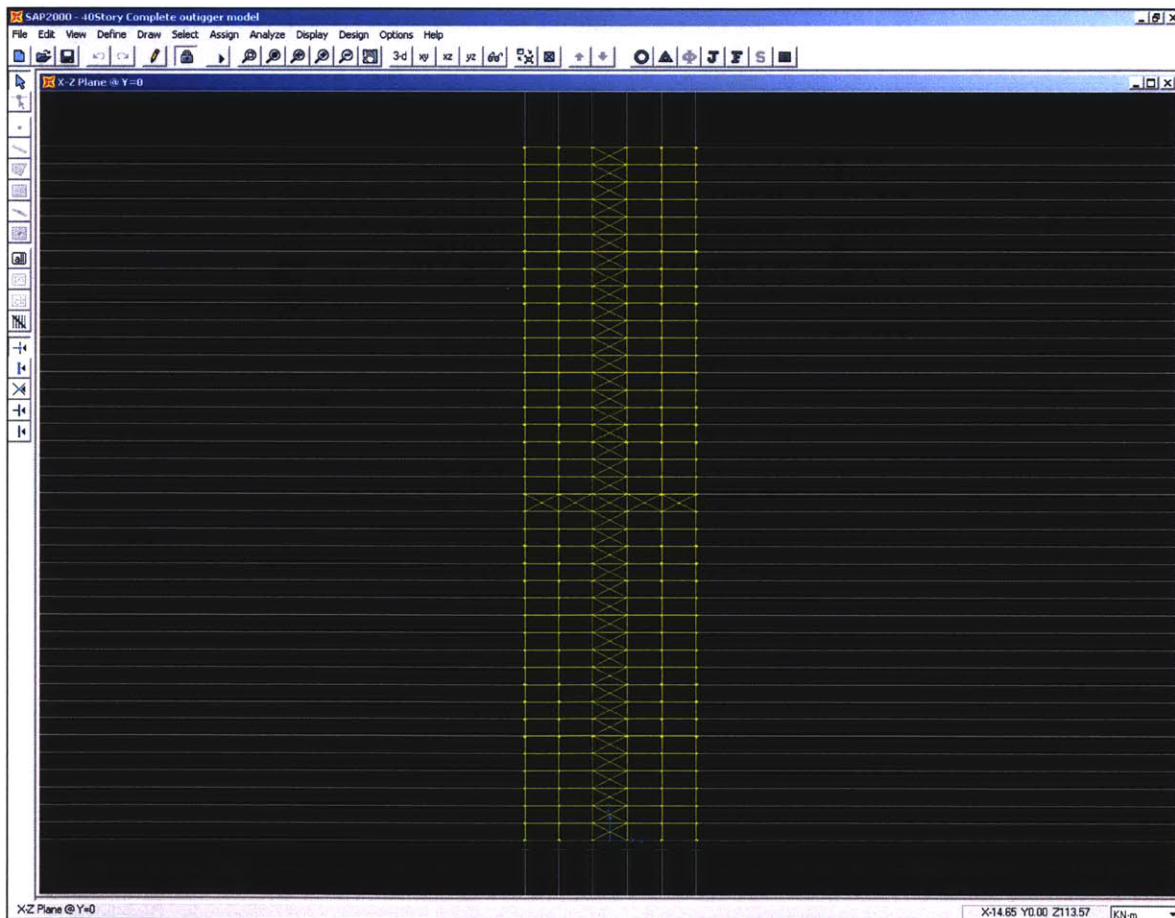
Table 5 - 1: Comparison of Top Story Drift with Outrigger Placement

Placed @ Story	ω	Top Story Drift
20	0.0341	1.76
40	0.0341	1.85
10	0.0341	2.47

5.3.2 Structural Efficiency

With the ability to place outriggers at the optimum location, a complete braced frame with outriggers incorporated was modeled. Two forty story structures with one and two outriggers was modeled in SAP and the elements were resized for top story drift control. The same virtual work optimization procedure performed on previous models was used.

The SAP models are shown in Figure 5 - 7 and Figure 5 - 8. The same loading of 26kN/m was applied uniformly across the windward face.

**Figure 5 - 7: Braced Frame with Single Outrigger**

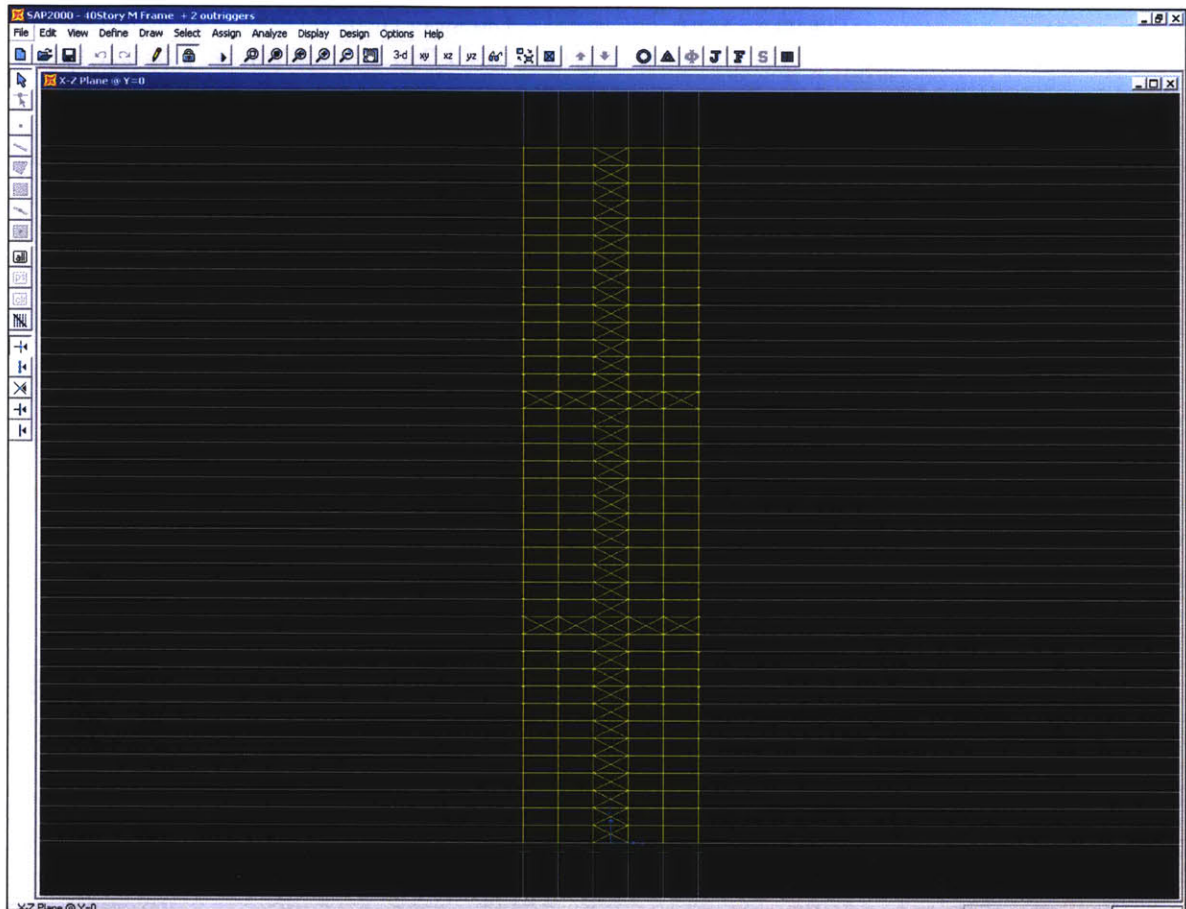


Figure 5 - 8: Braced Frame with 2 Outriggers

During each run, the elements sizes were adjusted up or down to meet the top story drift criteria with the minimum weight. Thus, material was sometimes removed from elements that did not make up much of the virtual work percentage. This allowed a reduction in steel volume while having little effect on drift.

The optimization for each model was run iteratively several times and the steel weight required was tabulated. The amount is compared illustrated in Figure 5 - 9 and tabulated in Table 5-2. Results were normalized to 8.74 which was the amount of steel required in a 10 story moment frame which has been consistently used as the base case for comparison.

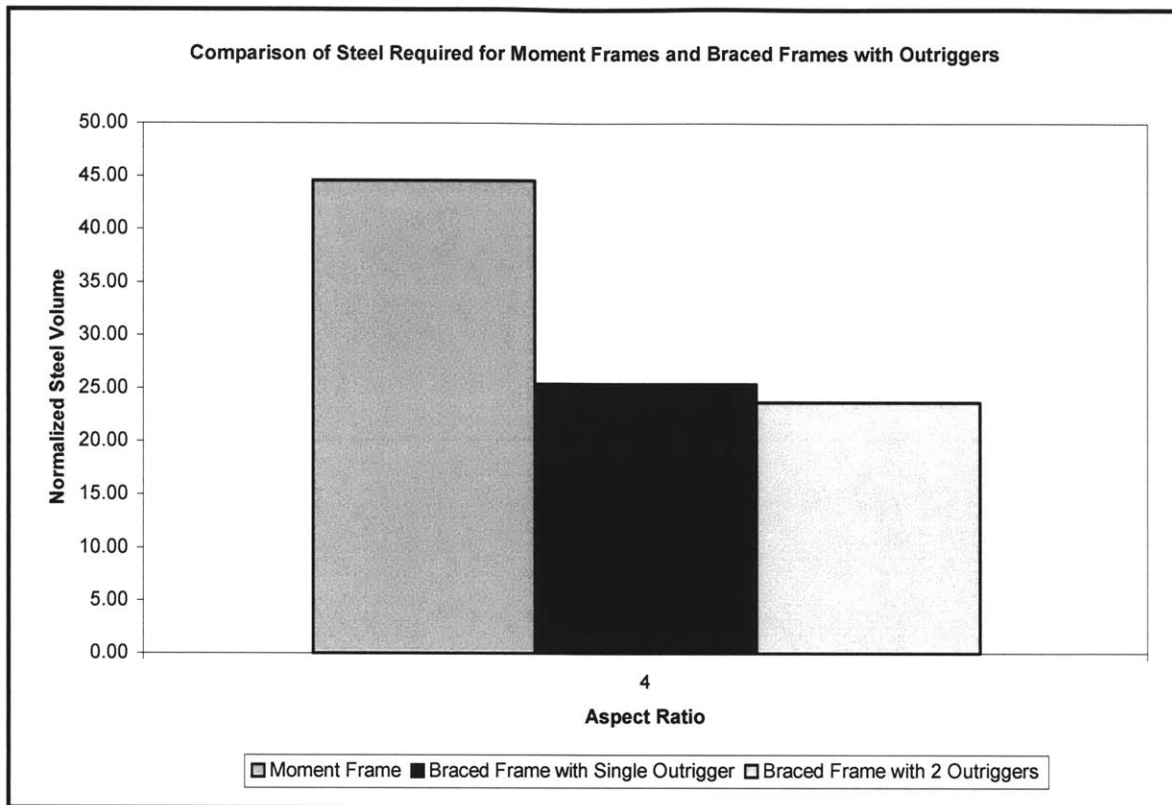


Figure 5 - 9: Graph of Steel Volume Required

Table 5 - 2: Comparison of Steel Volume Required

Structure Type	Steel Volume (m ³)	Normalized to 8.74
Moment Frame	390	44.62
Single Outrigger	222	25.40
Double Outrigger	207	23.68

From the above results, it is observed that the outrigger scheme provides significant savings in terms of steel volume required for drift control.

5.3.3 Deformed Shape and Design Issues

The deformation mode for a braced frame with outriggers was also of interest. It is not immediately apparent how the combined structure should deform. The deformed shape of the two outrigger braced frame is illustrated in Figure 5 - 10.

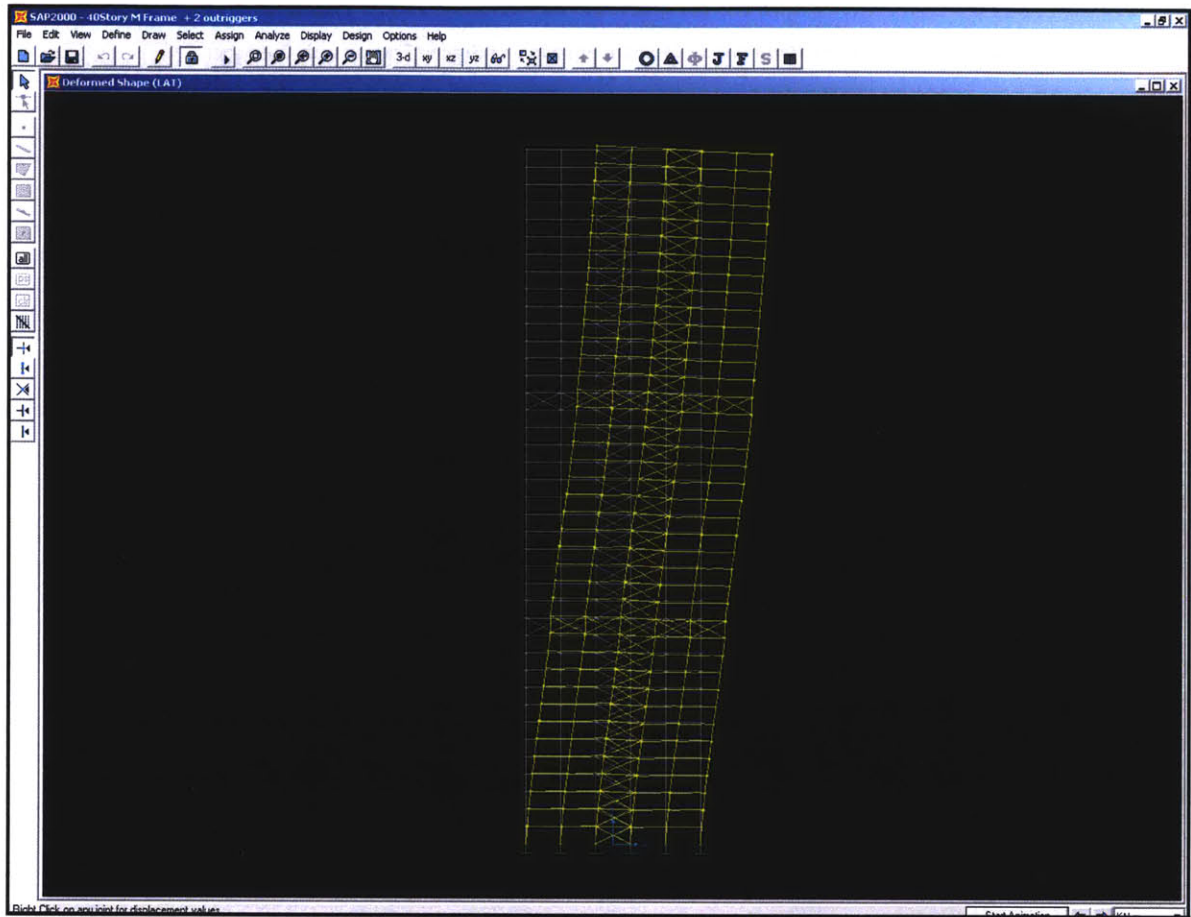


Figure 5 - 10: Deformed Shape (Braced Frame with 2 Outriggers)

The following observations are made with regards to the deformed shape. There are abrupt changes in curvature at the nodes at which the outriggers are attached, both at the perimeter columns and the interior joint between the outrigger and the core. This suggests the presence of large moments which should be carefully considered in design. The design of these connections are therefore critical. Majority of flexure (curvature) in the structure occurs at the base of the structure contrast to an isolated core where majority of flexure occurs at the top of the structure.

The virtual work diagram obtained from SAP is shown in Figure 5 - 11. It is observed that the maximum contribution arises at the base of the braced bay, particularly the diagonal webs of the braced bay. Surprisingly, the size of outrigger elements are shown to not affect the displacement of the structure any more than the stiffness columns or girder elements.

The structure is observed to go through a point of inflexion. In Figure 5 - 11, along the height of the structure, there is a sudden spike (identified by the gray elements) in the virtual work contribution by the braced bay truss element. This inflexion point is more clearly illustrated by the element moment diagram shown in Figure 5 - 12. A zone of almost zero moment is observed in the columns and girders at the particular floor. This implies that the story shear is primarily carried by the diagonal bracing element which explains the large virtual work contribution in those elements. This is another critical insight during the design of brace frame structures incorporating outriggers.

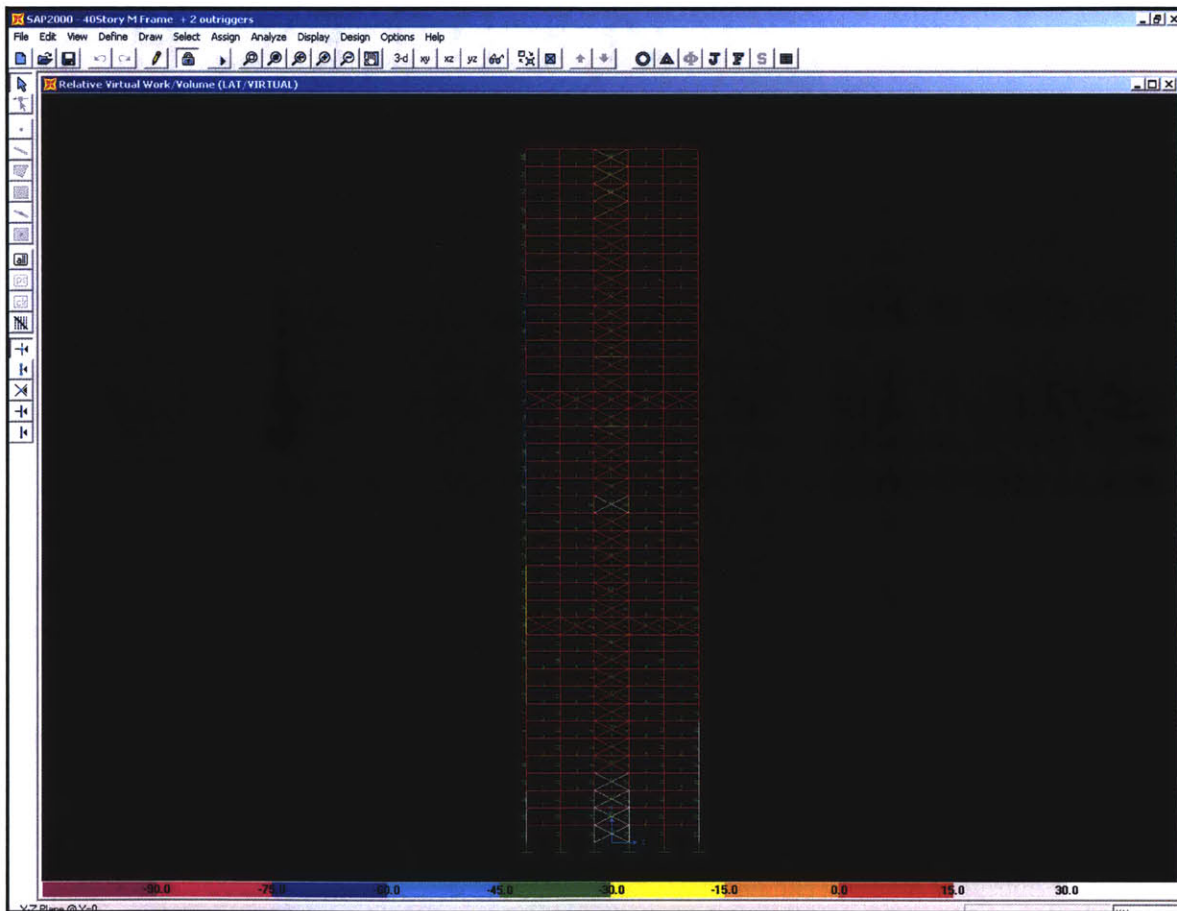


Figure 5 - 11: Virtual Work Diagram (Braced Frame with 2 Outriggers)

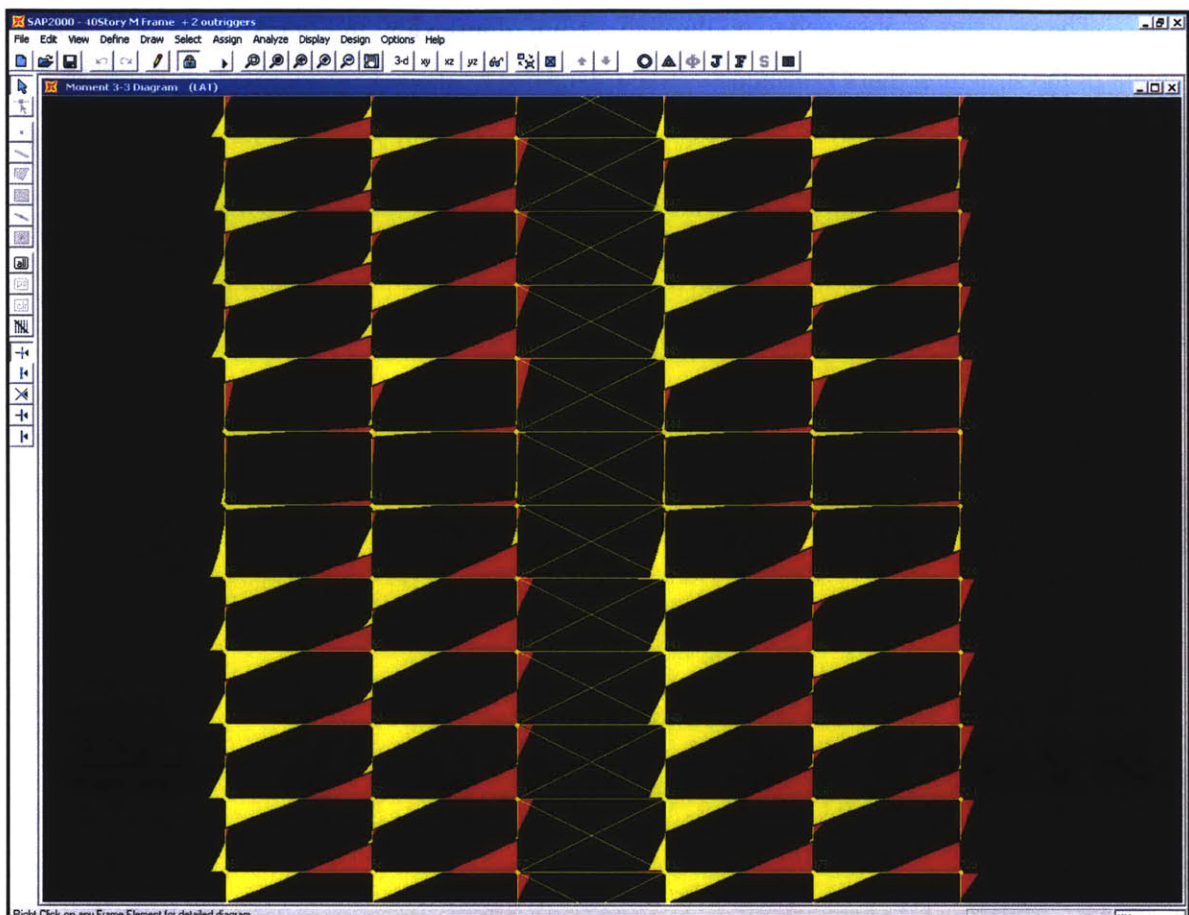


Figure 5 - 12: Location of Inflexion point in a Braced Frame with 2 Outriggers

Lastly, besides for deflection control, outriggers can be employed to reduce the moment that occurs at the base of the structure by providing a counter moment at the location at which it is joined to the core. From the SAP models available, the base moments of a braced frame without outriggers was compared to a braced frame incorporating outriggers. The moment at the base was found by multiplying the axial forces in the columns by half the braced bay width (3.5m). The results from this comparison are shown in Table 5-3. This reduction in base moment implies that outrigger schemes can be employed change the structural behavior of braced frames which is another tool in the structural engineer's arsenal to design safe yet structural efficient buildings.

Table 5 - 3: Comparison of Base Moments

Structure	Axial Force (kN)	Moment (kN-m)
Braced Frame (no outriggers)	8086	28301
Braced Frame (single outrigger)	7300	25500
Braced Frame (2 outriggers)	6800	23000

5.4 Conclusion (Braced Frame with Outriggers)

In this chapter, a relatively new lateral system was explored. The braced frame with outriggers seeks to engage the whole perimeter of the structure to resist the lateral loads applied. Outriggers were shown to influence the entire structure by reducing top story drift with only a small increase in material and also reduced the base moment in the rigid core (braced bay).

The optimum location of the outriggers was also demonstrated to depend on both the stiffness of the rigid core and the shear and bending stiffness of the outrigger. This suggests that it is possible to calibrate the outrigger to be placed at the optimum location determined by architectural requirements.

Certain key design issues were also explored in structures with outriggers. Due to the application of a countering moment by the outrigger, the displacement profile of the core was illustrated to go through a point of inflexion and this significantly differs from that of a normal rigid core which has been demonstrated to deform primarily in bending. The core then has to be reinforced in the location of the point of inflexion.

Chapter 6 explores a radically different approach to lateral stiffness in a tall structure which is the tubular structure.

5.5 References

- [1] www.som.com
- [2] B. S. Smith and A. Coull, Tall Building Structures: Analysis and Design, New York: John Wiley & Sons, Inc, 1991.
- [3] B. Taranath, Structural Analysis & Design of Tall Buildings, New York: McGraw-Hill Book Company, 1988.
- [4] W. Schueller, The Vertical Building Structure, New York: Van Nostrand Reinhold, 1990.
- [5] J. C. D. Hoenderkamp and M. C. M. Bakker, "Analysis of High-Rise Braced Frames with Outriggers," The Structural Design of Tall and Special Structures, Vol. 12, No. 4, Dec 2003, pp. 335-350.
- [6] J. C. D. Hoenderkamp and H. H. Snijder, "Simplified Analysis of Façade Rigger Braced High-Rise Structures," The Structural Design of Tall and Buldings, Vol. 9, No. 4, Sep 2000, pp. 309-319.

6 Chapter 6: Tubular Structures

6.1 Tubular Structures Introduction

The tubular structure is a relatively new form of high rise structural system. Buildings got taller as the field of structural engineering progressed and engineers have been hard pressed to find a new form that efficiently and safely carries the lateral loads applied. The tubular structure was the answer to the demand for height and new architectural forms.

The design of tubular structures involves engaging the entire perimeter of the building to resist the lateral loads that act on the structure. This involves closely spaced perimeter columns rigidly tied together by significantly deep spandrel beams. The World Trade Center (Figure 6 - 1) and Sears Tower (Figure 6 - 2) are much celebrated examples of this structural form. On observation of these structures, we are immediately struck by the verticality of the closely spaced columns which run up the entire face of the building and the relative slenderness of the tower.

The tubular structural form offers some distinct advantages that have led to its popularity in high rise construction. Firstly, it offers some clear advantages from a materials standpoint. Designed well, tubular forms have been known to utilize the same amount of material as would have been employed for a structure that was half as large and framed conventionally (Taranath 1998). Secondly, it allows great flexibility in the planning of the interior space since all the columns and the lateral system is concentrated on the perimeter of the structure. This essentially allows a column free space in the interior. This feature was one of the distinctions of the World Trade Center where the structure of the building was essentially the central core and the closely spaced perimeter columns. Lastly, the regularity the column schedule allows off-site fabrication and welding where speed can be achieved while still controlling for quality. For example, the columns of the World Trade Center was fabricated in panels off site and welded together on site. This allowed a repetitive construction sequence favored by both engineers and contractors.

The largest criticism to the tubular structural form is that while it allows high rise construction with great efficiency, it significantly reduces the size of openings in the building. So while occupants are working/living at great heights, their view of the world outside is rather obstructed. For example, in the World Trade Center, columns were spaced 3.33ft on center allowing narrow 19in wide by 78in high windows. Openings of these size would be naturally hard to implement in high rise residential construction. The finite rigidity of the girders and

connections also leads to a deviation from the standard linear distribution of axial forces across the flange and web columns assumed in regular beam theory. This non-linearity in axial force distribution is known as shear lag and is an effect that has to be accounted for in the design of tubular structures since it has an effect on the overall lateral stiffness of the structure.

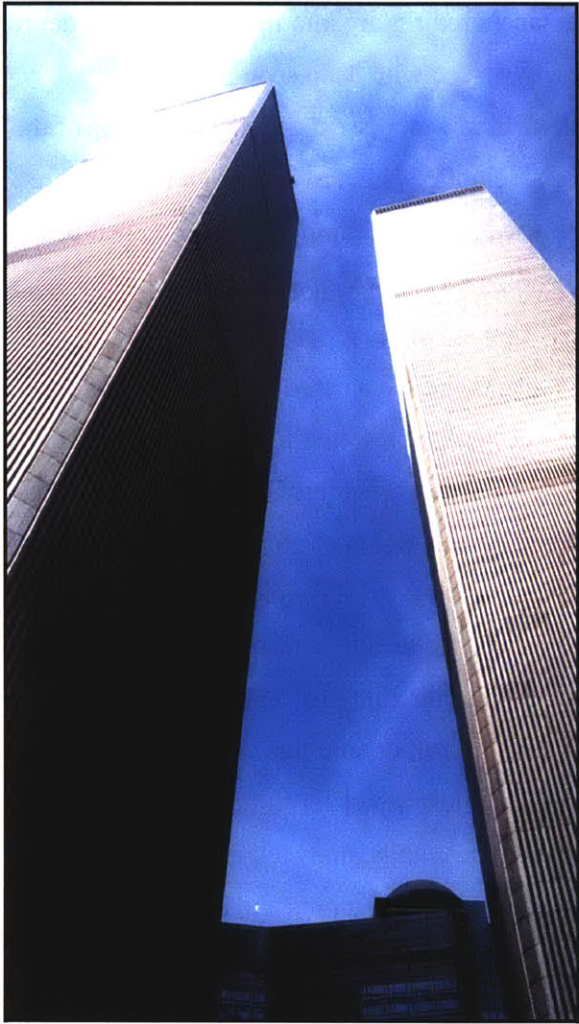


Figure 6 - 1: World Trade Center (New York) [1]

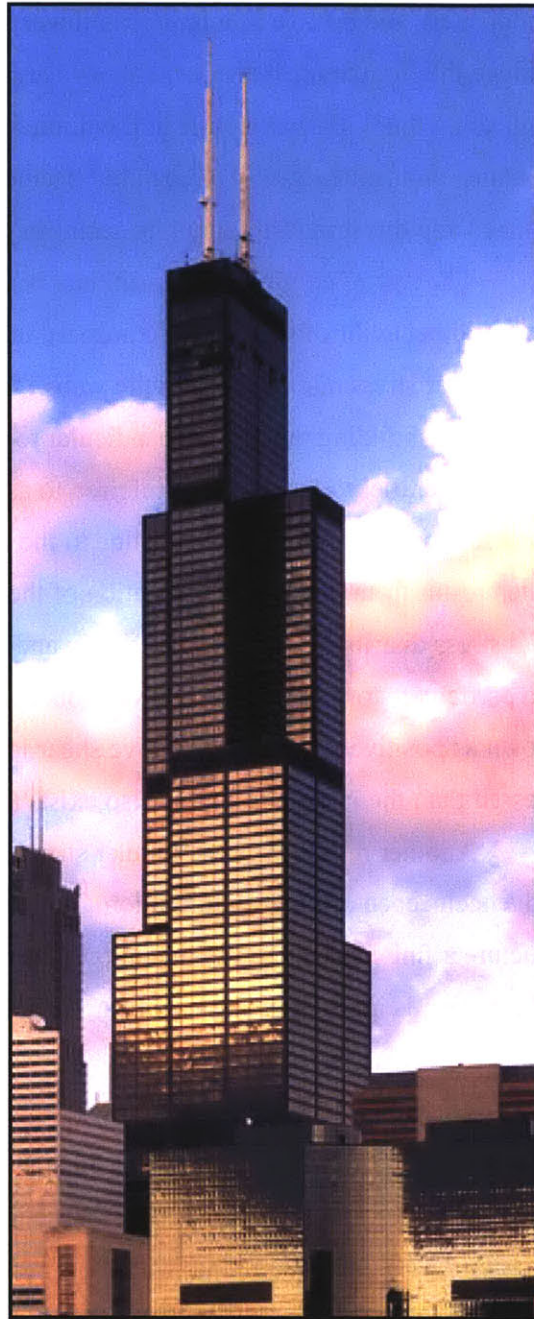


Figure 6 - 2: Sears Tower (Chicago) [1]

6.2 Structural Analysis

The strength of the tubular form arises from the utilization of the entire building perimeter to resist lateral loads. The goal is for the entire perimeter structure to function

compositely and behave as a large cantilever beam anchored rigidly into the ground. In order to achieve this composite behavior, columns are closely spaced with deep spandrel beams connecting them. However, due to the thinness of the tube wall (essentially the thickness of the columns) and finite rigidity of spandrel beams, the assumptions of classical beam bending are violated and the structure cannot be accurately analyzed as a pure cantilever bending beam.

The two assumptions in traditional beam bending theory which are violated by the structural behavior of tubular structures are the assumptions of plane sections remaining plane and a linear stress distributions in the webs. Since the analogy to a cantilever beam is made, the faces of the building that are perpendicular to the wind shall be referred to as the flanges while the faces parallel to the wind are referred to as the webs of the structure. Under lateral loading, plane sections do not remain plane due to the differential elongation of columns along the flange which result from the local deformation of the connecting spandrels. This leads to a non-linear axial stress distribution in both the flange and web panels and usually causes the corner columns in a particular story to be more heavily loaded than the interior columns. This phenomenon is known as positive shear lag. Negative shear lag, where the corner columns are less heavily stressed than the interior columns also exists and will be illustrated later in this chapter.

Another reason why the tubular structure cannot be readily analyzed as a cantilever beam is the occurrence of shear deformation. The finite rigidity of the columns and spandrels gives the structure a finite shear rigidity that allows shear deformation to occur. This shear mode of deformation is ignored in classical beam bending theory and has to be accounted for in the design of tubular structures.

According to Schueller (1990), structures with less than thirty percent of openings can be analyzed as a perforated tube and empirical studies have shown that as percentage of openings approach fifty percent, tubular action can no longer be developed and the shear mode of deformation begins to dominate with the structure behaving like a moment frame. Moment frames have been shown not to be structural efficient and thus moment frame behavior should be avoided.

6.2.1 Shear Lag

Shear lag is exhibited through a non-linearity in stress distribution across the flange and web sections of a beam. Along the flanges, this non-linearity can result in the corner/exterior

columns experiencing greater stress than the center/interior columns. This is known as positive shear lag. However, negative shear lag has been discovered to exist and this is the opposite of positive shear and the corner columns are observed to be less stressed than the center columns. Along the webs, shear lag results in a non-linear stress distribution in the web columns. This is illustrated in Figure 6 - 3. This deviation from traditional beam bending behavior naturally has implications on the bending stiffness of the built up structure. The presence of shear lag thus prevents the full potential in terms of rigidity of the structure to be exploited.

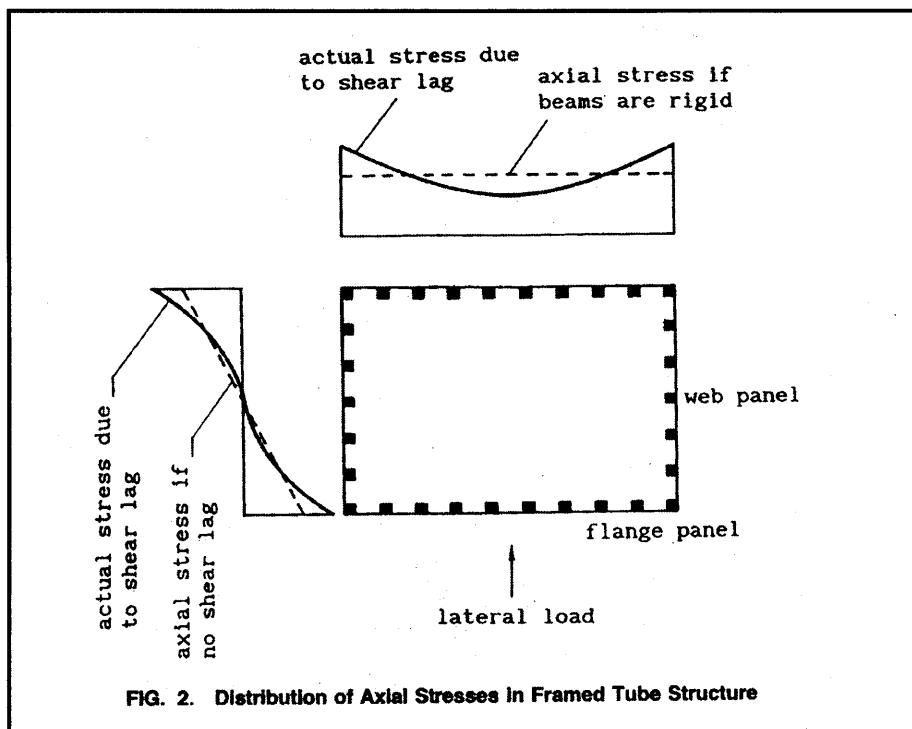


Figure 6 - 3: Axial Stress with Shear Lag [3]

6.2.1.1 Positive Shear Lag

Positive shear lag arises from local deformation of the spandrels which leads to the reduction in axial stress towards the center of the flange. This is shown in Figure 6-4. Assuming that the lateral loads are directed primarily to the corner columns, the corner column will deflect as shown. Through the linkage of the spandrel beams, the next interior column is displaced but by a smaller amount due to the flexibility of the spandrel. As the interior columns are progressively mobilized, the force generated in them are gradually less. In the same manner, the columns in the webs are progressively mobilized and the axial force distribution deviates from

the traditionally assumed linear profile. A parabolic distribution of axial stress in both the webs and flanges are observed as illustrated in Figure 6 - 3.

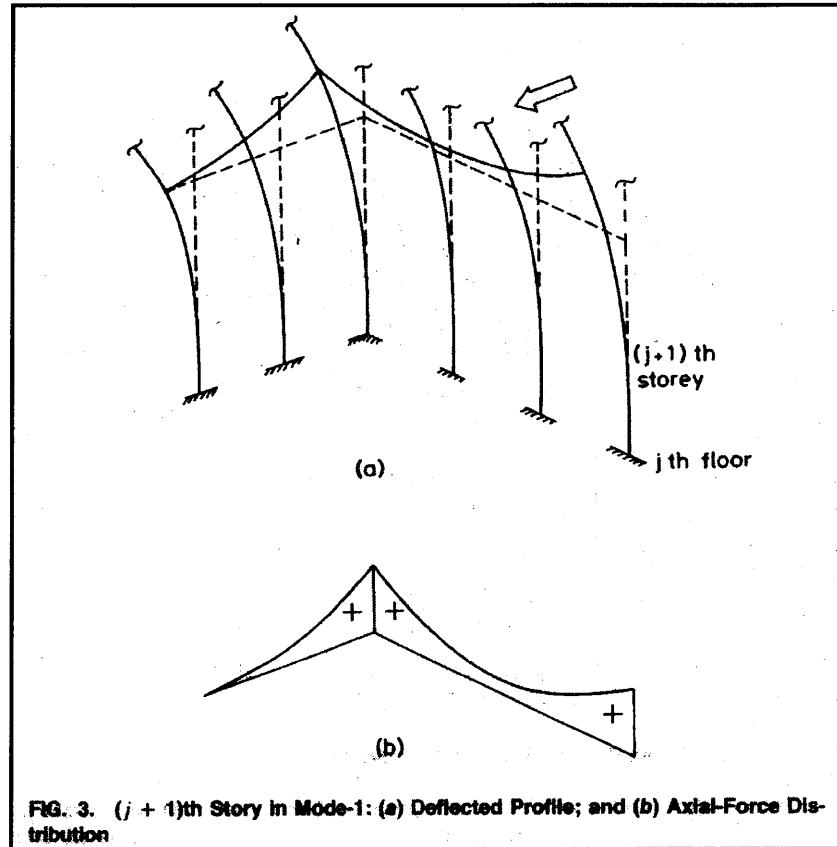


Figure 6 - 4: Deformation Resulting in Positive Shear Lag [4]

6.2.1.2 *Negative Shear Lag*

Negative shear lag arises from the differential vertical displacement of the studied story [4]. This is illustrated in Figure 6 - 5. As the building bends, the windward flange undergoes tension and the leeward flange compression. This implies that a vertical displacement occurs. However, due to the flexibility of the spandrels, this displacement is again non-uniform throughout the story and results in the deformation illustrated. This deformation leads to an increase in the axial forces in the center of the flange while reducing the axial forces in the corner columns. This displacement results in the differential stress distribution is known as negative shear lag.

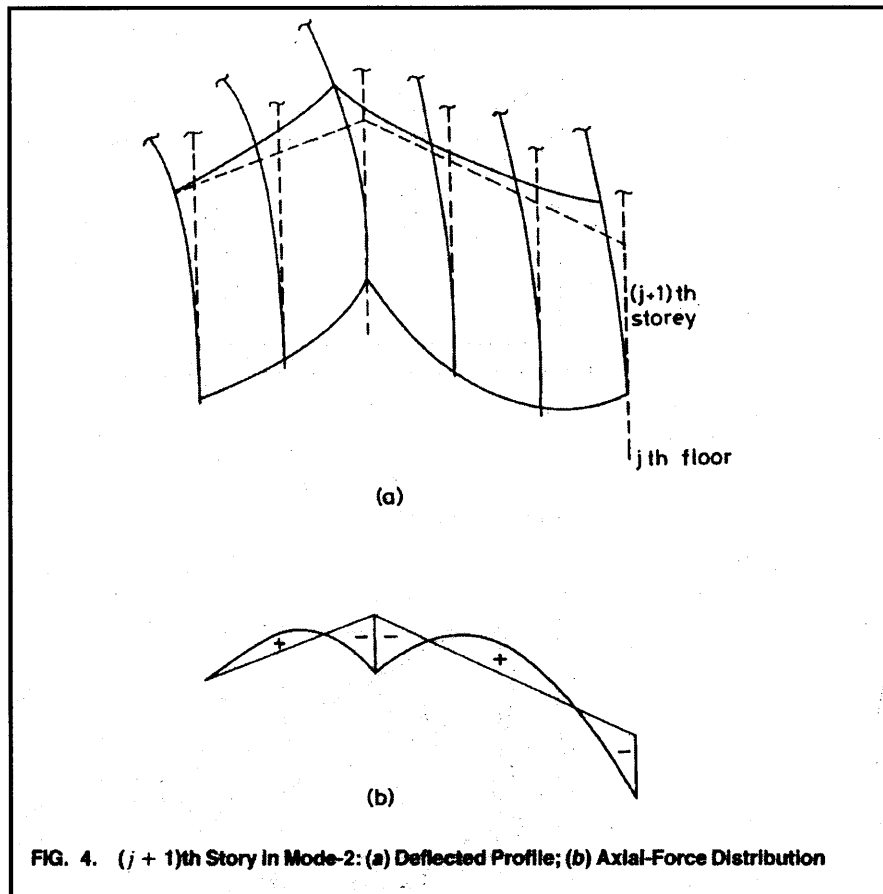


Figure 6 - 5: Deformation Resulting in Negative Shear Lag [4]

6.2.2 Quantification of Shear Lag

In order to quantify the magnitude and presence of shear lag, two measures have generally been used in research conducted. They involve either the ratio of the slopes of the stress distributions with and without shear lag (for the web panels) or the ratio of stress between the corner and center column (for the flange panels). In either case, as the ratios get to unity, shear lag then ceases to exist.

Kwan (1996) used the following measures of shear lag for his study. He defined α as the reduction in slope caused by shear lag in the web panel. Thus, shear lag in the web panels is seen to decrease as α decreases. This is illustrated in Figure 6 - 6.

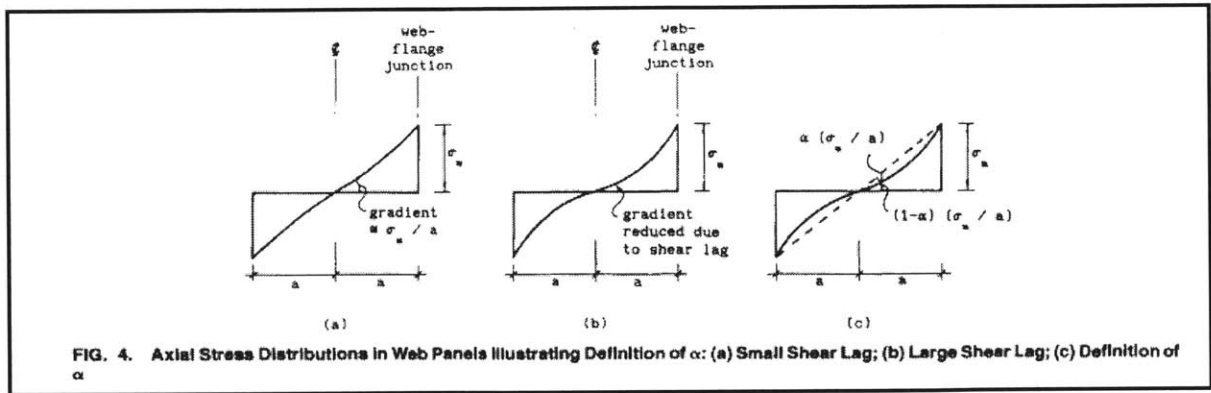


Figure 6 - 6: Quantification of Web Shear Lag [5]

Kwan used β to quantify the shear lag in the flange panels. This is computed as the reduction in axial stress in the center column compared to the corner column. Similar to α , the magnitude of shear lag decreases as the value of β decreases.

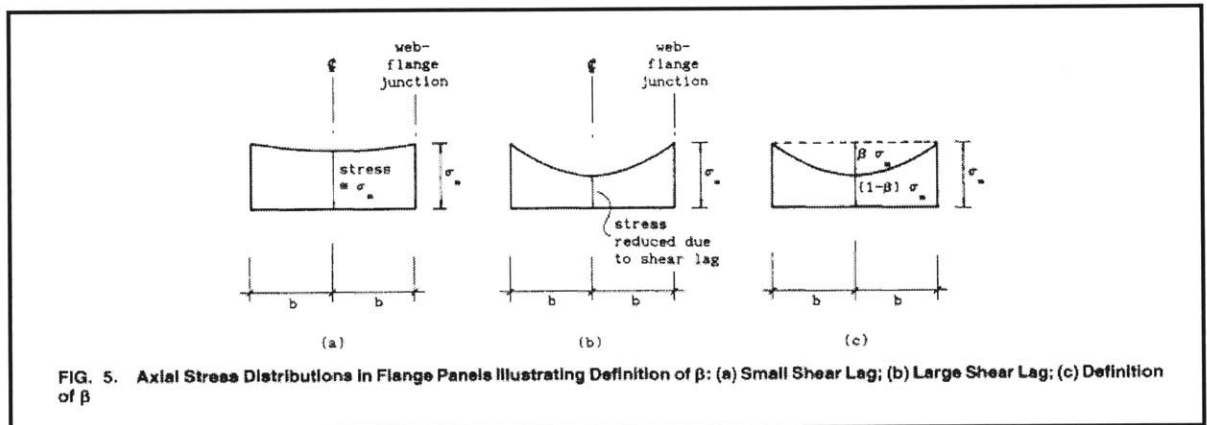


Figure 6 - 7: Quantification of Flange Shear Lag [5]

Lee, Lee and Lee (2002) utilized the ratio of axial force/stress between the corner flange column to the center column as their shear lag factor (p). In this situation, a value of p greater than unity indicates positive shear lag while a negative value indicates the presence of negative shear lag.

The SAP models presented later in the chapter will utilize a combination of both measures to grasp the structural behavior of the tubular form as geometric parameters change.

6.2.2.1 Variation of Shear Lag with Height

Both Lee, Lee and Lee (2002) and Singh and Nagpal (1994) demonstrated the variation of shear lag along the height of a structure. Lee, Lee and Lee proposed a method for analyzing the presence of shear lag with and without interior tubes. They compared their results to previous proposed methods and also a frame computer model (ETABS). Their results for a single tube are shown in Figure 6 - 8. As it is observed, the magnitude of shear lag quantified by p is noted to start out as a positive value at the base of the structure and gradually decrease towards the top of the structure. A point of zero shear lag is also observed. After this point, negative shear lag is seen to dominate and gradually increase towards the top of the structure.

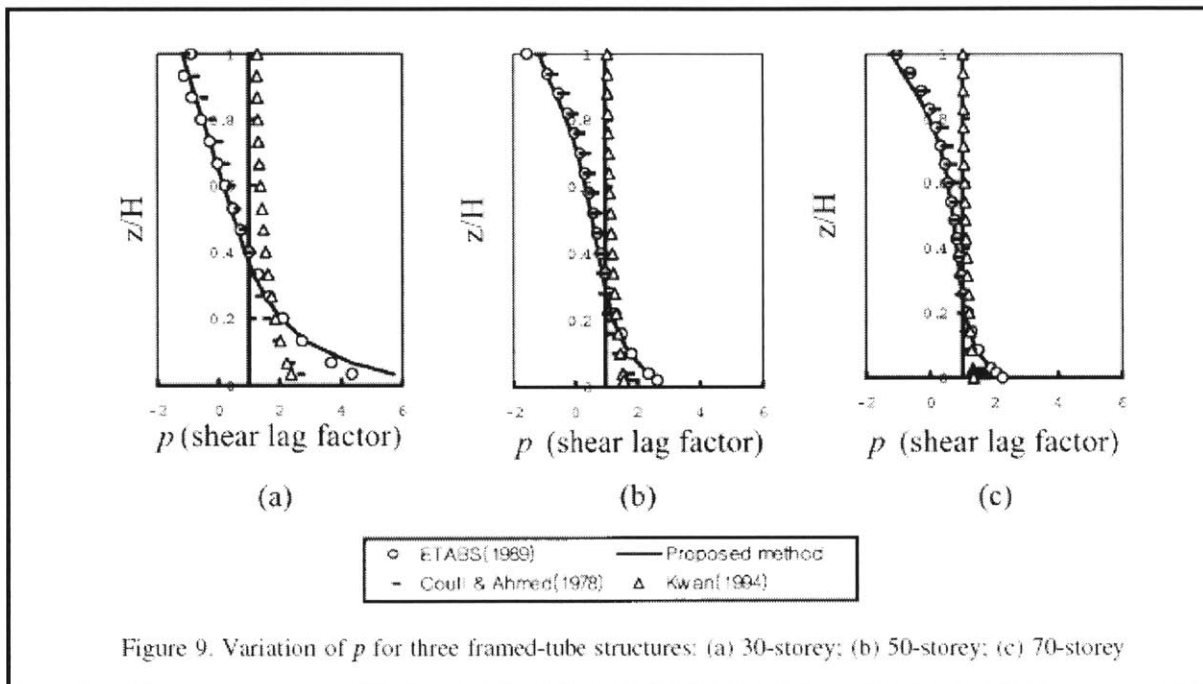


Figure 6 - 8: Variation of Shear Lag with Height [6]

Singh and Nagpal (1994) also demonstrated the variation of shear lag along the height of the structure. In their analysis of a forty story structure, they plot the variation of axial force in the flange columns with its distance from the center line. A large variation in axial force is observed at the base of the structure. However, this variation is seen to decrease along the height of the structure and at a certain point is zero. This point of zero shear lag is identified as the point of shear lag reversal. After this point, negative shear lag is seen to be present and the axial force in the center column is seen to be larger than that in the corner column.

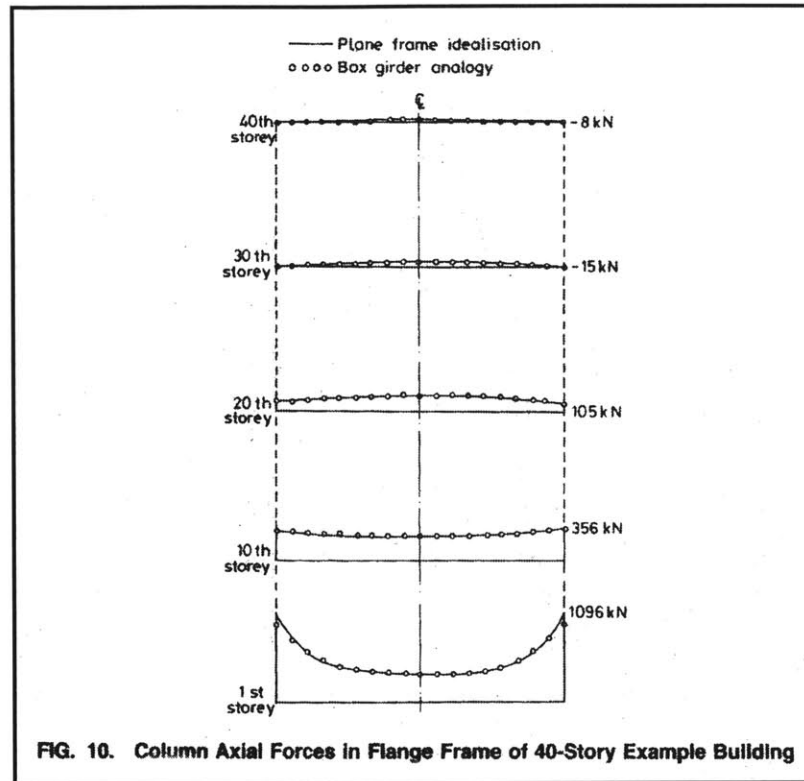


Figure 6 - 9: Variation of Shear Lag with Height [4]

This variation was confirmed by the SAP models run and this will be illustrated and discussed later in the chapter.

6.2.2.2 *Shear Lag Variation with Base Dimensions*

Kwan (1996) performed a parametric study of base shear lag by varying relative base dimensions of a structure. This was done using the finite element method. In his study, he used the reduction in slope α (web shear lag) and reduction in center column axial force β (flange shear lag) to quantify the magnitude of shear lag present.

It has been established that the magnitude of shear is most prominent at the base of a structure. He therefore focused his attention on the stress distributions at the base of the structure and computed shear lag coefficients for this location. Unlike previous studies that focused on the presence of shear lag in the flange panels and ignored shear lag in the web sections, he allowed for the occurrence of shear lag in the web panels in his analysis.

Figure 6 - 10 is adapted from his study and illustrates the variation of the magnitude of shear lag with different relative base dimensions. Figure 6 - 11 illustrates the structural model used and the dimensions of “a” and “b” used in Figure 6 - 10. He then proceeded to plot the computed shear lag coefficients, shown in Figure 6 - 12.

Model number (1)	$2a:2b:H$ (2)	Shear-lag coefficient α (3)	Shear-lag coefficient β (4)	Stress factor at fixed end (5)	Deflection factor at free end (6)
1	3:1:5	0.533	0.431	1.470	1.022
2	3:1:10	0.307	0.233	1.217	1.008
3	3:1:20	0.146	0.104	1.089	1.003
4	2:1:5	0.425	0.415	1.412	1.020
5	2:1:10	0.220	0.216	1.179	1.006
6	2:1:20	0.090	0.100	1.072	1.003
7	1:1:5	0.248	0.384	1.355	1.018
8	1:1:10	0.110	0.202	1.156	1.005
9	1:1:20	0.048	0.096	1.068	1.003
10	1:2:5	0.273	0.588	1.724	1.080
11	1:2:10	0.128	0.370	1.353	1.021
12	1:2:20	0.057	0.191	1.155	1.005
13	1:3:5	0.297	0.707	2.100	1.185
14	1:3:10	0.144	0.489	1.552	1.046
15	1:3:20	0.066	0.281	1.256	1.012

Figure 6 - 10: Variation of Shear with Base Dimensions [5]

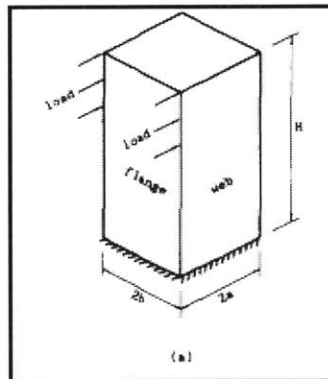


Figure 6 - 11: Structural Model [5]

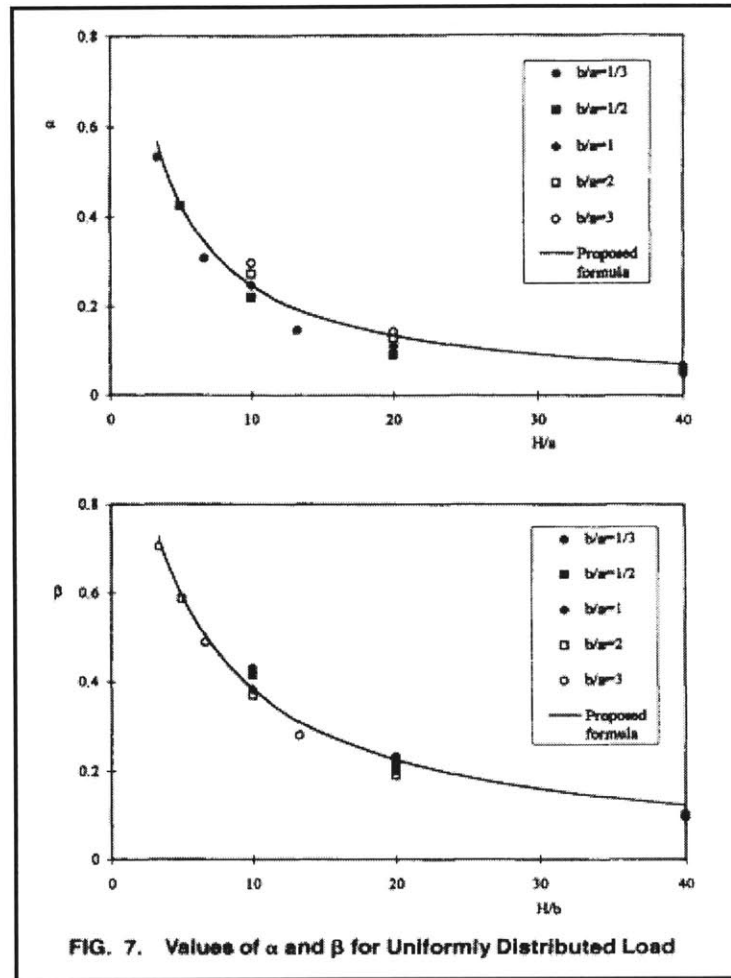


Figure 6 - 12: Plot of Shear Lag Coefficients with Varying H/a and H/b [5]

With the results and plots, the following was concluded. The magnitude of shear lag depended mainly on the ratio of H/a for α and H/b for β . He found that the magnitude of shear lag in both the flange and web panels decreased as the aspect ratios of the structures increased. This implies that shear lag is a phenomenon primarily associated with shorter structures. A gradual tapering in the shear lag coefficients was observed as the aspect ratios of the structures increased. This suggests that some degree of shear lag would occur at the base of the tubular structure regardless of height.

The ratio of flange to width (b/a) dimensions was found to have only a minor effect on the magnitude of base shear lag in both the web and flange panels. This is an insight not readily apparent from preliminary study of the structural behavior of tubular forms.

6.3 SAP Models (Tubular Structures)

SAP models with varying flange to width to height ratios were run to examine the validity of previous studies and also to look at some parameters which affect tubular behavior but has not been widely mentioned in the available literature. The SAP models were simple perimeter frames loaded at joints of the corner columns. As the ratio of the base and height dimensions were the parameters under study, the footprint of the structure was shrunk considerably to lessen the computational effort required. Columns were spaced one meter on center both in the web and flange panels with the maximum length of any base dimension not exceeding eighteen columns. Height of the structure was varied and a standard floor to floor height of 3.5 meters was maintained.

As the study only focused on the presence of and magnitude of shear lag, section sizes were kept constant throughout the structure. For each structure, the imposed loading was uniform point loads throughout the height of the structure and was of a magnitude to give a reasonable top story deflection of around $H/500$.

The SAP models analyzed were of the dimensions as follows in Table 6 - 1. The aspect ratios of models 1, 2 and 3 were kept constant at 4, with a column spacing of 1m and floor to floor height of 3.5m. These models were used to establish the effect of varying base dimensions on the occurrence of shear lag in the webs and flange panels. The next two models (4 and 5) were used to determine the effect of varying height keeping the base dimensions the same. These models gave insight into the effect of the ratios H/F and H/W had on the occurrence of shear lag. The last model (6) was used to examine the effect of increased lateral loading on the structure. It was desired to determine if the magnitude of loading affected the magnitude of shear lag that occurs.

Table 6 - 1: SAP Models Analyzed

Model Number	Flange (F) (columns)	Web (W) (columns)	Height (H) (Stories)	F/W	H/F	H/W
1	9	27	30	0.33	3.33	1.11
2	18	18	20	1	1.11	1.11
3	28	10	10	2.8	0.36	1.00
4	18	18	40	1	2.22	2.22
5	9	27	60	0.33	6.67	2.22
6	28	10	10	2.8	0.36	1.00

6.3.1 Shear Lag Coefficients

Two measures were used to quantify the occurrence of and magnitude of shear lag. The measure of flange shear lag was the ratio of the axial force in the center column compared to the corner column. The smaller the ratio, the greater the occurrence of shear lag since in a perfect beam, it is assumed that the flange is under a constant state of stress. An example of the output from SAP and the calculation of flange shear lag is shown in Table 6 - 2.

In order to quantify the magnitude of web shear lag, the ratio of the slopes at the vertical symmetric axis of the plot was used. To compute this value, two slopes were required. The first slope was the slope of the graph from the center point to the last point on the plot. The other slope was the tangent of the graph at the center point. In traditional beam theory, a linear distribution of stress along the web is assumed. This implies that the tangent slope at the center point and the slope from center to end point should be the same. In the presence of shear lag, this does not occur. The difference in slope between the ideal case and actual case thus provides a measure of shear lag present. The greater the variation, the greater the presence of shear lag. In Figure 6 - 14, the axial force distribution is clearly non-linear and this illustrates how the difference in slope can be used to capture the shear lag effect.

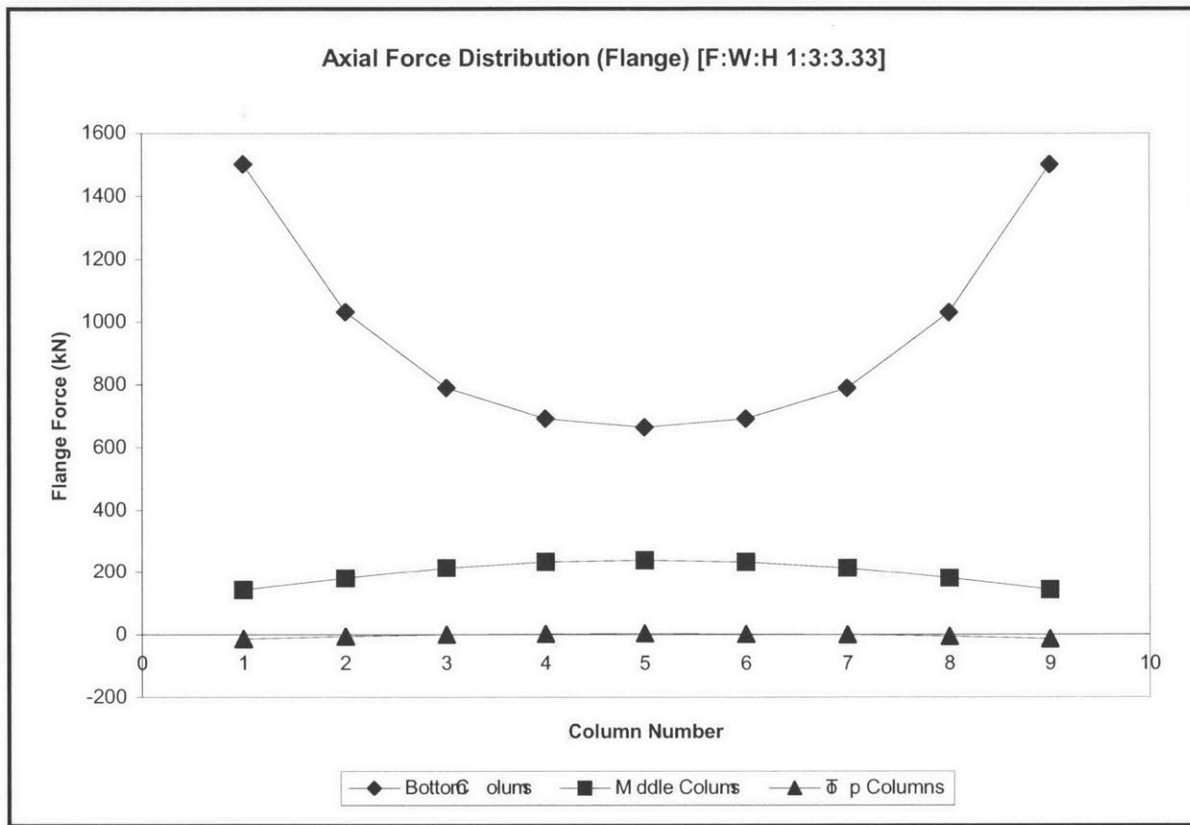


Figure 6 - 13: Flange Axial Force Distribution for Model 1

Table 6 - 2: Flange Axial Forces for Model 1 (Bottom Column)

Column Number	Axial Force (kN)
1	1502.47
2	1031.63
3	790.88
4	691.49
5	663.80
6	691.49
7	790.88
8	1031.63
9	1502.47
Shear Lag Coefficient	$1502/663 = 0.442$

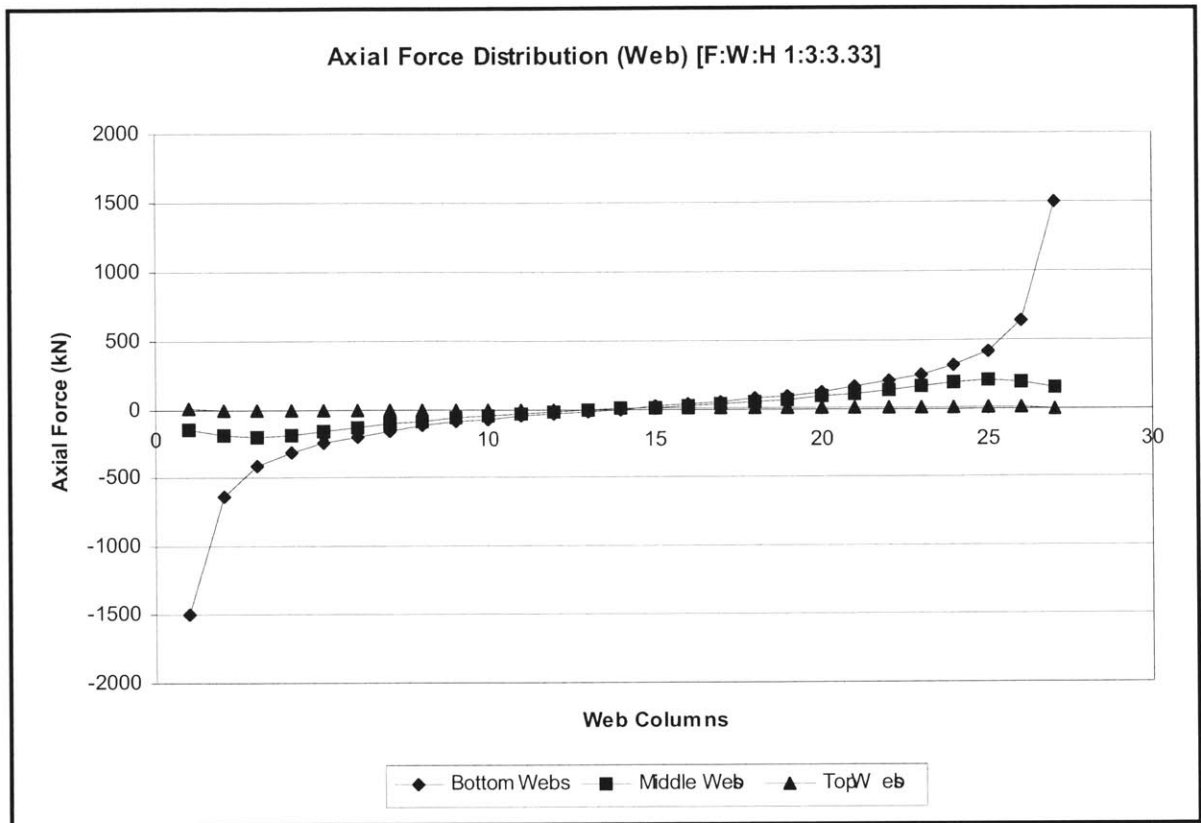


Figure 6 - 14: Web Axial Force Distribution for Model 1

6.3.2 SAP Model Results

The distribution of axial forces across both the web and flange was graphed for each of the six models. This section will discuss the findings from the six models and their agreement with previous studies examined. As the base of the structure has been found to experience the greatest degree of shear lag, the shear lag coefficients for both the flange and web panels are calculated at this location.

The shear lag coefficients for both the web and flange panel for the six models are tabulated in Table 6-3. Figure 6 - 15 and Figure 6 - 16 graph the variation of flange and web shear lag respectively with varying H/F and H/W. Complete graphs are attached in Appendix F.

Table 6 - 3: Computed Shear Lag Coefficients

Flange Analysis (Ratio of Axial Forces of Center to Corner Column)						
	Model 1	Model 2	Model 3	Model 4	Model 5	Model 6
Bottom Columns	0.442	0.130	0.003	0.285	0.620	0.003
Middle Columns	1.667	2.570	0.022	1.993	1.132	0.022
Top Columns	-0.270	-0.020	0.005	-0.418	-0.113	0.005

Web Analysis (Ratio of Slopes)						
	Model 1	Model 2	Model 3	Model 4	Model 5	Model 6
Bottom Columns	0.143	0.113	0.089	0.265	0.346	0.088
Middle Columns	1.083	2.998	1.054	2.326	3.157	1.055
Top Columns	-0.409	-0.282	-0.668	-0.463	-1.018	-0.668

6.3.2.1 *Variation of Flange and Web Shear with H/F and H/W*

The shear lag coefficients for the bottom columns for the models are tabulated in Table 6 - 4. From Figure 6 - 15, it is immediately apparent that flange shear lag decreases with increasing H/F. In other words, the greater the aspect ratio of the building, the smaller the effect of shear lag in the structure. The high R^2 value of the fitted trendline gives confidence in this finding. A tapering of the graph is also observed in Figure 6 - 15. From the few data points, it is noticed that as the aspect ratio (H/F) of the structure increased, there was a realistic limit to the elimination of shear lag. This can be attributed to the inherent flexibility of the connecting spandrels, which is the primary cause of shear lag.

Table 6 - 4: Variation of Flange Shear Lag with H/F

Model No.	H/F	Flange Shear Lag Coefficient (Bottom Columns)
1	3.330	0.442
2	1.110	0.130
3	0.360	0.003
4	2.220	0.285
5	6.670	0.620

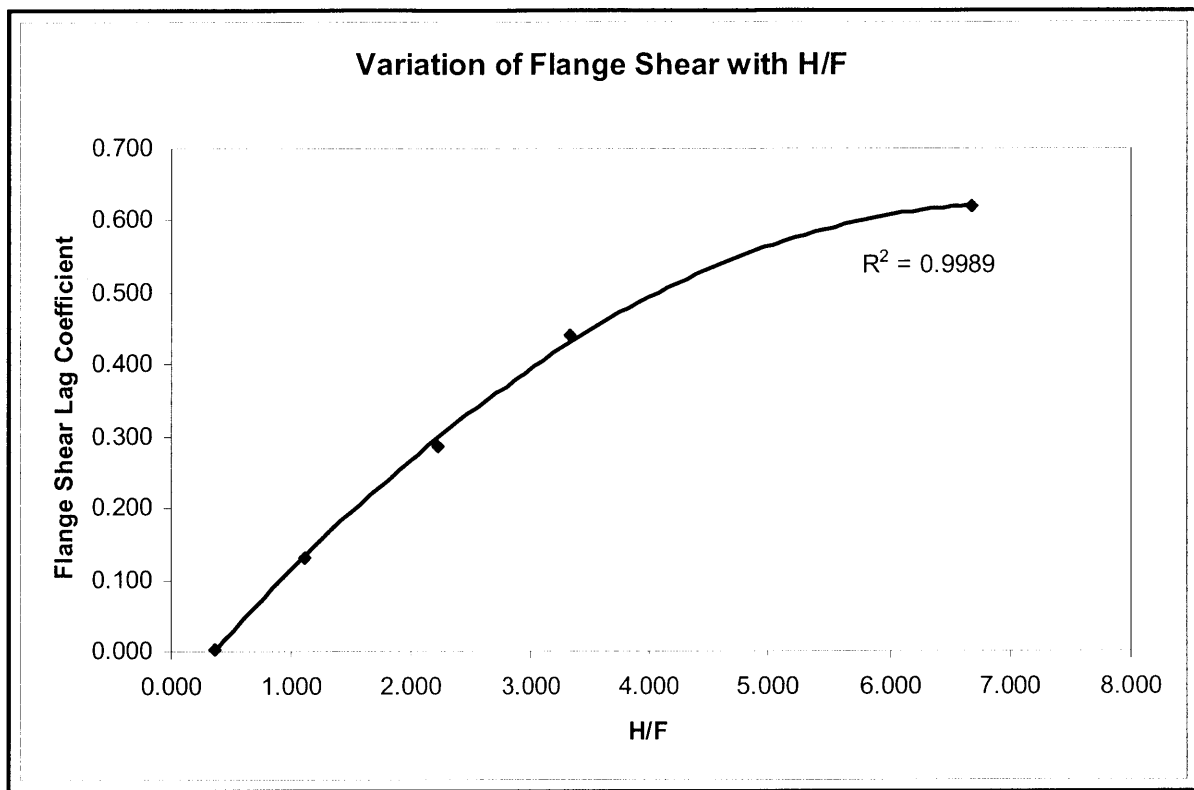


Figure 6 - 15: Variation of Flange Shear Lag with H/F

Figure 6 - 16 illustrates the variation of web shear lag with H/W. The same trend as that in flange shear lag is observed. As the ratio H/W increases, web shear lag is observed to decrease. Although only five points were obtained, the upwards trend is clearly observed. A realistic limit to the elimination of web shear lag should also be expected since spandrels have a finite rigidity.

Table 6 - 5: Variation of Web Shear Lag with H/W

Model No.	H/W	Web Shear Lag Coefficient (Bottom Columns)
1	1.111	0.143
2	1.111	0.113
3	1.000	0.089
4	2.222	0.265
5	2.222	0.346
6	1.000	0.088

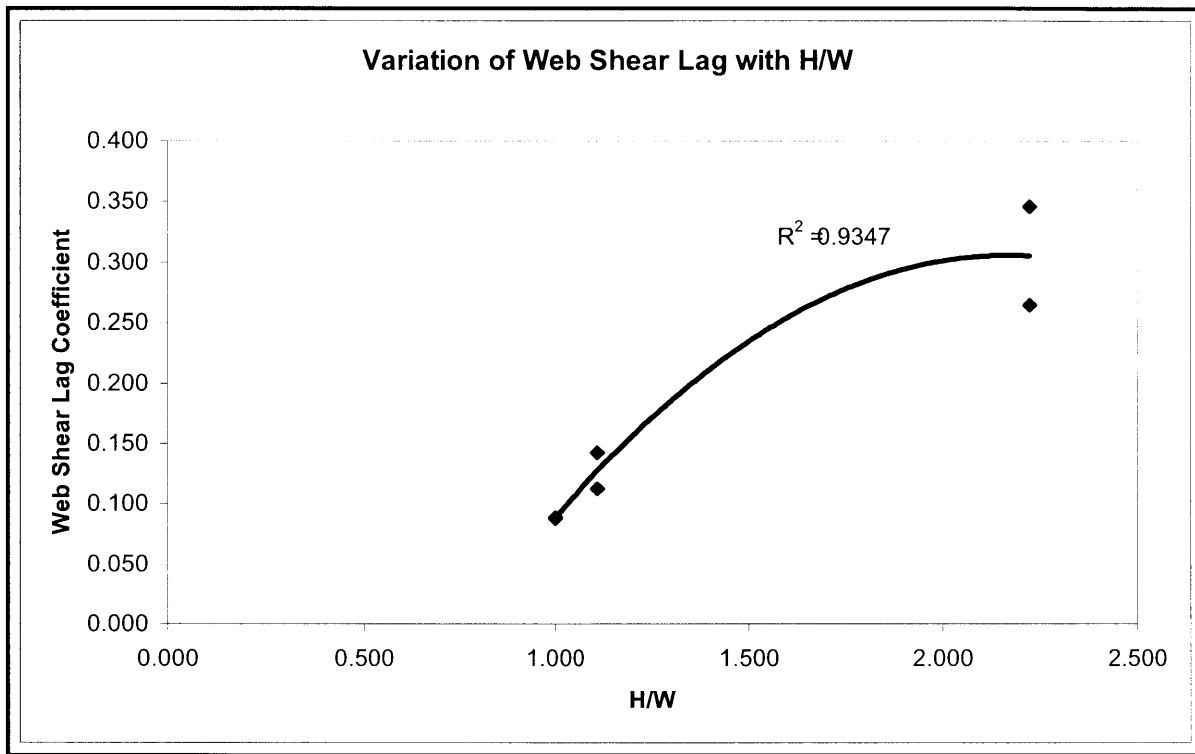


Figure 6 - 16: Variation of Web Shear Lag with H/W

From Figure 6 - 15 and Figure 6 - 16, it is then concluded that shear lag in both the web and flange panels is a concern primarily with shorter structures. These graphs also provide a preliminary estimate of how much the interior columns will be engaged in a particular structure under lateral loading.

6.3.2.2 *Variation of Flange and Web Shear Lag with Height*

From the SAP models, the degree of shear lag was also found to vary along the height of the structure. Both the web and flange shear lag coefficients for each of the six models were plotted and are attached in Appendix F. All plots exhibited a decrease in shear lag towards the top of the structure. In some instances along the flange panels, negative shear was found to dominate at the top of the structure. Negative shear lag is the situation where the corner column is less stressed than the center columns. For example, in the top story in model 4, the flange shear lag coefficient was found to be -0.418 . Although this value is large, it is also critical to look at the magnitudes of the axial forces in this location. The axial force in the top columns for model 4 was 18.4kN and -44.1kN for the center and corner column respectively. Although a

large measure of shear lag is calculated, the magnitude of the axial forces in these columns is such that the shear lag is not something of concern.

6.3.2.3 Variation of Flange Shear Lag with F/W

The effect of the ratio of F/W on the occurrence of flange shear lag was also examined. The variation of flange shear lag was plotted with respect of F/W. This is shown in Figure 6 - 17. With the six models run, five different ratios of F/W were obtained. For each ratio of F/W, two flange shear lag coefficients were obtained due to each model with a similar F/W value had two different heights. As previously established, the H/F ratio is a key determinant of the degree of shear lag that occurs. The data points with the larger flange shear lag coefficient for each value of F/W is then the model with the greater H/F ratio.

With this in mind, the data exhibited a general downwards trend as the ratio of F/W increased. The ratio of F/W is an analogous measure of the width to depth ratio of a beam. It is observed that as the building gets wider (F/W increases) with respect to its depth, the occurrence of flange shear lag is seen to increase. This should be expected since there is a greater number of interior columns to be engaged from the corner. More spandrel deformation occurs and a progressively smaller axial load is transferred from the corners.

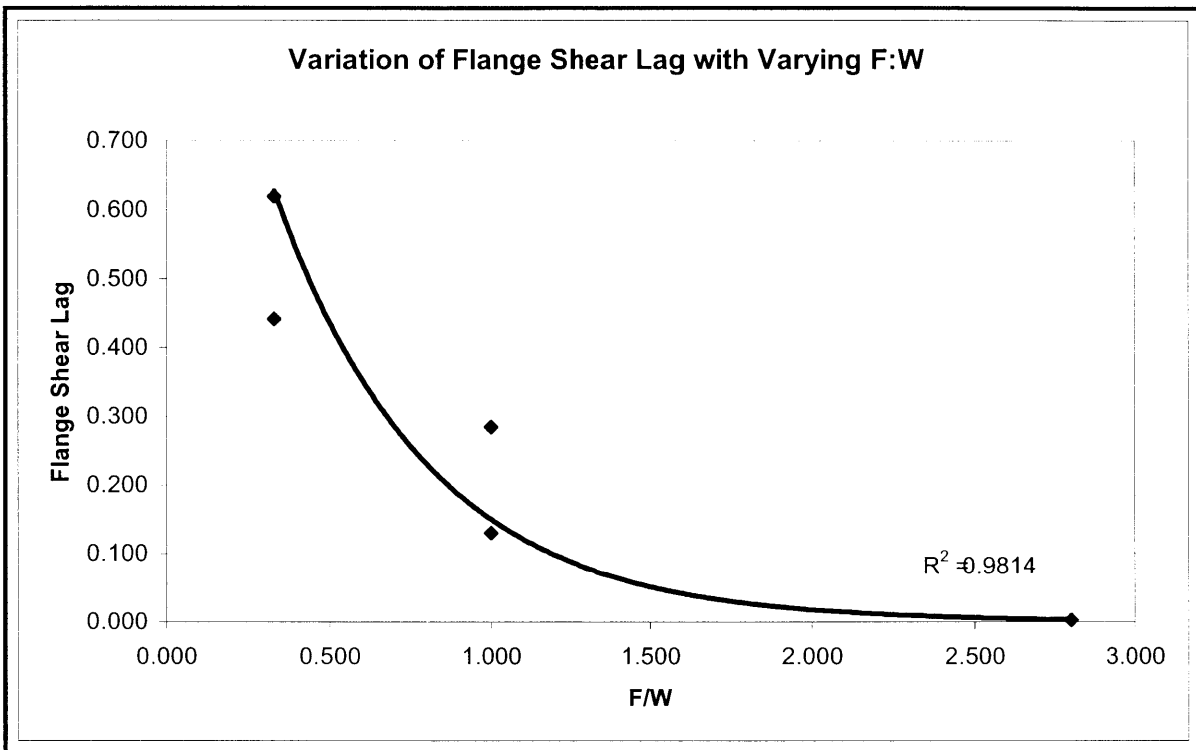


Figure 6 - 17: Variation of Flange Shear Lag with F:W

6.3.2.4 *Effect of Increased Girder Stiffness on Flange Shear Lag*

In order to study the effect of the girder stiffness on the degree of shear lag present, model 1 was run with the girder stiffness modified upwards by 2 times and also 5 times. The degree of shear lag computed was compared to the original model with no modification of girder properties. This comparison is shown in Table 6 - 6.

Table 6 - 6: Flange Shear Lag with Varying Girder Stiffness

Model	Flange Shear Lag (Bottom Column)	Girder Stiffness Modification
1	0.442	0
1a	0.464	2x
1b	0.493	5x

Girder stiffness is demonstrated to have an effect on the flange shear lag. An increased girder stiffness leads to a smaller degree of flange shear lag as shown in Table 6 - 4. Naturally, there are other manners to increase the stiffness of the girders such as reducing its span, but this

does not detract from the fact that girder stiffness plays a important role in the negation of shear lag.

6.3.2.5 Braced Tube Structures

Pure tubular forms have demonstrated to experience shear lag in both the flange and web panels. A hybrid structural form that allows the building to function totally compositely is much desired. Large scale bracing imposed on the web and flange panels have been shown to significantly reduce the degree of shear lag present in the panels. This scheme was modeled in SAP (Figure 6 - 18) and the results are shown in Table 6 - 7. Bracing was introduced into model 1 to study its effect on shear lag.

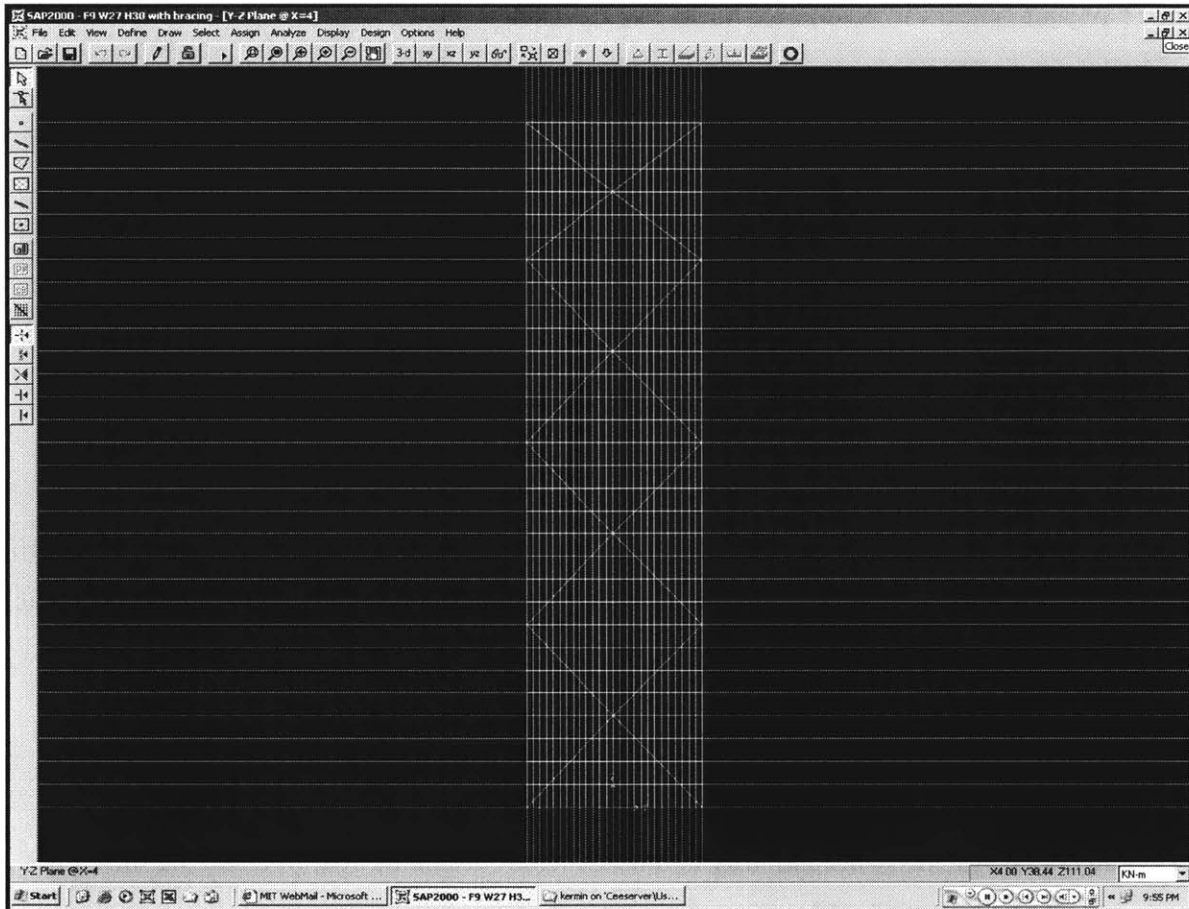


Figure 6 - 18: Tubular Structure with Bracing

Table 6 - 7: Shear Lag Coefficients with Bracing Introduced

Model	Flange Shear Lag Coefficient	Web Shear Lag Coefficient
1 (without bracing)	0.442	0.143
1 (with bracing)	0.833	0.311

Large scale bracing is seen to have a significant effect on the degree of shear lag present in the structure. The introduction of bracing into model 1 reduced the degree of shear lag present by almost half in both the flange and web panels (increases in shear lag coefficient). Bracing essentially increases the vertical rigidity between two adjacent stories such that the inter-story vertical displacement is constrained to be the same. This behavior targets the occurrence of positive and negative shear lag at its cause and has proven to be very effective in practice. The most successful implementation of this scheme has been in the John Hancock Center in Chicago where the structural form has been often classified as a braced tube, engaging the full composite action of the structure to resist the lateral loads.

6.4 Conclusion (Tubular Structures)

The tubular structure has been shown to behave radically different from previously explored lateral systems. The similarity to other schemes lies in the goal of engaging the entire perimeter structure of the building to participate in the lateral resistance. However, the tubular structure does so different by seeking to make the building function like a large cantilever beam attached to the ground. This has been demonstrated to be hard to achieve due to the occurrence of shear lag.

The phenomenon of shear lag has been researched to compose of both a positive and negative component. The magnitude of positive shear lag has been illustrated to occur most prominently at the base of the structure and decrease along the height. A point of shear lag reversal has also been illustrated to exist. This is the point at which shear lag ceases to exist and beyond this point, towards the top of the structure, negative shear lag is seen to dominate.

The effects of varying base dimensions and height of the structure on the magnitude of shear lag in both the web and flange panels was also discussed. Both flange and web shear lag was demonstrated to depend mostly on the height of the structure. Shear lag was seen to be most prominent in shorter structures (structures with small aspect ratios).

Finally, methods of reducing shear lag was explored. Large scale bracing was seen to be the most effective tool in accomplishing this.

6.5 References

- [1] www.emporis.com
- [2] W. Schueller, The Vertical Building Structure, New York: Van Nostrand Reinhold, 1990.
- [3] A.K. H. Kwan, "Simple Method For Approximate Analysis of Framed Tube Structures," Journal of Structural Engineering, Vol. 120, No. 4, Apr 1994, pp. 1221-1239.
- [4] Y. Singh and A. K. Nagpal, "Negative Shear Lag in Framed-Tube Buildings," Journal of Structural Engineering, Vol. 120, No. 11, Nov 1994, pp. 3105-3121.
- [5] K. Kwan, "Shear Lag Shear/Core Walls," Journal of Structural Engineering, Vol. 122, No. 9, Sep. 1996, pp.1097-1104.
- [6] K. Lee, L. Lee, E. Lee, "Predication of Shear-Lag Effects in Framed-Tube Structures with Internal Tubes(s)," The Structural Design of Tall Buildings, Vol. 11, No.2, Jun 2002, pp. 79-92.
- [7] Taranath, Structural Analysis & Design of Tall Buildings, New York: McGraw-Hill Book Company, 1988.
- [8] S. Smith and A. Coull, Tall Building Structures: Analysis and Design, New York: John Wiley & Sons, Inc, 1991.

7 Chapter 7: Stiffness Distribution for Braced Frames

7.1 Introduction

It has been demonstrated in previous chapters and in other literature that the structural engineering of tall buildings is centered on controlling both the dynamic and static motion of the structure. Various lateral schemes have been explored in previous chapters and this chapter will focus on understanding the methodology and implications of different distributions of lateral stiffness between the various elements. The goal is to obtain an accurate understanding of how the structure might perform under the lateral loadings during the preliminary stage of design. This gives the engineer a sense of what section sizes might be required for key structural elements.

This section will utilize an example of a planar frame with six columns. Bracing is assumed to run across three bays of the structure giving it lateral stiffness. The aspect ratios will be computed using this three bay width as the base. Girder spacing was maintained at 3.5m on center vertically and columns 7m on center horizontally.

7.2 Methodology for Analyzing Stiffness Distributions

The following equations and parameters are defined in order to understand the effect of different stiffness distributions in a structure.

$$\begin{aligned}
 u(H) &= \gamma H - \frac{\chi H^2}{2} \\
 s &= \frac{\frac{\chi H^2}{2}}{\gamma H} \\
 u_H &= (1+s)\gamma H \\
 \alpha &= (1+s)\gamma && (7-1 \text{ to } 7-8) \\
 V &= D_T \gamma \\
 D_T &= D_{brace} + D_{frame} \\
 f &= \frac{\varepsilon^d}{\varepsilon^c} \\
 s &= \frac{H \sin(2\theta)}{2fB}
 \end{aligned}$$

where:

γ	-	transverse shearing strain
χ	-	bending deformation parameter
H	-	Height of structure
s	-	ratio of bending to shear deformation
α	-	allowable drift ratio
V	-	Story shear
D_T	-	Shear rigidity
f	-	Ratio of allowable diagonal strain to chord/column strain
B	-	Width of structure

For each model, the following procedure was followed using Equations 7-1 to 7-6.

Equations 7 - 7 and 7 – 8 were used for preliminary design and this will be discussed later in the chapter.

- 1) Assume a preliminary s (e.g. $s = 1/2$)
- 2) Assume allowable drift α (e.g. $\alpha = 1/500$)
- 3) Compute allowable γ
- 4) Compute story shear V
- 5) Compute required structure shear rigidity ($D_t = V/\gamma$)
- 6) Pick an allocation of stiffness to bracing (e.g. ratio = 80%)
- 7) Compute required D_{brace} ($0.8 * D_T/\gamma$)

- 8) Pick diagonal cross sectional area to satisfy truss rigidity requirement
- 9) Pick column inertia to satisfy frame rigidity requirement
- 10) Compute shear deflection for whole structure
- 11) Compute cantilever beam bending deflection
- 12) Compute s (beam bending deflection / shear deflection)

The size of the sections for each model studied was selected based on its stiffness capacity, cross sectional area of the diagonal elements and moment of inertias for the column elements. The moment and axial capacities of the required sections were found to be greater than that required for strength considerations. The dominance of stiffness requirements over strength requirements was again illustrated here.

7.3 Results of Parametric Study

Three models of varying aspect ratios were run. This gave an insight into the expected ratio of bending to shear deformation for different aspect ratios. A fourth study was performed to understand the sensitivity of the original analysis to a change in the initial assumed value of “ s ”. The four models analyzed are shown in Table 7 - 1.

Table 7 - 1: Braced Frame Models Analyzed

Model	Storys	Aspect Ratio	Assumed “ s ”
1	20	3.37	0.5
2	30	5	0.5
3	40	6.67	0.5
4	30	5	0.25

For each of the 4 models analyzed, elements were sized as discussed in the previous section and the “ s ” value was computed. The results of this study are illustrated in Figure 7 - 1. The results are inline with what is generally expected from the structures of different heights. Complete calculations and results are attached in Appendix G.

Firstly, for a given “ p ”, the forty story structure exhibits a higher value of “ s ” implying that the frame’s deformation was more attributed to bending compared to shear. This is in contrast to the shorter structures where the “ s ” values are smaller implying that the deformation was mainly attributed to shear.

Second, regardless of aspect ratio, all models demonstrated an exponential increase in the value of “s” as the percentage of stiffness directed to the diagonal (p) increased. This implies that as the stiffness of the braced bay which essentially behaves like a cantilever beam increases relative to the stiffness of the shear columns, the bending deformations increasingly dominates the deformation mode.

Third, in the twenty story structure with a relatively low aspect ratio, the structure is dominated by shear deformation regardless of the value of “p” assigned. This implies that the introduction of diagonals do not serve to shift the dominance of deformation from shear to bending deformation. This suggests that the determining factor for the dominant mode of deformation in structures is its height.

Fourth, the assumed value of “s” in the beginning of each analysis had little impact on the final results. This is demonstrated by the small variance in results between the two thirty story models studied. With the two trend lines plotted, the expected value of “s” for each starting value of “s” was approximately equal at low values of “p” and appreciable deviation was only noticed above “p” values of 80%.

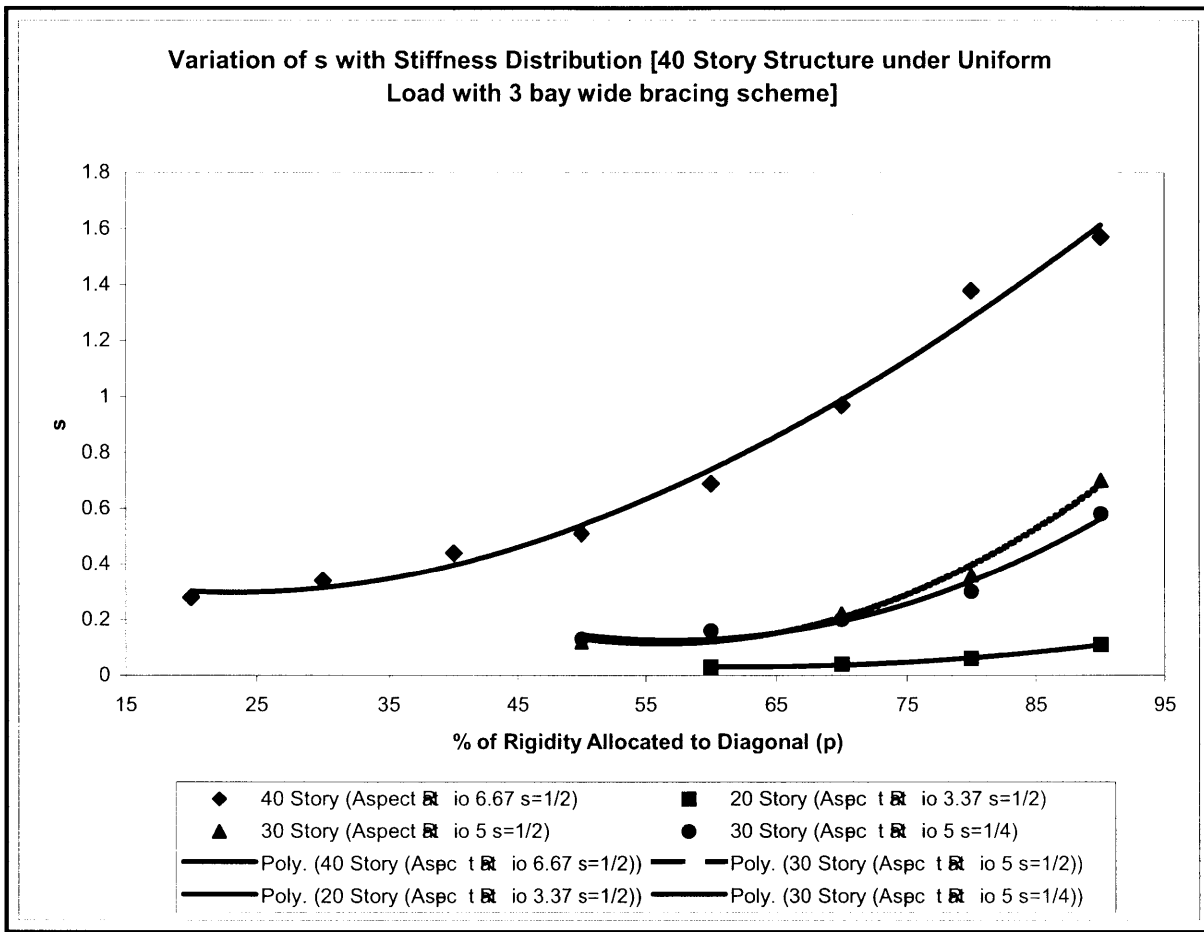


Figure 7 - 1: Variation of “ s ” with Aspect Ratios

7.4 Implications for Design

With the results presented, it is possible to draw some implications for the design of the lateral systems for structures. With an aspect ratio defined, it is possible to define the desired value of “ s ” for a structure, based on the parameter “ f ”. Next, referring to a graph with the variation of “ s ” with a multitude of aspect ratios, it is possible to obtain the desired value of “ s ” by selecting a value of “ p ”.

With this value of “ p ”, it is possible to select element sizes to obtain that percentage of shear rigidity and theoretically obtain the desired value of “ s ”.

7.5 Conclusion

This chapter has outlined the equations and parameters needed to understand how a particular allocation of stiffness distribution can affect the relative contributions of the two

modes of deformation that is present in a structure. The results of this study for structures of different aspect ratios was also presented and discussed. Finally, the implications for the actual selection of shear stiffness distribution was examined.

7.6 References

- [1] J. J. Connor, Introduction to Structural Motion Control, New Jersey: Prentice Hall, 2003.

Appendix A

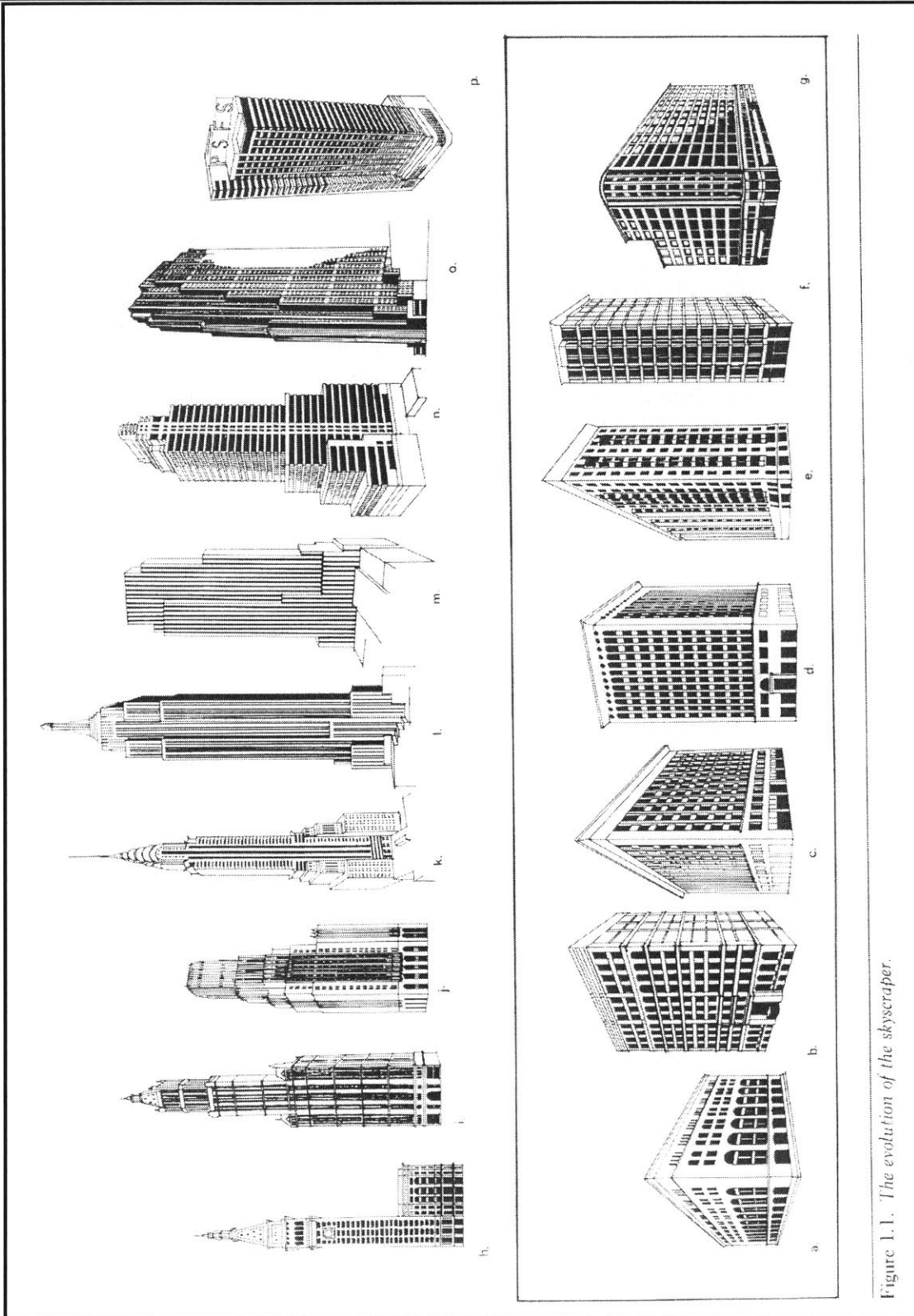


Figure 1.1. The evolution of the skyscraper.

Figure A - 1: Evolution of Skyscraper Form

Appendix B

Calculation of Wind Loads

$$p = qGCp - qhGCPi$$

alpha	5
2/alpha	0.4
zg	457

Kzt	1.2996
K1	1
K2	1
K3	0.14

V	49	m/s
V ²	2401	

Base	35	m
Story Height	3.5	m

Stories	height (m)	Kz	qz
0	0	0.00	0
5	18	0.55	1199
10	35	0.72	1582
15	53	0.85	1861
20	70	0.95	2088
25	88	1.04	2282
30	105	1.12	2455
35	123	1.19	2611
40	140	1.25	2754
45	158	1.31	2887

10 Storys			
1582			
p (windward)	p (leeward)	p total	nodal force
		Kn/M ²	Kn
483	-348	0.83	51
728	-348	1.08	66

20 Storys			
2088			
p (windward)	p (leeward)	p total	nodal force
391	-459	0.85	52
637	-459	1.10	67
815	-459	1.27	78
960	-459	1.42	87

Calculation of Wind Loads

I	1.15
with Cat III	

GCp windward	0.64
GCp leeward	-0.4

Gcpi (windward)	0.18
Gcpi (leeward)	-0.18

30 Stories			
2450			
p (windward)	p (leeward)	p total	nodal force
326	-539	0.87	53
572	-539	1.11	68
750	-539	1.29	79
895	-539	1.43	88
1020	-539	1.56	95
1130	-539	1.67	102

40 Stories			
2754			
p (windward)	p (leeward)	p total	nodal force
272	-606	0.88	54
517	-606	1.12	69
695	-606	1.30	80
840	-606	1.45	89
965	-606	1.57	96
1076	-606	1.68	103
1175	-606	1.78	109
1267	-606	1.87	115

Calculation of Section Properties

Lateral Systems for Tall Buildings
Appendix B

Fy 344737 kPa
 Breadth 0.6 m
 c 0.3 m

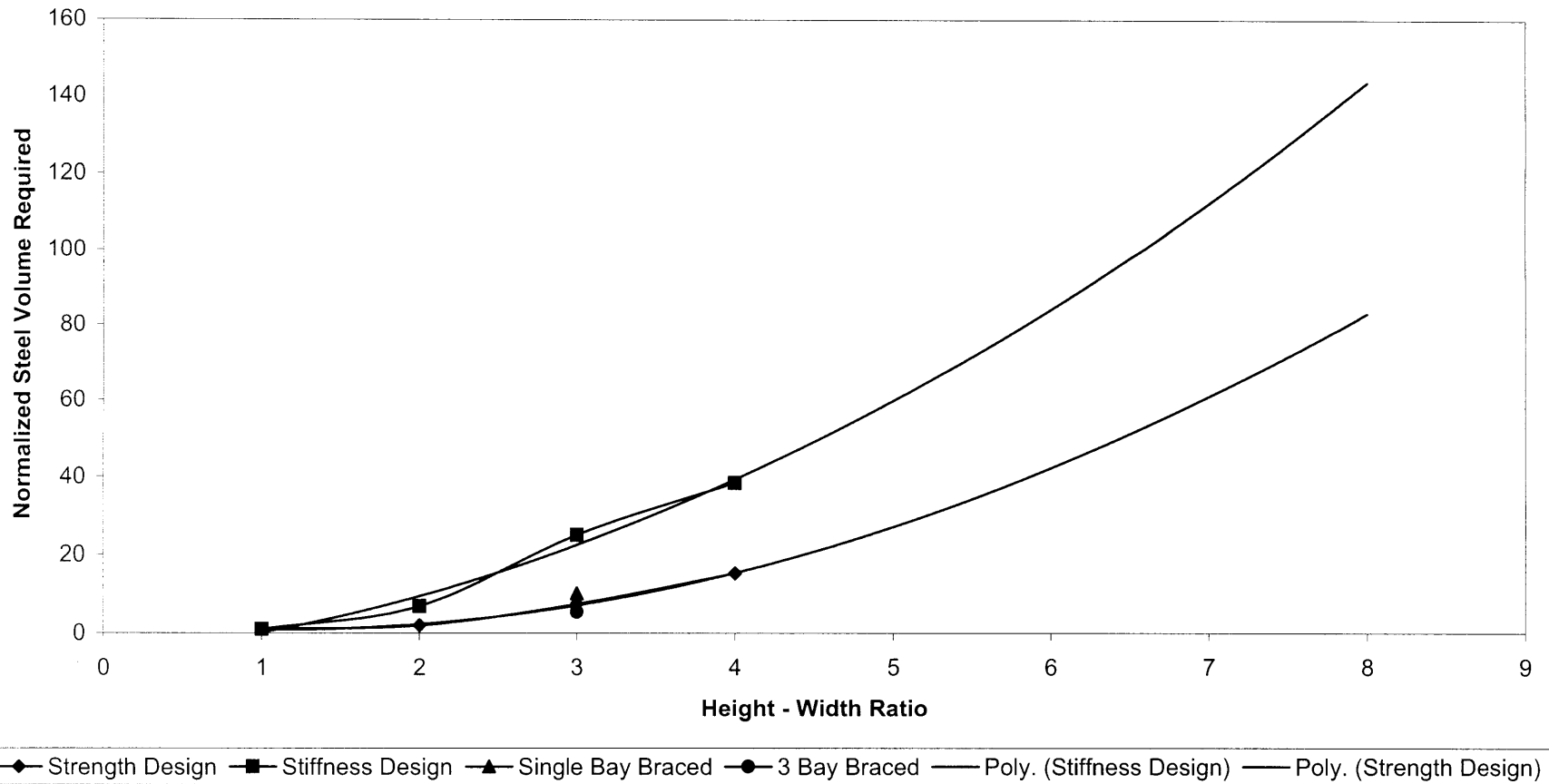
t	b ⁴	(b-2t) ⁴	MOI (m ⁴)	S [I/c (m ³)]	Z (m ³)	Mp (kN-m)	My (kN-m)	Pn (kN)	Area (m ²)
0.01	0.1296	0.11316496	1.370E-03	5.E-03	0.00534	1841	1574	8136	0.024
0.02	0.1296	0.09834496	2.605E-03	9.E-03	0.01056	3640	2993	15996	0.046
0.03	0.1296	0.08503056	3.714E-03	1.E-02	0.01566	5399	4268	23580	0.068
0.04	0.1296	0.07311616	4.707E-03	2.E-02	0.02064	7115	5409	30888	0.090
0.05	0.1296	0.0625	5.592E-03	2.E-02	0.0255	8791	6426	37921	0.110
0.06	0.1296	0.05308416	6.376E-03	2.E-02	0.03024	10425	7327	44678	0.130
0.07	0.1296	0.04477456	7.069E-03	2.E-02	0.03486	12018	8123	51159	0.148
0.08	0.1296	0.03748096	7.677E-03	3.E-02	0.03936	13569	8821	57364	0.166
0.09	0.1296	0.03111696	8.207E-03	3.E-02	0.04374	15079	9431	63294	0.184
0.1	0.1296	0.0256	8.667E-03	3.E-02	0.048	16547	9959	68947	0.200
0.11	0.1296	0.02085136	9.062E-03	3.E-02	0.05214	17975	10414	74325	0.216
0.12	0.1296	0.01679616	9.400E-03	3.E-02	0.05616	19360	10802	79427	0.230
0.13	0.1296	0.01336336	9.686E-03	3.E-02	0.06006	20705	11131	84254	0.244
0.14	0.1296	0.01048576	9.926E-03	3.E-02	0.06384	22008	11406	88804	0.258
0.15	0.1296	0.0081	1.013E-02	3.E-02	0.0675	23270	11635	93079	0.270
0.16	0.1296	0.00614656	1.029E-02	3.E-02	0.07104	24490	11822	97078	0.282
0.17	0.1296	0.00456976	1.042E-02	3.E-02	0.07446	25669	11973	100801	0.292
0.18	0.1296	0.00331776	1.052E-02	4.E-02	0.07776	26807	12093	104248	0.302
0.19	0.1296	0.00234256	1.060E-02	4.E-02	0.08094	27903	12186	107420	0.312
0.2	0.1296	0.0016	1.067E-02	4.E-02	0.084	28958	12257	110316	0.320

Appendix C

Steel Volumes Required for Moment Frames and Braced Frames

Stories	Height (m)	Aspect Ratio	Deflection Criteria (m)	Moment Frame		Bracing		Normalized Values			
				Strength Based Steel Vol	Stiffness Based Steel Vol	Single Bay Bracing	3 Bay Wide Bracing	Strength (Normalized)	Stiffness (Normalized)	Single Bay Bracing (normalized)	3 Bay Bracing (normalized)
10	35	1	0.07	8.74	8.74			1.00	1.00		
20	70	2	0.14	17.02	60.59			1.95	6.93		
30	105	3	0.21	65.3	219	88.79	47.87	7.47	25.06	10.16	5.48
40	140	4	0.28	133.73	336			15.30	38.44		

Percentage Increase in Steel Required



Portal Analysis for Moment Frames

Columns	6		Beam Length / floor	35	m
Spacing	7	m	Column Length / floor	21	m
Story Height	3.5	m	Total Steel Length / Floor	56	m
Axial Loading	82	kN			

**Portal Analysis
10 Story**

Story	Nodal Force (kN)	Story Shear (kN)	Column Shear (end) (kN)	Column Moments (kN-m)	Beam Moments (kN)	Beam Shears (kN)	Lateral Column Axial Forces (kN)	Gravity Axial Col Forces (kN)	Total Column Axial Load (kN)	
10	66	66	13	23	23	7	7	82	89	8.05%
9	66	132	26	46	69	20	26	164	190	16.10%
8	66	198	40	69	116	33	59	246	305	24.15%
7	66	264	53	92	162	46	106	328	434	32.20%
6	66	330	66	116	208	59	165	410	575	40.24%
5	51	381	76	133	249	71	236	492	728	47.99%
4	51	432	86	151	285	81	317	574	891	55.30%
3	51	483	97	169	320	92	409	656	1065	62.33%
2	51	534	107	187	356	102	511	738	1249	69.19%
1	51	585	117	205	392	112	623	820	1443	75.91%

20 Story

Story	Nodal Force (kN)	Story Shear (kN)	Column Shear (end) (kN)	Column Moments (kN-m)	Beam Moments (kN)	Beam Shears (kN)	Lateral Column Axial Forces (kN)	Gravity Axial Col Forces (kN)	Total Column Axial Load (kN)	
20	87	87	17	30	30	9	9	82	91	10.61%
19	87	174	35	61	91	26	35	164	199	21.22%
18	87	261	52	91	152	44	78	246	324	31.83%
17	87	348	70	122	213	61	139	328	467	42.44%
16	87	435	87	152	274	78	218	410	628	53.05%
15	78	513	103	180	332	95	312	492	804	63.48%
14	78	591	118	207	386	110	423	574	997	73.64%
13	78	669	134	234	441	126	549	656	1205	83.64%
12	78	747	149	261	496	142	690	738	1428	93.54%
11	78	825	165	289	550	157	848	820	1668	103.35%
10	67	892	178	312	601	172	1019	902	1921	112.99%
9	67	959	192	336	648	185	1204	984	2188	122.39%
8	67	1026	205	359	695	199	1403	1066	2469	131.59%
7	67	1093	219	383	742	212	1615	1148	2763	140.65%
6	67	1160	232	406	789	225	1840	1230	3070	149.59%
5	52	1212	242	424	830	237	2077	1312	3389	158.32%
4	52	1264	253	442	867	248	2325	1394	3719	166.77%
3	52	1316	263	461	903	258	2583	1476	4059	174.99%
2	52	1368	274	479	939	268	2851	1558	4409	183.00%
1	52	1420	284	497	976	279	3130	1640	4770	190.85%

Portal Analysis for Moment Frames

**Column Design
10 Story**

Column Width = 0.4m

Mu	116	Pu	575	Inertia	3.96E-04	Set 2
Mn	682	Pn	5377	Area (m ³)	0.0156	
Mu / 0Mn	0.20	Pu/0Pn	0.126			
Pu/0Pn > 0.2		Pu/0Pn <0.2		Total Steel Vol (5 Floors)	4.368	
	0.30		0.26			
Mu	205	Pu	1443	Inertia	3.96E-04	Set 1
Mn	682	Pn	5377	Area (m ³)	0.0156	
Mu / 0Mn	0.35	Pu/0Pn	0.316			
Pu/0Pn > 0.2		Pu/0Pn <0.2		Total Steel Vol (5 Floors)	4.368	
	0.63		0.51			

20 Story

Column Width = 0.4m

Mu	152	Pu	628	Inertia	3.96E-04	Set 4
Mn	682	Pn	5377	Area	0.0156	
Mu / 0Mn	0.26	Pu/0Pn	0.137			
Pu/0Pn > 0.2		Pu/0Pn <0.2		Total Steel Vol (5 Floors)	4.368	
	0.37		0.33			
Mu	289	Pu	1668	Inertia	3.96E-04	Set 3
Mn	682	Pn	5377	Area	0.0156	
Mu / 0Mn	0.50	Pu/0Pn	0.365			
Pu/0Pn > 0.2		Pu/0Pn <0.2		Total Steel Vol (5 Floors)	4.368	
	0.81		0.68			
Mu	406	Pu	3070	Inertia	7.34E-04	Set 2
Mn	1265	Pn	10480	Area	0.0304	
Mu / 0Mn	0.38	Pu/0Pn	0.345			
Pu/0Pn > 0.2		Pu/0Pn <0.2		Total Steel Vol (5 Floors)	8.512	
	0.68		0.55			
Mu	497	Pu	4770	Inertia	7.34E-04	Set 1
Mn	1265	Pn	10480	Area	0.0304	
Mu / 0Mn	0.46	Pu/0Pn	0.535			
Pu/0Pn > 0.2		Pu/0Pn <0.2		Total Steel Vol (5 Floors)	8.512	
	0.95		0.73			

Portal Analysis for Moment Frames

E 1.99E+08 kPa

Strength Based Design Displacement Analysis

10 Story

Inertia (col)	Inertia (beam)	Area	Vh ² /12	h / EI (col)	1/ (EI/L)	Uk (interstory)	% contribution	Disp (m)	SAP	% Error	Max Disp	Steel Vol	
3.96E-04	3.96E-04	0.0156	67	7.40E-06	1.78E-05	0.002	2%	0.087	0.088	-0.59%	0.07	0.87	Set 2
3.96E-04	3.96E-04	0.0156	135	7.40E-06	1.78E-05	0.003	4%	0.086				0.87	
3.96E-04	3.96E-04	0.0156	202	7.40E-06	1.78E-05	0.005	6%	0.082			25.71%	0.87	
3.96E-04	3.96E-04	0.0156	270	7.40E-06	1.78E-05	0.007	8%	0.077				0.87	
3.96E-04	3.96E-04	0.0156	337	7.40E-06	1.78E-05	0.008	10%	0.071				0.87	Set 1
3.96E-04	3.96E-04	0.0156	389	7.40E-06	1.78E-05	0.010	11%	0.062				0.87	
3.96E-04	3.96E-04	0.0156	441	7.40E-06	1.78E-05	0.011	13%	0.052				0.87	
3.96E-04	3.96E-04	0.0156	493	7.40E-06	1.78E-05	0.012	14%	0.041				0.87	
3.96E-04	3.96E-04	0.0156	545	7.40E-06	1.78E-05	0.014	16%	0.029				0.87	
3.96E-04	3.96E-04	0.0156	597	7.40E-06	1.78E-05	0.015	17%	0.015				0.87	
8.736													

20 Story

Inertia (col)	Inertia (beam)	Area	Vh ² /12	h / EI (col)	1/ (EI/L)	Uk (interstory)	% contribution	Disp (m)	SAP	% Error	Max Disp	Steel Vol	
3.96E-04	3.96E-04	0.0156	89	7.40E-06	1.78E-05	0.002	1%	0.282	0.3	-6.07%	0.14	0.87	Set 4
3.96E-04	3.96E-04	0.0156	178	7.40E-06	1.78E-05	0.004	2%	0.280				0.87	
3.96E-04	3.96E-04	0.0156	266	7.40E-06	1.78E-05	0.007	2%	0.275			114.29%	0.87	
3.96E-04	3.96E-04	0.0156	355	7.40E-06	1.78E-05	0.009	3%	0.268				0.87	
3.96E-04	3.96E-04	0.0156	444	7.40E-06	1.78E-05	0.011	4%	0.259				0.87	Set 3
3.96E-04	3.96E-04	0.0156	524	7.40E-06	1.78E-05	0.013	5%	0.248				0.87	
3.96E-04	3.96E-04	0.0156	603	7.40E-06	1.78E-05	0.015	5%	0.235				0.87	
3.96E-04	3.96E-04	0.0156	683	7.40E-06	1.78E-05	0.017	6%	0.220				0.87	
3.96E-04	3.96E-04	0.0156	763	7.40E-06	1.78E-05	0.019	7%	0.203				0.87	
3.96E-04	3.96E-04	0.0156	842	7.40E-06	1.78E-05	0.021	8%	0.184				0.87	
7.34E-04	7.34E-04	0.0304	911	3.99E-06	9.58E-06	0.012	4%	0.162				1.70	Set 2
7.34E-04	7.34E-04	0.0304	979	3.99E-06	9.58E-06	0.013	5%	0.150				1.70	
7.34E-04	7.34E-04	0.0304	1047	3.99E-06	9.58E-06	0.014	5%	0.137				1.70	
7.34E-04	7.34E-04	0.0304	1116	3.99E-06	9.58E-06	0.015	5%	0.122				1.70	
7.34E-04	7.34E-04	0.0304	1184	3.99E-06	9.58E-06	0.016	6%	0.107				1.70	
7.34E-04	7.34E-04	0.0304	1237	3.99E-06	9.58E-06	0.017	6%	0.091				1.70	
7.34E-04	7.34E-04	0.0304	1290	3.99E-06	9.58E-06	0.018	6%	0.074				1.70	
7.34E-04	7.34E-04	0.0304	1343	3.99E-06	9.58E-06	0.018	6%	0.057				1.70	
7.34E-04	7.34E-04	0.0304	1397	3.99E-06	9.58E-06	0.019	7%	0.039				1.70	
7.34E-04	7.34E-04	0.0304	1450	3.99E-06	9.58E-06	0.020	7%	0.020				1.70	
17.024													

Portal Analysis for Moment Frames

Stiffness Based Design Displacement Analysis

10 Story

Inertia (col)	Inertia (beam)	Area	Vh ² /12	h / EI (col)	1/(EI/L)	Uk (interstory)	Disp (m)	Steel Vol

0.00

20 Story

Inertia (col)	Inertia (beam)	Area	Vh ² /12	h / EI (col)	1/(EI/L)	Uk (interstory)	Disp (m)	Total Steel Vol
1.02E-03	1.02E-03	0.0444	89	2.87E-06	6.90E-06	0.001	0.134	2.49
1.02E-03	1.02E-03	0.0444	178	2.87E-06	6.90E-06	0.002	0.133	2.49
1.02E-03	1.02E-03	0.0444	266	2.87E-06	6.90E-06	0.003	0.131	2.49
1.02E-03	1.02E-03	0.0444	355	2.87E-06	6.90E-06	0.003	0.128	2.49
1.02E-03	1.02E-03	0.0444	444	2.87E-06	6.90E-06	0.004	0.125	2.49
1.02E-03	1.02E-03	0.0444	524	2.87E-06	6.90E-06	0.005	0.121	2.49
1.02E-03	1.02E-03	0.0444	603	2.87E-06	6.90E-06	0.006	0.116	2.49
1.02E-03	1.02E-03	0.0444	683	2.87E-06	6.90E-06	0.007	0.110	2.49
1.02E-03	1.02E-03	0.0444	763	2.87E-06	6.90E-06	0.007	0.103	2.49
1.02E-03	1.02E-03	0.0444	842	2.87E-06	6.90E-06	0.008	0.096	2.49
1.26E-03	1.26E-03	0.0576	911	2.33E-06	5.58E-06	0.007	0.087	3.23
1.26E-03	1.26E-03	0.0576	979	2.33E-06	5.58E-06	0.008	0.080	3.23
1.26E-03	1.26E-03	0.0576	1047	2.33E-06	5.58E-06	0.008	0.072	3.23
1.26E-03	1.26E-03	0.0576	1116	2.33E-06	5.58E-06	0.009	0.064	3.23
1.26E-03	1.26E-03	0.0576	1184	2.33E-06	5.58E-06	0.009	0.055	3.23
1.46E-03	1.46E-03	0.07	1237	2.01E-06	4.82E-06	0.008	0.046	3.92
1.46E-03	1.46E-03	0.07	1290	2.01E-06	4.82E-06	0.009	0.037	3.92
1.46E-03	1.46E-03	0.07	1343	2.01E-06	4.82E-06	0.009	0.029	3.92
1.46E-03	1.46E-03	0.07	1397	2.01E-06	4.82E-06	0.010	0.019	3.92
1.46E-03	1.46E-03	0.07	1450	2.01E-06	4.82E-06	0.010	0.010	3.92

60.59

Portal Analysis for Moment Frames

Portal Analysis

30 Story

Story	Nodal Force (kN)	Story Shear (kN)	Column Shear (end) (kN)	Column Moments (kN-m)	Beam Moments (kN)	Beam Shears (kN)	Lateral Column Axial Forces (kN)	Gravity Axial Col Forces (kN)	Total Column Axial Load (kN)	
30	102	102	20	36	36	10	10	82	92	12.44%
29	102	204	41	71	107	31	41	164	205	24.88%
28	102	306	61	107	179	51	92	246	338	37.32%
27	102	408	82	143	250	71	163	328	491	49.76%
26	102	510	102	179	321	92	255	410	665	62.20%
25	95	605	121	212	390	112	367	492	859	74.49%
24	95	700	140	245	457	131	497	574	1071	86.59%
23	95	795	159	278	523	150	647	656	1303	98.55%
22	95	890	178	312	590	169	815	738	1553	110.43%
21	95	985	197	345	656	188	1003	820	1823	122.26%
20	88	1073	215	376	720	206	1208	902	2110	133.96%
19	88	1161	232	406	782	223	1432	984	2416	145.50%
18	88	1249	250	437	844	241	1673	1066	2739	156.91%
17	88	1337	267	468	905	259	1931	1148	3079	168.23%
16	88	1425	285	499	967	276	2208	1230	3438	179.47%
15	79	1504	301	526	1025	293	2500	1312	3812	190.58%
14	79	1583	317	554	1080	309	2809	1394	4203	201.51%
13	79	1662	332	582	1136	325	3134	1476	4610	212.30%
12	79	1741	348	609	1191	340	3474	1558	5032	222.97%
11	79	1820	364	637	1246	356	3830	1640	5470	233.54%
10	68	1888	378	661	1298	371	4201	1722	5923	243.95%
9	68	1956	391	685	1345	384	4585	1804	6389	254.17%
8	68	2024	405	708	1393	398	4983	1886	6869	264.22%
7	68	2092	418	732	1441	412	5395	1968	7363	274.13%
6	68	2160	432	756	1488	425	5820	2050	7870	283.90%
5	53	2213	443	775	1531	437	6257	2132	8389	293.49%
4	53	2266	453	793	1568	448	6705	2214	8919	302.85%
3	53	2319	464	812	1605	459	7164	2296	9460	312.01%
2	53	2372	474	830	1642	469	7633	2378	10011	320.98%
1	53	2425	485	849	1679	480	8113	2460	10573	329.78%
Base Shear	2425									

Portal Analysis for Moment Frames

Column Design

30 Story

Column Width = 0.4m

Mu	179	Pu	665	Inertia	3.96E-04	Set 6
Mn	682	Pn	5377	Area	0.0156	
Mu / 0Mn	0.31	Pu/0Pn	0.145			
Pu/0Pn > 0.2		Pu/0Pn <0.2				
0.42		0.38		Total Steel Vol (5 Floors)	4.368	
Mu	345	Pu	1823	Inertia	3.96E-04	Set 5
Mn	682	Pn	5377	Area	0.0156	
Mu / 0Mn	0.59	Pu/0Pn	0.399			
Pu/0Pn > 0.2		Pu/0Pn <0.2				
0.93		0.79		Total Steel Vol (5 Floors)	4.368	
Mu	499	Pu	3438	Inertia	7.34E-04	Set 4
Mn	1265	Pn	10480	Area	0.03	
Mu / 0Mn	0.46	Pu/0Pn	0.386			
Pu/0Pn > 0.2		Pu/0Pn <0.2				
0.80		0.66		Total Steel Vol (5 Floors)	8.4	
Mu	637	Pu	5470	Inertia	1.02E-03	Set 3
Mn	1758	Pn	15306	Area	0.044	
Mu / 0Mn	0.43	Pu/0Pn	0.420			
Pu/0Pn > 0.2		Pu/0Pn <0.2				
0.80		0.64		Total Steel Vol (5 Floors)	12.32	
Mu	756	Pu	7870	Inertia	1.26E-03	Set 2
Mn	2171	Pn	19857	Area	0.058	
Mu / 0Mn	0.41	Pu/0Pn	0.466			
Pu/0Pn > 0.2		Pu/0Pn <0.2				
0.83		0.64		Total Steel Vol (5 Floors)	16.24	
Mu	849	Pu	10573	Inertia	1.46E-03	Set 1
Mn	2514	Pn	24132	Area	0.07	
Mu / 0Mn	0.40	Pu/0Pn	0.515			
Pu/0Pn > 0.2		Pu/0Pn <0.2				
0.87		0.65		Total Steel Vol (5 Floors)	19.6	

Portal Analysis for Moment Frames

Strength Based Design Displacement Analysis

30 Story

Inertia (col)	Inertia (beam)	Area	Vh ² /12	h / EI (col)	1/ (EI/L)	Uk (interstory)	% contribution	Disp (m)	SAP	% Error	Max Disp	Steel Vol	
3.96E-04	3.96E-04	0.0156	104	7.40E-06	1.78E-05	0.003	1%	0.473	0.544	-12.98%	0.21	0.87	Set 6
3.96E-04	3.96E-04	0.0156	208	7.40E-06	1.78E-05	0.005	1%	0.471				0.87	
3.96E-04	3.96E-04	0.0156	312	7.40E-06	1.78E-05	0.008	2%	0.466			159.05%	0.87	
3.96E-04	3.96E-04	0.0156	417	7.40E-06	1.78E-05	0.010	2%	0.458				0.87	
3.96E-04	3.96E-04	0.0156	521	7.40E-06	1.78E-05	0.013	3%	0.447				0.87	Set 5
3.96E-04	3.96E-04	0.0156	618	7.40E-06	1.78E-05	0.016	3%	0.434				0.87	
3.96E-04	3.96E-04	0.0156	715	7.40E-06	1.78E-05	0.018	4%	0.419				0.87	
3.96E-04	3.96E-04	0.0156	812	7.40E-06	1.78E-05	0.020	4%	0.401				0.87	
3.96E-04	3.96E-04	0.0156	909	7.40E-06	1.78E-05	0.023	5%	0.380				0.87	Set 4
3.96E-04	3.96E-04	0.0156	1006	7.40E-06	1.78E-05	0.025	5%	0.357				0.87	
7.34E-04	7.34E-04	0.03	1095	3.99E-06	9.58E-06	0.015	3%	0.332				1.68	
7.34E-04	7.34E-04	0.03	1185	3.99E-06	9.58E-06	0.016	3%	0.317				1.68	
7.34E-04	7.34E-04	0.03	1275	3.99E-06	9.58E-06	0.017	4%	0.301				1.68	Set 3
7.34E-04	7.34E-04	0.03	1365	3.99E-06	9.58E-06	0.019	4%	0.284				1.68	
7.34E-04	7.34E-04	0.03	1455	3.99E-06	9.58E-06	0.020	4%	0.265				1.68	
1.02E-03	1.02E-03	0.044	1535	2.87E-06	6.90E-06	0.015	3%	0.245				2.46	
1.02E-03	1.02E-03	0.044	1616	2.87E-06	6.90E-06	0.016	3%	0.230				2.46	Set 2
1.02E-03	1.02E-03	0.044	1697	2.87E-06	6.90E-06	0.017	4%	0.215				2.46	
1.02E-03	1.02E-03	0.044	1777	2.87E-06	6.90E-06	0.017	4%	0.198				2.46	
1.02E-03	1.02E-03	0.044	1858	2.87E-06	6.90E-06	0.018	4%	0.181				2.46	
1.26E-03	1.26E-03	0.058	1927	2.33E-06	5.58E-06	0.015	3%	0.163				3.25	Set 1
1.26E-03	1.26E-03	0.058	1997	2.33E-06	5.58E-06	0.016	3%	0.147				3.25	
1.26E-03	1.26E-03	0.058	2066	2.33E-06	5.58E-06	0.016	3%	0.131				3.25	
1.26E-03	1.26E-03	0.058	2136	2.33E-06	5.58E-06	0.017	4%	0.115				3.25	
1.46E-03	1.46E-03	0.07	2205	2.33E-06	5.58E-06	0.017	4%	0.098				3.25	Set 1
1.46E-03	1.46E-03	0.07	2259	2.01E-06	4.82E-06	0.015	3%	0.081				3.92	
1.46E-03	1.46E-03	0.07	2313	2.01E-06	4.82E-06	0.016	3%	0.065				3.92	
1.46E-03	1.46E-03	0.07	2367	2.01E-06	4.82E-06	0.016	3%	0.050				3.92	
1.46E-03	1.46E-03	0.07	2421	2.01E-06	4.82E-06	0.017	3%	0.033				3.92	Set 1
1.46E-03	1.46E-03	0.07	2476	2.01E-06	4.82E-06	0.017	4%	0.017				3.92	

65.296

Portal Analysis for Moment Frames

Stiffness Based Design Displacement Analysis

30 Story

Inertia (col)	Inertia (beam)	Area	Vh ² /12	h / EI (col)	1/(EI/L)	Uk (interstory)	Disp (m)	Total Steel Vol
1.94E-03	1.94E-03	0.116	104	1.51E-06	3.63E-06	0.001	0.205	6.50
1.94E-03	1.94E-03	0.116	208	1.51E-06	3.63E-06	0.001	0.205	6.50
1.94E-03	1.94E-03	0.116	312	1.51E-06	3.63E-06	0.002	0.204	6.50
1.94E-03	1.94E-03	0.116	417	1.51E-06	3.63E-06	0.002	0.202	6.50
1.94E-03	1.94E-03	0.116	521	1.51E-06	3.63E-06	0.003	0.200	6.50
1.94E-03	1.94E-03	0.116	618	1.51E-06	3.63E-06	0.003	0.197	6.50
1.94E-03	1.94E-03	0.116	715	1.51E-06	3.63E-06	0.004	0.194	6.50
1.94E-03	1.94E-03	0.116	812	1.51E-06	3.63E-06	0.004	0.190	6.50
1.94E-03	1.94E-03	0.116	909	1.51E-06	3.63E-06	0.005	0.186	6.50
1.94E-03	1.94E-03	0.116	1006	1.51E-06	3.63E-06	0.005	0.181	6.50
2.00E-03	2.00E-03	0.12	1095	1.47E-06	3.52E-06	0.005	0.176	6.72
2.00E-03	2.00E-03	0.12	1185	1.47E-06	3.52E-06	0.006	0.171	6.72
2.00E-03	2.00E-03	0.12	1275	1.47E-06	3.52E-06	0.006	0.165	6.72
2.00E-03	2.00E-03	0.12	1365	1.47E-06	3.52E-06	0.007	0.159	6.72
2.00E-03	2.00E-03	0.12	1455	1.47E-06	3.52E-06	0.007	0.152	6.72
2.10E-03	2.10E-03	0.1404	1535	1.40E-06	3.35E-06	0.007	0.144	7.86
2.10E-03	2.10E-03	0.1404	1616	1.40E-06	3.35E-06	0.008	0.137	7.86
2.10E-03	2.10E-03	0.1404	1697	1.40E-06	3.35E-06	0.008	0.130	7.86
2.10E-03	2.10E-03	0.1404	1777	1.40E-06	3.35E-06	0.008	0.121	7.86
2.10E-03	2.10E-03	0.1404	1858	1.40E-06	3.35E-06	0.009	0.113	7.86
2.12E-03	2.12E-03	0.1456	1927	1.38E-06	3.32E-06	0.009	0.104	8.15
2.12E-03	2.12E-03	0.1456	1997	1.38E-06	3.32E-06	0.009	0.095	8.15
2.12E-03	2.12E-03	0.1456	2066	1.38E-06	3.32E-06	0.010	0.086	8.15
2.12E-03	2.12E-03	0.1456	2136	1.38E-06	3.32E-06	0.010	0.076	8.15
2.12E-03	2.12E-03	0.1456	2205	1.38E-06	3.32E-06	0.010	0.066	8.15
2.12E-03	2.12E-03	0.1456	2259	1.38E-06	3.32E-06	0.011	0.056	8.15
2.12E-03	2.12E-03	0.1456	2313	1.38E-06	3.32E-06	0.011	0.045	8.15
2.12E-03	2.12E-03	0.1456	2367	1.38E-06	3.32E-06	0.011	0.034	8.15
2.12E-03	2.12E-03	0.1456	2421	1.38E-06	3.32E-06	0.011	0.023	8.15
2.12E-03	2.12E-03	0.1456	2476	1.38E-06	3.32E-06	0.012	0.012	8.15

219.41

Portal Analysis

40 Story

Story	Nodal Force (kN)	Story Shear (kN)	Column Shear (end) (kN)	Column Moments (kN-m)	Beam Moments (kN)	Beam Shears (kN)	Lateral Column Axial Forces (kN)	Gravity Axial Col Forces (kN)	Total Column Axial Load (kN)	
40	115	115	23	40	40	12	12	82	94	14.02%
39	115	230	46	81	121	35	46	164	210	28.05%
38	115	345	69	121	201	58	104	246	350	42.07%
37	115	460	92	161	282	81	184	328	512	56.10%
36	115	575	115	201	362	104	288	410	698	70.12%
35	109	684	137	239	441	126	413	492	905	84.02%
34	109	793	159	278	517	148	561	574	1135	97.75%
33	109	902	180	316	593	170	731	656	1387	111.37%
32	109	1011	202	354	670	191	922	738	1660	124.92%
31	109	1120	224	392	746	213	1135	820	1955	138.41%
30	103	1223	245	428	820	234	1369	902	2271	151.81%
29	103	1326	265	464	892	255	1624	984	2608	165.06%
28	103	1429	286	500	964	276	1900	1066	2966	178.21%
27	103	1532	306	536	1036	296	2196	1148	3344	191.27%
26	103	1635	327	572	1108	317	2513	1230	3743	204.27%
25	96	1731	346	606	1178	337	2849	1312	4161	217.16%
24	96	1827	365	639	1245	356	3205	1394	4599	229.91%
23	96	1923	385	673	1313	375	3580	1476	5056	242.54%
22	96	2019	404	707	1380	394	3974	1558	5532	255.08%
21	96	2115	423	740	1447	413	4388	1640	6028	267.53%
20	89	2204	441	771	1512	432	4819	1722	6541	279.87%
19	89	2293	459	803	1574	450	5269	1804	7073	292.08%
18	89	2382	476	834	1636	468	5737	1886	7623	304.17%
17	89	2471	494	865	1699	485	6222	1968	8190	316.15%
16	89	2560	512	896	1761	503	6725	2050	8775	328.05%
15	80	2640	528	924	1820	520	7245	2132	9377	339.82%
14	80	2720	544	952	1876	538	7781	2214	9995	351.45%
13	80	2800	560	980	1932	552	8333	2296	10629	362.94%
12	80	2880	576	1008	1988	568	8901	2378	11279	374.31%
11	80	2960	592	1036	2044	584	9485	2460	11945	385.57%
10	69	3029	606	1060	2096	599	10084	2542	12626	396.69%
9	69	3098	620	1084	2144	613	10697	2624	13321	407.64%
8	69	3167	633	1108	2193	627	11323	2706	14029	418.44%
7	69	3236	647	1133	2241	640	11963	2788	14751	429.10%
6	69	3305	661	1157	2289	654	12618	2870	15488	439.63%
5	54	3359	672	1176	2332	666	13284	2952	16236	450.00%
4	54	3413	683	1195	2370	677	13961	3034	16995	460.15%
3	54	3467	693	1213	2408	688	14649	3116	17765	470.13%
2	54	3521	704	1232	2446	699	15348	3198	18546	479.92%
1	54	3575	715	1251	2484	710	16058	3280	19338	489.56%

Base Shear 3575
Distributed Load 26 kN/m

Portal Analysis for Moment Frames

Column Design

40 Story

Column Width = 0.4m

Mu	201	Pu	698	Inertia	3.96E-04	Set 8
Mn	682	Pn	5377	Area	0.0156	
Mu / 0Mn	0.35	Pu/0Pn	0.153			
Pu/0Pn > 0.2	0.46	Pu/0Pn < 0.2	0.42	Total Steel Vol (5 Floors)	4.368	
Mu	392	Pu	1955	Inertia	7.34E-04	Set 7
Mn	1265	Pn	10480	Area	0.03	
Mu / 0Mn	0.36	Pu/0Pn	0.219			
Pu/0Pn > 0.2	0.54	Pu/0Pn < 0.2	0.47	Total Steel Vol (5 Floors)	8.4	
Mu	572	Pu	3743	Inertia	1.02E-03	Set 6
Mn	1758	Pn	15306	Area	0.044	
Mu / 0Mn	0.38	Pu/0Pn	0.288			
Pu/0Pn > 0.2	0.63	Pu/0Pn < 0.2	0.53	Total Steel Vol (5 Floors)	12.32	
Mu	740	Pu	6028	Inertia	1.02E-03	Set 5
Mn	1758	Pn	15306	Area	0.044	
Mu / 0Mn	0.50	Pu/0Pn	0.463			
Pu/0Pn > 0.2	0.90	Pu/0Pn < 0.2	0.73	Total Steel Vol (5 Floors)	12.32	
Mu	896	Pu	8775	Inertia	1.26E-03	Set 4
Mn	2171	Pn	19857	Area	0.058	
Mu / 0Mn	0.49	Pu/0Pn	0.520			
Pu/0Pn > 0.2	0.95	Pu/0Pn < 0.2	0.75	Total Steel Vol (5 Floors)	16.24	
Mu	1036	Pu	11945	Inertia	1.62E-03	Set 3
Mn	2794	Pn	28131	Area	0.082	
Mu / 0Mn	0.44	Pu/0Pn	0.500			
Pu/0Pn > 0.2	0.89	Pu/0Pn < 0.2	0.69	Total Steel Vol (5 Floors)	22.96	
Mu	1157	Pu	15488	Inertia	1.75E-03	Set 2
Mn	3021	Pn	31854	Area	0.092	
Mu / 0Mn	0.45	Pu/0Pn	0.572			
Pu/0Pn > 0.2	0.97	Pu/0Pn < 0.2	0.74	Total Steel Vol (5 Floors)	25.76	
Mu	1251	Pu	19338	Inertia	1.94E-03	Set 1
Mn	3341	Pn	38473	Area	0.112	
Mu / 0Mn	0.44	Pu/0Pn	0.591			
Pu/0Pn > 0.2	0.98	Pu/0Pn < 0.2	0.74	Total Steel Vol (5 Floors)	31.36	

Strength Based Design Displacement Analysis

40 Story

Inertia (col)	Inertia (beam)	Area	Vh ² /12	h / EI (col)	1/ (EI/L)	Uk (interstory)	% contribution	Disp (m)	SAP	% Error	Max Disp	Steel Vol	
3.96E-04	3.96E-04	0.0156	117	7.40E-06	1.78E-05	0.003	1%	0.641	0.79	-18.85%	0.28	0.87	Set 8
3.96E-04	3.96E-04	0.0156	235	7.40E-06	1.78E-05	0.006	1%	0.638				0.87	
3.96E-04	3.96E-04	0.0156	352	7.40E-06	1.78E-05	0.009	2%	0.632			182.14%	0.87	
3.96E-04	3.96E-04	0.0156	470	7.40E-06	1.78E-05	0.012	2%	0.623				0.87	
3.96E-04	3.96E-04	0.0156	587	7.40E-06	1.78E-05	0.015	3%	0.612				0.87	
7.34E-04	7.34E-04	0.03	698	3.99E-06	9.58E-06	0.009	2%	0.597				1.68	Set 7
7.34E-04	7.34E-04	0.03	810	3.99E-06	9.58E-06	0.011	2%	0.587				1.68	
7.34E-04	7.34E-04	0.03	921	3.99E-06	9.58E-06	0.013	3%	0.576				1.68	
7.34E-04	7.34E-04	0.03	1032	3.99E-06	9.58E-06	0.014	3%	0.564				1.68	
7.34E-04	7.34E-04	0.03	1143	3.99E-06	9.58E-06	0.016	3%	0.550				1.68	
1.02E-03	1.02E-03	0.044	1248	2.87E-06	6.90E-06	0.012	3%	0.534				2.46	Set 6
1.02E-03	1.02E-03	0.044	1354	2.87E-06	6.90E-06	0.013	3%	0.522				2.46	
1.02E-03	1.02E-03	0.044	1459	2.87E-06	6.90E-06	0.014	3%	0.509				2.46	
1.02E-03	1.02E-03	0.044	1564	2.87E-06	6.90E-06	0.015	3%	0.495				2.46	
1.02E-03	1.02E-03	0.044	1669	2.87E-06	6.90E-06	0.016	3%	0.479				2.46	
1.02E-03	1.02E-03	0.044	1767	2.87E-06	6.90E-06	0.017	4%	0.463				2.46	Set 5
1.02E-03	1.02E-03	0.044	1865	2.87E-06	6.90E-06	0.018	4%	0.446				2.46	
1.02E-03	1.02E-03	0.044	1963	2.87E-06	6.90E-06	0.019	4%	0.427				2.46	
1.02E-03	1.02E-03	0.044	2061	2.87E-06	6.90E-06	0.020	4%	0.408				2.46	
1.02E-03	1.02E-03	0.044	2159	2.87E-06	6.90E-06	0.021	4%	0.388				2.46	
1.26E-03	1.26E-03	0.058	2250	2.33E-06	5.58E-06	0.018	4%	0.367				3.25	Set 4
1.26E-03	1.26E-03	0.058	2341	2.33E-06	5.58E-06	0.019	4%	0.349				3.25	
1.26E-03	1.26E-03	0.058	2432	2.33E-06	5.58E-06	0.019	4%	0.331				3.25	
1.26E-03	1.26E-03	0.058	2522	2.33E-06	5.58E-06	0.020	4%	0.312				3.25	
1.26E-03	1.26E-03	0.058	2613	2.33E-06	5.58E-06	0.021	4%	0.292				3.25	
1.62E-03	1.62E-03	0.082	2695	1.81E-06	4.34E-06	0.017	4%	0.271				4.59	Set 3
1.62E-03	1.62E-03	0.082	2777	1.81E-06	4.34E-06	0.017	4%	0.254				4.59	
1.62E-03	1.62E-03	0.082	2858	1.81E-06	4.34E-06	0.018	4%	0.237				4.59	
1.62E-03	1.62E-03	0.082	2940	1.81E-06	4.34E-06	0.018	4%	0.220				4.59	
1.62E-03	1.62E-03	0.082	3022	1.81E-06	4.34E-06	0.019	4%	0.202				4.59	
1.75E-03	1.75E-03	0.092	3092	1.68E-06	4.02E-06	0.018	4%	0.183				5.15	Set 2
1.75E-03	1.75E-03	0.092	3163	1.68E-06	4.02E-06	0.018	4%	0.165				5.15	
1.75E-03	1.75E-03	0.092	3233	1.68E-06	4.02E-06	0.018	4%	0.147				5.15	
1.75E-03	1.75E-03	0.092	3303	1.68E-06	4.02E-06	0.019	4%	0.129				5.15	
1.75E-03	1.75E-03	0.092	3374	1.68E-06	4.02E-06	0.019	4%	0.110				5.15	
1.94E-03	1.94E-03	0.112	3429	1.51E-06	3.63E-06	0.018	4%	0.091				6.27	Set 1
1.94E-03	1.94E-03	0.112	3484	1.51E-06	3.63E-06	0.018	4%	0.073				6.27	
1.94E-03	1.94E-03	0.112	3539	1.51E-06	3.63E-06	0.018	4%	0.055				6.27	
1.94E-03	1.94E-03	0.112	3594	1.51E-06	3.63E-06	0.018	4%	0.037				6.27	
1.94E-03	1.94E-03	0.112	3649	1.51E-06	3.63E-06	0.019	4%	0.019				6.27	

133.73

Portal Analysis for Moment Frames

Stiffness Based Design Displacement Analysis

40 Story

Inertia (col)	Inertia (beam)	Area	Vh ² /12	h / EI (col)	1/ (EI/L)	Uk (interstory)	Disp (m)	Total Steel Vol
2.13E-03	2.13E-03	0.15	117	1.38E-06	3.30E-06	0.001	0.392	8.40
2.13E-03	2.13E-03	0.15	235	1.38E-06	3.30E-06	0.001	0.391	8.40
2.13E-03	2.13E-03	0.15	352	1.38E-06	3.30E-06	0.002	0.390	8.40
2.13E-03	2.13E-03	0.15	470	1.38E-06	3.30E-06	0.002	0.389	8.40
2.13E-03	2.13E-03	0.15	587	1.38E-06	3.30E-06	0.003	0.387	8.40
2.13E-03	2.13E-03	0.15	698	1.38E-06	3.30E-06	0.003	0.384	8.40
2.13E-03	2.13E-03	0.15	810	1.38E-06	3.30E-06	0.004	0.381	8.40
2.13E-03	2.13E-03	0.15	921	1.38E-06	3.30E-06	0.004	0.377	8.40
2.13E-03	2.13E-03	0.15	1032	1.38E-06	3.30E-06	0.005	0.372	8.40
2.13E-03	2.13E-03	0.15	1143	1.38E-06	3.30E-06	0.005	0.368	8.40
2.13E-03	2.13E-03	0.15	1248	1.38E-06	3.30E-06	0.006	0.362	8.40
2.13E-03	2.13E-03	0.15	1354	1.38E-06	3.30E-06	0.006	0.356	8.40
2.13E-03	2.13E-03	0.15	1459	1.38E-06	3.30E-06	0.007	0.350	8.40
2.13E-03	2.13E-03	0.15	1564	1.38E-06	3.30E-06	0.007	0.343	8.40
2.13E-03	2.13E-03	0.15	1669	1.38E-06	3.30E-06	0.008	0.336	8.40
2.13E-03	2.13E-03	0.15	1767	1.38E-06	3.30E-06	0.008	0.328	8.40
2.13E-03	2.13E-03	0.15	1865	1.38E-06	3.30E-06	0.009	0.320	8.40
2.13E-03	2.13E-03	0.15	1963	1.38E-06	3.30E-06	0.009	0.311	8.40
2.13E-03	2.13E-03	0.15	2061	1.38E-06	3.30E-06	0.010	0.302	8.40
2.13E-03	2.13E-03	0.15	2159	1.38E-06	3.30E-06	0.010	0.292	8.40
2.13E-03	2.13E-03	0.15	2250	1.38E-06	3.30E-06	0.011	0.282	8.40
2.13E-03	2.13E-03	0.15	2341	1.38E-06	3.30E-06	0.011	0.272	8.40
2.13E-03	2.13E-03	0.15	2432	1.38E-06	3.30E-06	0.011	0.261	8.40
2.13E-03	2.13E-03	0.15	2522	1.38E-06	3.30E-06	0.012	0.249	8.40
2.13E-03	2.13E-03	0.15	2613	1.38E-06	3.30E-06	0.012	0.238	8.40
2.13E-03	2.13E-03	0.15	2695	1.38E-06	3.30E-06	0.013	0.225	8.40
2.13E-03	2.13E-03	0.15	2777	1.38E-06	3.30E-06	0.013	0.213	8.40
2.13E-03	2.13E-03	0.15	2858	1.38E-06	3.30E-06	0.013	0.200	8.40
2.13E-03	2.13E-03	0.15	2940	1.38E-06	3.30E-06	0.014	0.186	8.40
2.13E-03	2.13E-03	0.15	3022	1.38E-06	3.30E-06	0.014	0.173	8.40
2.13E-03	2.13E-03	0.15	3092	1.38E-06	3.30E-06	0.014	0.158	8.40
2.13E-03	2.13E-03	0.15	3163	1.38E-06	3.30E-06	0.015	0.144	8.40
2.13E-03	2.13E-03	0.15	3233	1.38E-06	3.30E-06	0.015	0.129	8.40
2.13E-03	2.13E-03	0.15	3303	1.38E-06	3.30E-06	0.015	0.114	8.40
2.13E-03	2.13E-03	0.15	3374	1.38E-06	3.30E-06	0.016	0.099	8.40
2.13E-03	2.13E-03	0.15	3429	1.38E-06	3.30E-06	0.016	0.083	8.40
2.13E-03	2.13E-03	0.15	3484	1.38E-06	3.30E-06	0.016	0.067	8.40
2.13E-03	2.13E-03	0.15	3539	1.38E-06	3.30E-06	0.017	0.050	8.40
2.13E-03	2.13E-03	0.15	3594	1.38E-06	3.30E-06	0.017	0.034	8.40
2.13E-03	2.13E-03	0.15	3649	1.38E-06	3.30E-06	0.017	0.017	8.40

336.00

Appendix D

Calculation of Shear Stiffness for Diagonal and Columns

Model Parameters	
Base Shear	2425 kN
Base Moment	145180 kN-m
no of columns	6
no of stories	30
allowable gamma	0.002
allowable disp	0.007 m
h	3.5 m
L _b	7 m
% allocated to Brace	70%
Stiffness Ratio	2.33 D _{truss} /D _{frame}
f	3

Brace Parameters		
A ^d	0.02 m ²	area of diagonal
A ^c	0.03 m ²	area of chord
Inertia of eachChords	7.34E-04 m ⁴	
Inertia of Braced Bay	7.35E-01 m ⁴	
E	2.00E+08 kPA	mod of elasticity
theta	0.46 rad	diagonal angle

Frame Parameters	
I _c	7.34E-04 m ⁴
I _b	7.34E-04 m ⁴
r	2.00

Required Shear Stiffness for Desired Distribution					
Required D _{truss}	848,750	kN/m	Required D _{frame}	103,929	kN/m

Truss Shear Stiffness	
D _{truss}	2.86E+06 kN/theta

Frame Shear Stiffness	
K _{interior}	27391 kN/theta
K _{bracing chord}	27391 kN/theta
K _{corner}	16435 kN/theta
D _{frame (6 columns)}	71,217 kN/theta

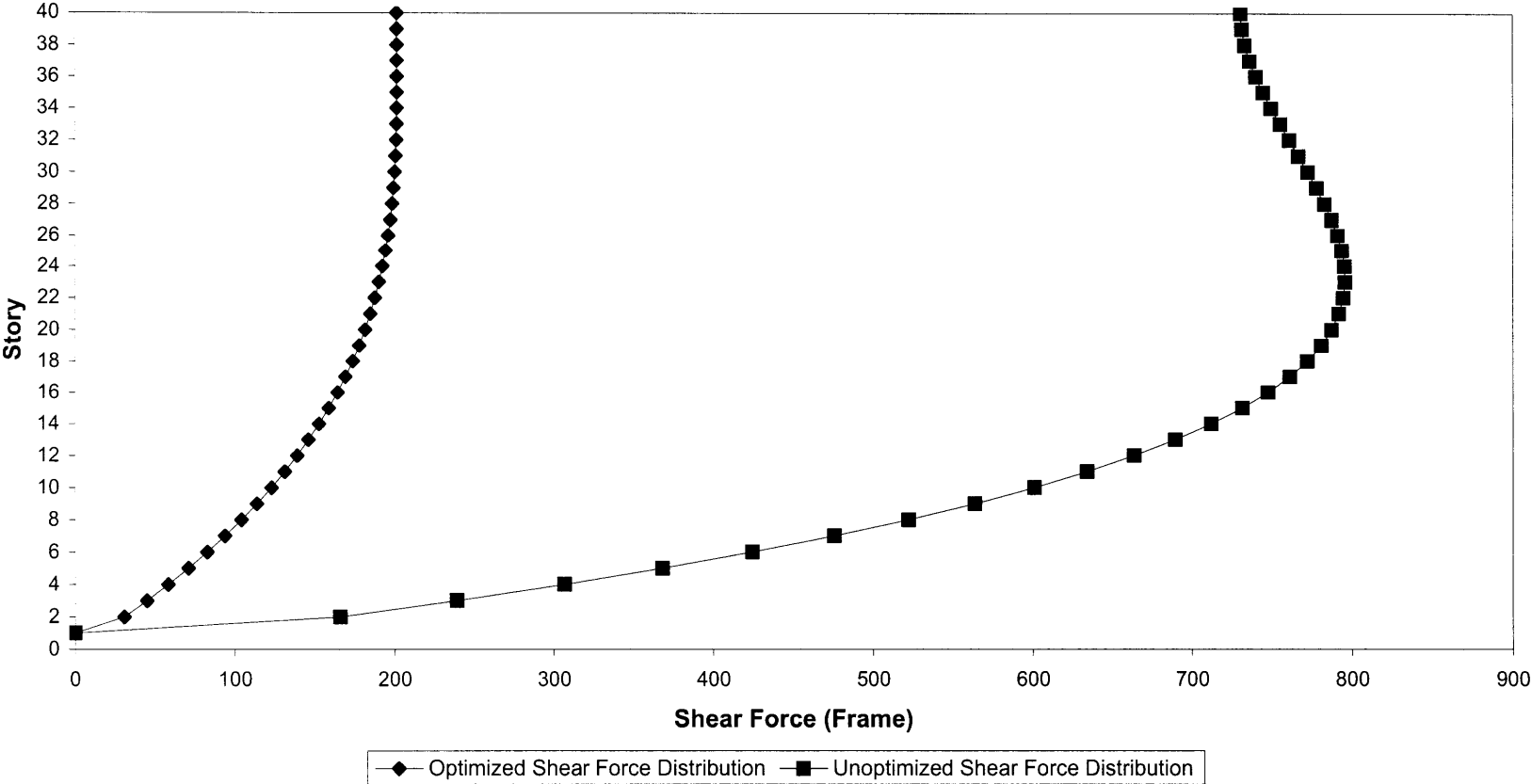
Truss Bending Stiffness	
D _{bending}	1.47E+08 kN-m/theta

Expected Results	
Total Shear Stiffness	2,933,384 kN/theta
Expected Gamma	8.27E-04 theta
Expected Shear Disp (x-dir)	2.89E-03 m
Expected Bending Disp (x-dir)	2.36E-04 m
Total Expected Displacement (x-dir)	3.13E-03 m
Expected Shear Contribution by Brace	98%

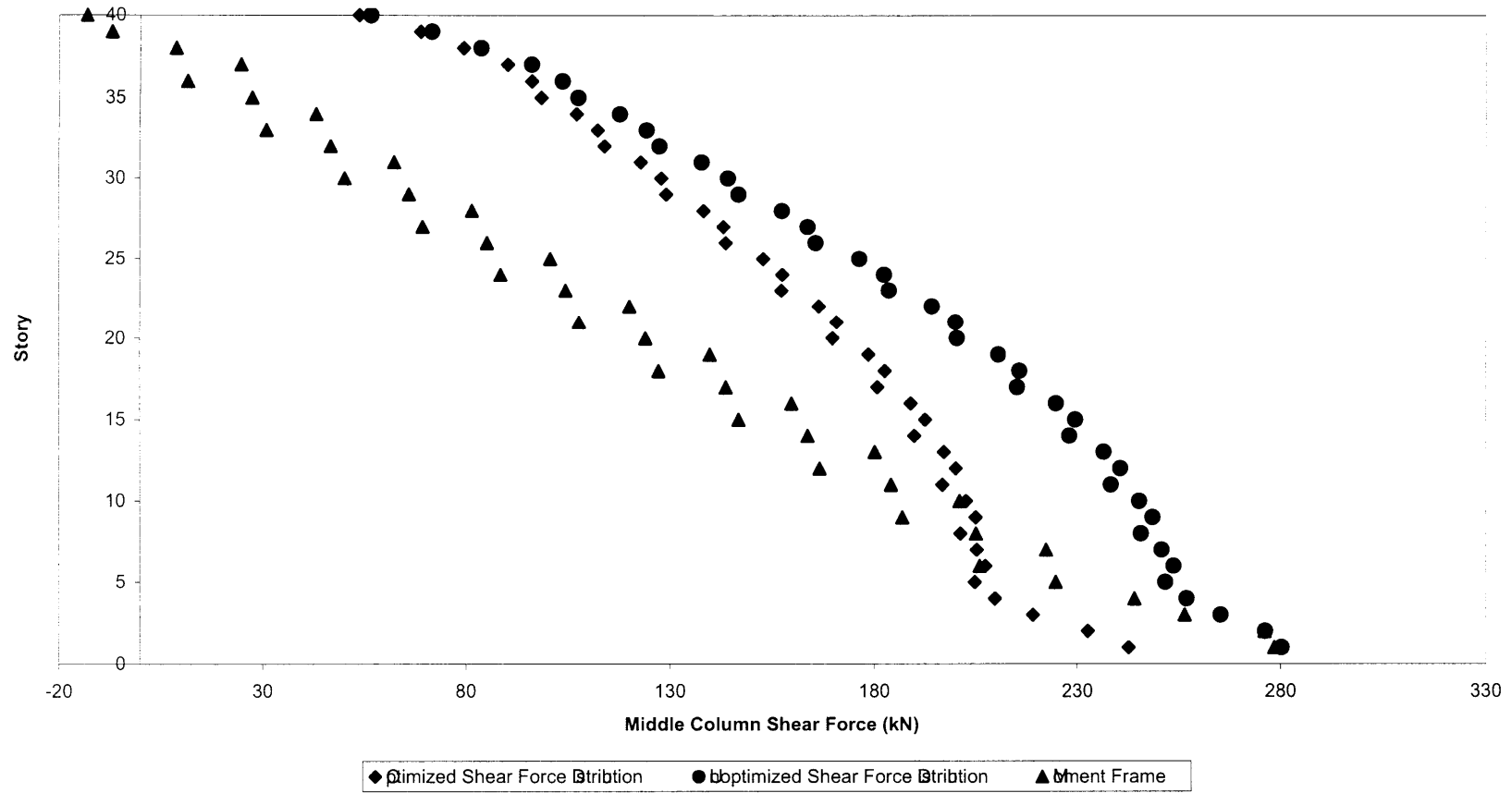
Calculated Forces from SAP Displacement (with increased column area -- min axial deformation)			
SAP Displacement (x dir)	3.12E-03 m		
SAP Displacement (Z dir)	2.42E-04 m		
Gamma	8.91E-04		
Bracing Force (x-dir)	2040.00 kN	Column Shear Force	381.00 kN
Total Shear Force	2421.00 kN	Ratio of Brace to Frame	84%
% difference from hand calc (Disp)	-0.29%		
% difference from hand calc (Brace Contribution)	-13.64%		

Calculated Forces from SAP Displacement (Standard column area -- with axial deformation)			
SAP Displacement (x dir)	4.06E-03 m		
SAP Displacement (Z dir)	1.23E-03 m		
Gamma	1.16E-03		
Bracing Force (x-dir)	1984.00 kN	Column Shear Force	435.00 kN
Total Shear Force	2419.00 kN	Ratio of Brace to Frame	82%
% difference from hand calc (Disp)	29.75%		
% difference from hand calc (Brace Contribution)	-15.94%		

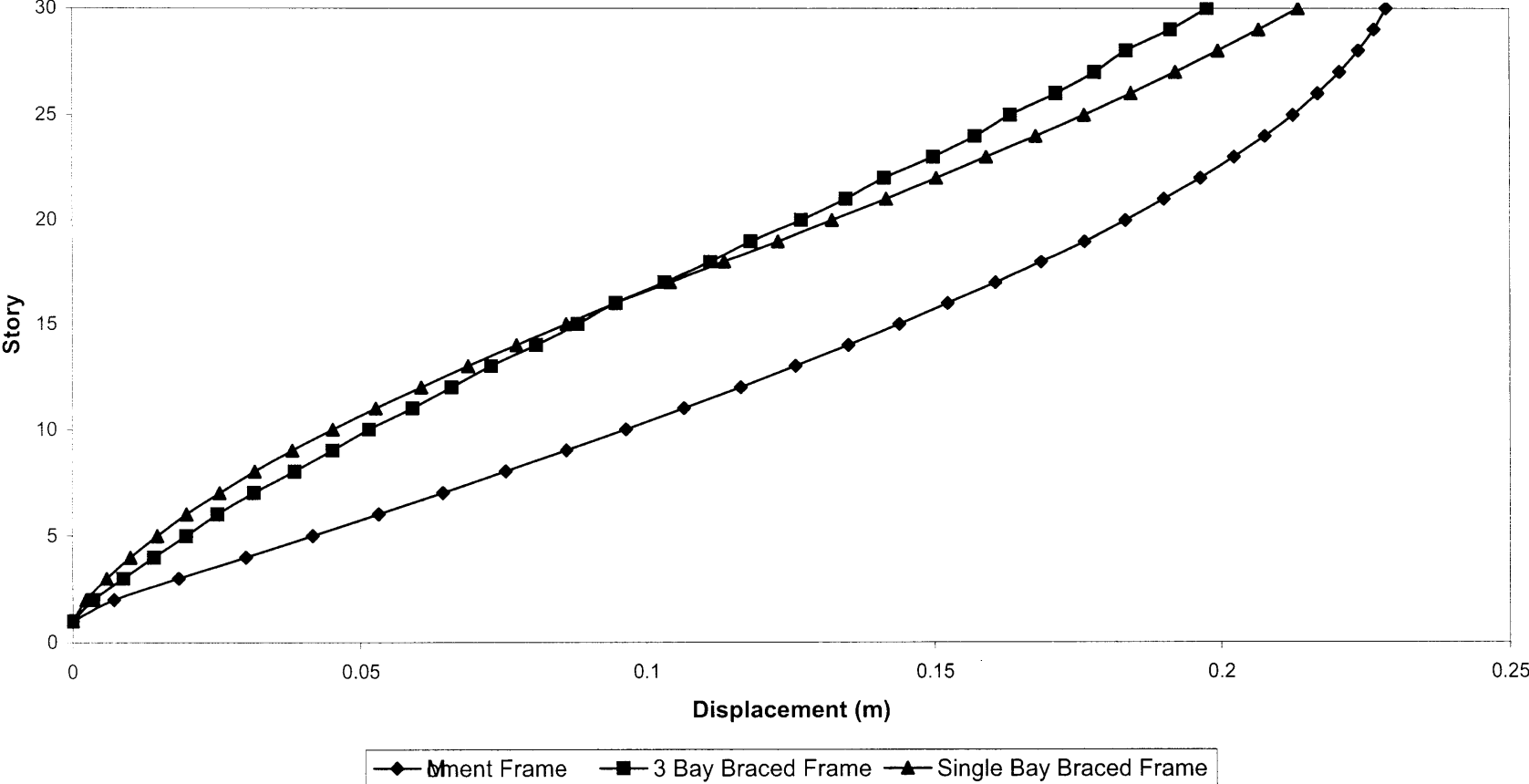
Theoretical Frame Shear Force Distribution in Braced Frames



Frame Shear Force Distribution of Optimized and Unoptimized Braced Frames (SAP Model)



Displacement Profile of Braced Frames and Moment Frames



Theoretical Frame Shear Distribution with Original Model Properties

H	140	m	No of Columns	6	Column Length	3.5	m
w	26	kN/m	No of Girders	5	Girder Length	7	m
E	2.00E+08						
Inertia Columns	1.63E-03						
Inertia Brace	18		GA	5.64E+05	kN/m ²		
G	1.16E-03		EI	3.60E+09			
C	2.79E-03						
alpha ^2	1.57E-04						
alpha	0.0125						
alpha H	1.75						

wH	1/alphaH	sinh(aH)	cosh(aH)	(aH*sinh(aH) + 1) / cosh(aH)
3640	0.57	2.80	2.97	1.99

Story	z	sinh(aZ)	cosh(aZ)	Term 1	Term 2	Term 3	Shear (Bracing)	External Shear	Shear (Frame)
1	0	0	1	-2078.06	0.00	-1.75	3640.00	3640	0.00
2	7	0.09	1.00	-2078.06	0.17	-1.76	3292.03	3458	165.97
3	10.5	0.13	1.01	-2078.06	0.26	-1.77	3127.69	3367	239.31
4	14	0.18	1.02	-2078.06	0.35	-1.78	2969.34	3276	306.66
5	17.5	0.22	1.02	-2078.06	0.44	-1.79	2816.68	3185	368.32
6	21	0.27	1.03	-2078.06	0.53	-1.81	2669.43	3094	424.57
7	24.5	0.31	1.05	-2078.06	0.62	-1.83	2527.30	3003	475.70
8	28	0.36	1.06	-2078.06	0.71	-1.86	2390.01	2912	521.99
9	31.5	0.40	1.08	-2078.06	0.80	-1.89	2257.31	2821	563.69
10	35	0.45	1.10	-2078.06	0.90	-1.92	2128.94	2730	601.06
11	38.5	0.50	1.12	-2078.06	0.99	-1.96	2004.65	2639	634.35
12	42	0.55	1.14	-2078.06	1.09	-2.00	1884.21	2548	663.79
13	45.5	0.60	1.17	-2078.06	1.19	-2.04	1767.38	2457	689.62
14	49	0.65	1.19	-2078.06	1.30	-2.09	1653.94	2366	712.06
15	52.5	0.71	1.22	-2078.06	1.40	-2.14	1543.67	2275	731.33
16	56	0.76	1.26	-2078.06	1.51	-2.20	1436.36	2184	747.64
17	59.5	0.82	1.29	-2078.06	1.62	-2.26	1331.81	2093	761.19
18	63	0.87	1.33	-2078.06	1.73	-2.32	1229.81	2002	772.19
19	66.5	0.93	1.37	-2078.06	1.85	-2.39	1130.17	1911	780.83
20	70	0.99	1.41	-2078.06	1.97	-2.47	1032.70	1820	787.30
21	73.5	1.05	1.45	-2078.06	2.09	-2.55	937.21	1729	791.79
22	77	1.12	1.50	-2078.06	2.22	-2.63	843.51	1638	794.49
23	80.5	1.19	1.55	-2078.06	2.36	-2.72	751.44	1547	795.56
24	84	1.26	1.61	-2078.06	2.49	-2.81	660.80	1456	795.20
25	87.5	1.33	1.66	-2078.06	2.64	-2.91	571.44	1365	793.56
26	91	1.40	1.72	-2078.06	2.78	-3.02	483.16	1274	790.84
27	94.5	1.48	1.78	-2078.06	2.93	-3.13	395.82	1183	787.18
28	98	1.56	1.85	-2078.06	3.09	-3.24	309.23	1092	782.77
29	101.5	1.64	1.92	-2078.06	3.26	-3.36	223.24	1001	777.76
30	105	1.73	1.99	-2078.06	3.43	-3.49	137.68	910	772.32
31	108.5	1.81	2.07	-2078.06	3.60	-3.63	52.38	819	766.62
32	112	1.91	2.15	-2078.06	3.79	-3.77	-32.82	728	760.82
33	115.5	2.00	2.24	-2078.06	3.98	-3.92	-118.09	637	755.09
34	119	2.10	2.33	-2078.06	4.18	-4.08	-203.57	546	749.57
35	122.5	2.21	2.42	-2078.06	4.38	-4.24	-289.45	455	744.45
36	126	2.32	2.52	-2078.06	4.60	-4.42	-375.89	364	739.89
37	129.5	2.43	2.63	-2078.06	4.82	-4.60	-463.04	273	736.04
38	133	2.55	2.74	-2078.06	5.06	-4.79	-551.09	182	733.09
39	136.5	2.67	2.85	-2078.06	5.30	-4.99	-640.19	91	731.19
40	140	2.80	2.97	-2078.06	5.55	-5.20	-730.52	0	730.52

average 657
std 196

Optimized Theoretical Frame Shear Distribution by Fixing a Value of alpha

H	140	m	No of Columns	6	Column Length	3.5	m
w	26	kN/m	No of Girders	5	Girder Length	7	m
E	2.00E+08						
Inertia Columns	1.63E-03						
Inertia Brace	9		GA	5.64E+05	kN/m ²		
G	1.16E-03		EI	1.80E+09			
C	2.79E-03						
alpha ^2	2.00E-05		(FIXING A VALUE OF ALPHA HERE)				
alpha	0.004						
alpha H	0.63						

wH	1/alphaH	sinh(aH)	cosh(aH)	(aH*sinh(aH) + 1) / cosh(aH)
3640	1.60	0.67	1.20	1.18

Story	z	sinh(aZ)	cosh(aZ)	Term 1	Term 2	Term 3	Shear (Bracing)	External Shear	Shear (Frame)
1	0	0	1	-5813.78	0.00	-0.63	3640.00	3640	0.00
2	7	0.03	1.00	-5813.78	0.04	-0.63	3427.11	3458	30.89
3	10.5	0.05	1.00	-5813.78	0.06	-0.63	3321.94	3367	45.06
4	14	0.06	1.00	-5813.78	0.07	-0.63	3217.58	3276	58.42
5	17.5	0.08	1.00	-5813.78	0.09	-0.63	3114.01	3185	70.99
6	21	0.09	1.00	-5813.78	0.11	-0.63	3011.21	3094	82.79
7	24.5	0.11	1.01	-5813.78	0.13	-0.63	2909.14	3003	93.86
8	28	0.13	1.01	-5813.78	0.15	-0.63	2807.78	2912	104.22
9	31.5	0.14	1.01	-5813.78	0.17	-0.63	2707.12	2821	113.88
10	35	0.16	1.01	-5813.78	0.19	-0.63	2607.11	2730	122.89
11	38.5	0.17	1.01	-5813.78	0.20	-0.64	2507.75	2639	131.25
12	42	0.19	1.02	-5813.78	0.22	-0.64	2408.99	2548	139.01
13	45.5	0.20	1.02	-5813.78	0.24	-0.64	2310.83	2457	146.17
14	49	0.22	1.02	-5813.78	0.26	-0.64	2213.24	2366	152.76
15	52.5	0.24	1.03	-5813.78	0.28	-0.64	2116.19	2275	158.81
16	56	0.25	1.03	-5813.78	0.30	-0.65	2019.65	2184	164.35
17	59.5	0.27	1.04	-5813.78	0.32	-0.65	1923.61	2093	169.39
18	63	0.29	1.04	-5813.78	0.34	-0.65	1828.04	2002	173.96
19	66.5	0.30	1.04	-5813.78	0.36	-0.65	1732.92	1911	178.08
20	70	0.32	1.05	-5813.78	0.38	-0.66	1638.23	1820	181.77
21	73.5	0.33	1.05	-5813.78	0.39	-0.66	1543.93	1729	185.07
22	77	0.35	1.06	-5813.78	0.41	-0.66	1450.02	1638	187.98
23	80.5	0.37	1.07	-5813.78	0.43	-0.67	1356.46	1547	190.54
24	84	0.38	1.07	-5813.78	0.45	-0.67	1263.23	1456	192.77
25	87.5	0.40	1.08	-5813.78	0.47	-0.67	1170.31	1365	194.69
26	91	0.42	1.08	-5813.78	0.49	-0.68	1077.68	1274	196.32
27	94.5	0.44	1.09	-5813.78	0.51	-0.68	985.31	1183	197.69
28	98	0.45	1.10	-5813.78	0.53	-0.69	893.18	1092	198.82
29	101.5	0.47	1.10	-5813.78	0.55	-0.69	801.28	1001	199.72
30	105	0.49	1.11	-5813.78	0.57	-0.70	709.56	910	200.44
31	108.5	0.50	1.12	-5813.78	0.59	-0.70	618.03	819	200.97
32	112	0.52	1.13	-5813.78	0.62	-0.71	526.64	728	201.36
33	115.5	0.54	1.14	-5813.78	0.64	-0.71	435.38	637	201.62
34	119	0.56	1.14	-5813.78	0.66	-0.72	344.23	546	201.77
35	122.5	0.58	1.15	-5813.78	0.68	-0.72	253.17	455	201.83
36	126	0.59	1.16	-5813.78	0.70	-0.73	162.16	364	201.84
37	129.5	0.61	1.17	-5813.78	0.72	-0.73	71.20	273	201.80
38	133	0.63	1.18	-5813.78	0.74	-0.74	-19.75	182	201.75
39	136.5	0.65	1.19	-5813.78	0.77	-0.75	-110.70	91	201.70
40	140	0.67	1.20	-5813.78	0.79	-0.75	-201.68	0	201.68
								average	157
								std	56

Appendix E

Design of Braced Frame with Single Outrigger

H	140	m
a	3.5	m
b	14	m
d	17.5	m
h	3.5	m
E	2.00E+08	kN/m ²

Inertia (Outrigger)	
Area	0.05 m ²
Inertia	0.306 m ⁴
EI	6.13E+07
(EI) _o	1.20E+08

Column Stiffness	
Column Area	0.0912
EA	18240000

Core Stiffness	
Area	0.0912
Inertia	2.2344
EI	446880000

alpha	0.16
beta	4.67E-01
w	0.034

Outrigger Diamter	Area	w	Placed @ story	delta
0.260	0.053	0.034	20	1.76
0.26	0.053	0.034	40	1.85
0.26	0.053	0.034	10	2.47

Design of Braced Frame with Single Outrigger

Moment Frame

Displacement Controlled Moment Frame Design							
	d	thickness	Area	Total Length	No of Storys	Vol	Delta
Column set 1	0.44	0.15	0.1740	21	30	110	0.29
Girders set 1	0.44	0.15	0.1740	35	30	183	
Column set 2	0.44	0.15	0.1740	21	10	37	
Girders set 2	0.44	0.15	0.1740	35	10	61	
						390	m ³

Maximum Allowable Drift 0.28

Braced Frame without Outriggers

Braced Frame Displacement Controlled Design without outrigger							
	d	thickness	Area	Total Length	Story	Vol	Delta
Column set 1	0.44	0.06	0.0912	21	40	77	0.27
Girders	0.44	0.06	0.0912	35	40	128	
Bracing	0.2	0.07	0.0286	626		18	
						222	m ³

Core Column Axial Forces 8086 kN
Moment 28301

Braced Frame Strength Based Design without outrigger							
	d	thickness	Area	Total Length		Vol	Delta
Column set 1	0.4	0.06	0.0816	840		69	0.37
Girders	0.4	0.06	0.0816	1400		114	
Bracing	0.15	0.02	8.16E-03	626		5	
						188	m ³

Braced Frame with Outriggers

With Outrigger (at midheight)							
	d	thickness	Area	Total Length		Vol	Delta
Column set 1	0.44	0.06	0.0912	840		77	0.25
Girders	0.44	0.06	0.0912	1330		121	
Bracing	0.15	0.05	0.0157	626		10	
Outrigger	0.26		5.31E-02	133		7	
						215	m ³

With Outrigger (with column change) Run 2							
	d	thickness	Area	Total Length	No of Storys	Vol	Delta
Column set 1	0.44	0.04	0.0640	21	30	40	0.32
Girders set 1	0.44	0.04	0.0640	35	28	63	
Column set 2	0.44	0.06	0.0912	21	10	19	
Girders set 2	0.44	0.06	0.0912	35	10	32	
Bracing	0.15	0.05	0.0157	626		10	
Outrigger	0.26		0.0531	133		7	
						171	m ³

With Outrigger (with column change) Run 3							
	d	thickness	Area	Total Length	No of Storys	Vol	Delta
Column set 1	0.44	0.04	0.0640	21	30	40	0.32
Girders set 1	0.44	0.04	0.0640	35	28	63	
Column set 2	0.44	0.07	0.1036	21	10	22	
Girders set 2	0.44	0.07	0.1036	35	10	36	
Bracing	0.15	0.05	0.0157	626		10	
Outrigger	0.26		0.0531	133		7	
						178	

Note: Frame Action Takes Over in order to control drift

With Outrigger (with column change) Run 4							
	d	thickness	Area	Total Length	No of Storys	Vol	Delta
Column set 1	0.44	0.05	0.0780	21	30	49	0.28
Girders set 1	0.44	0.05	0.0780	35	28	76	
Column set 2	0.44	0.08	0.1152	21	10	24	
Girders set 2	0.44	0.08	0.1152	35	10	40	
Bracing	0.15	0.05	0.0157	626		10	
Outrigger	0.26		0.0531	133		7	
						207	

Core Column Axial Forces 7300 kN
Moment 25550 kN-m

Design of Braced Frame with 2 Outriggers

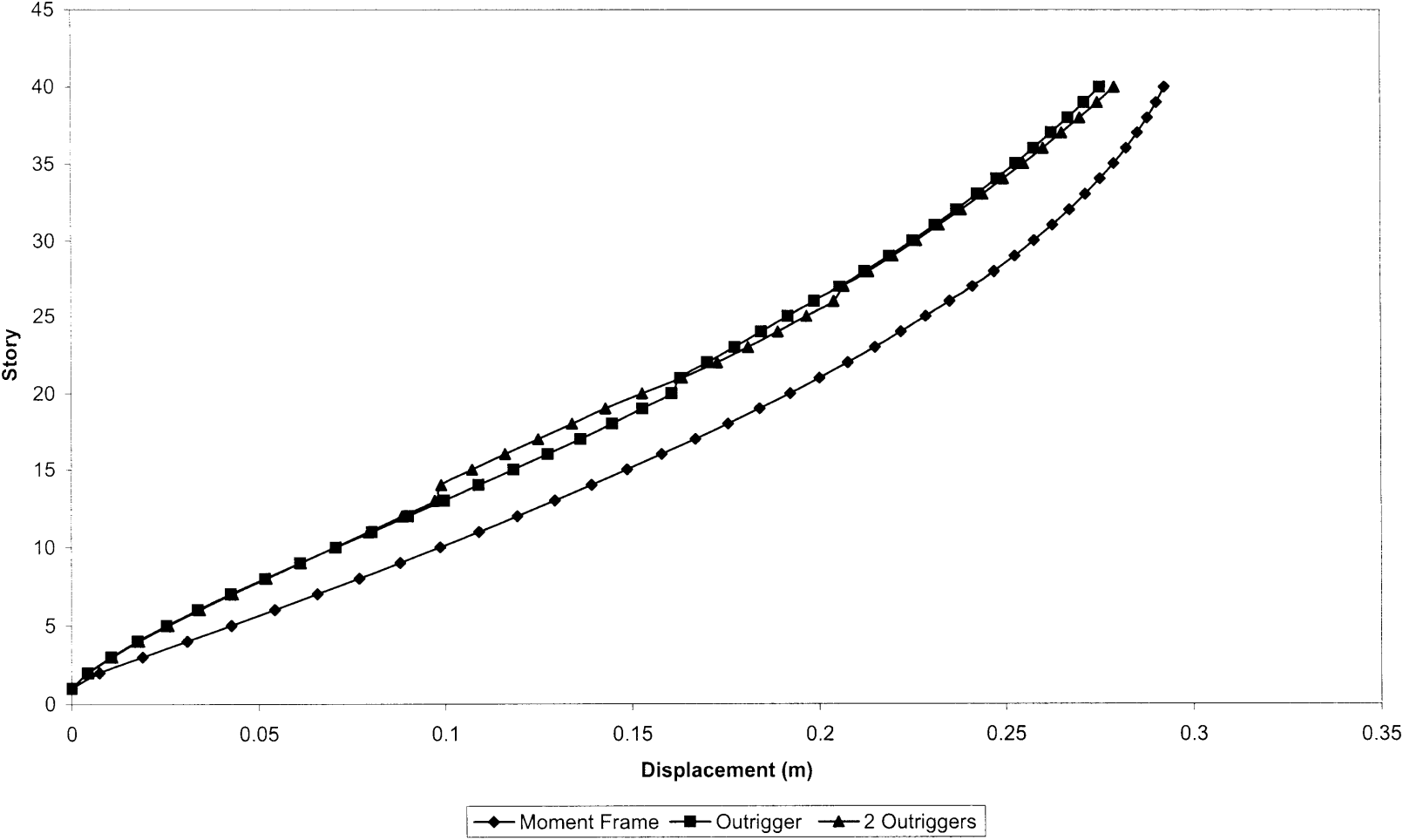
Braced Frame with 2 Outriggers

With Outrigger 2 (with column change)								Maximum Drift
	d	thickness	Area	Total Length	No of Storys	Vol	Delta	
Column set 1	0.44	0.05	0.0780	21	30	49	0.26	0.28
Girders set 1	0.44	0.05	0.0780	35	26	71		
Column set 2	0.44	0.06	0.0912	21	10	19		
Girders set 2	0.44	0.06	0.0912	35	10	32		
Bracing	0.15	0.05	0.0157	626	1	10		
Outrigger	0.26		0.0531	133	2	14		
195 m ³								

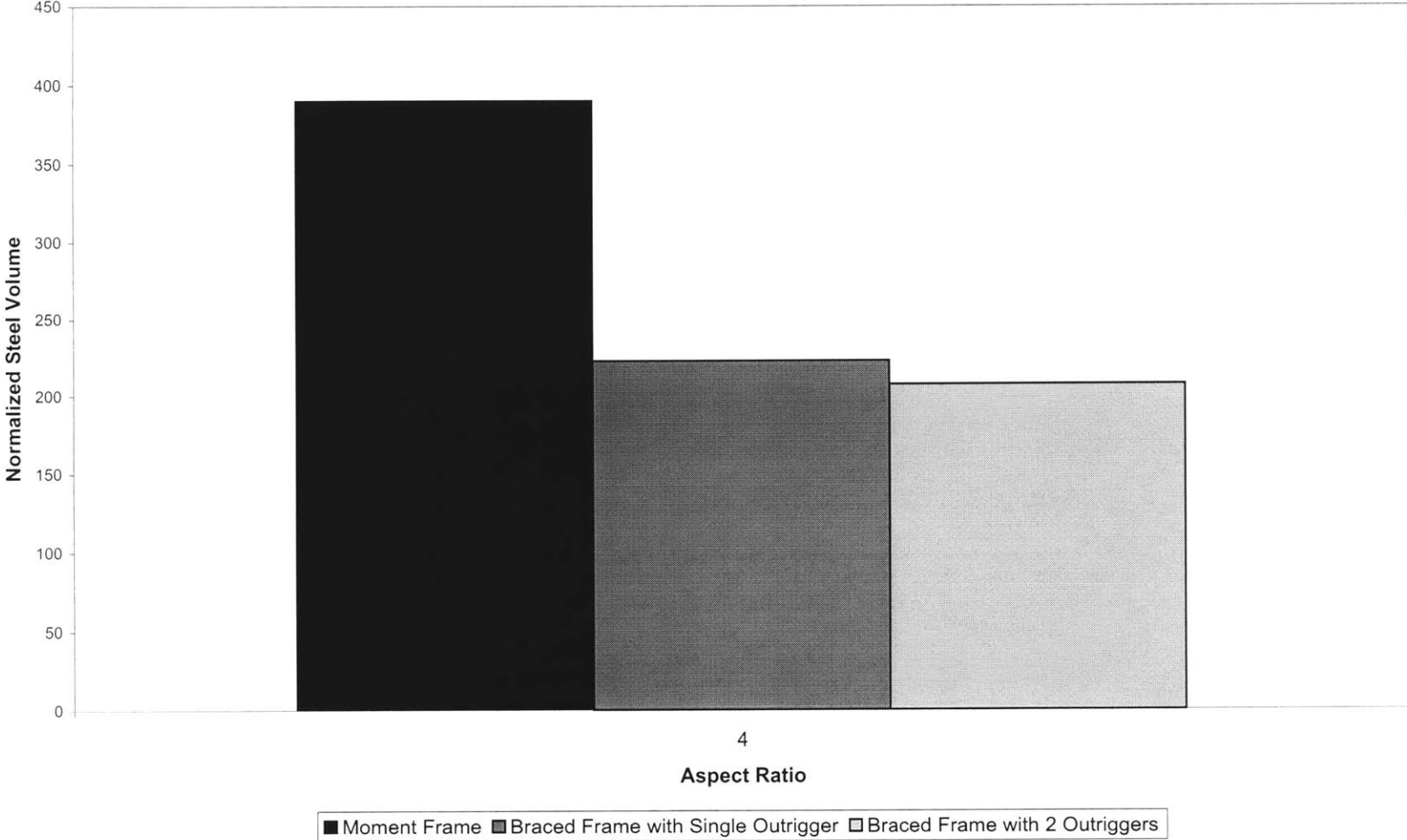
With Outrigger 2 (with column change)								
	d	thickness	Area	Total Length	No of Storys	Vol	Delta	
Column set 1	0.44	0.04	0.0640	21	30	40	0.3	
Girders set 1	0.44	0.04	0.0640	35	26	58		
Column set 2	0.44	0.06	0.0912	21	10	19		
Girders set 2	0.44	0.06	0.0912	35	10	32		
Bracing	0.15	0.05	0.0157	626	1	10		
Outrigger	0.26		0.0531	133	2	14		
174 m ³								

With Outrigger 2 (with column change)								Axial Force	Moment
	d	thickness	Area	Total Length	No of Storys	Vol	Delta		
Column set 1	0.44	0.045	0.0711	21	30	45	0.28	6800	23800
Girders set 1	0.44	0.045	0.0711	35	26	65			
Column set 2	0.44	0.06	0.0912	21	10	19			
Girders set 2	0.44	0.06	0.0912	35	10	32			
Bracing	0.15	0.05	0.0157	626	1	10			
Outrigger	0.26		0.0531	133	2	14			
184 m ³									

Displacement Profiles (Outrigger and Moment Frame)



Comparison of Steel Required for Moment Frames and Braced Frames with Outriggers



Appendix F

Tabulation of Tubular Structures Analyzed and Shear Lag Coefficients

Model	b No of Flange Columns	a No of web Columns	Storys	Height	Loading	F/W	H/F	H/W	Total Number of Elements
1	9	27	30	105	Flange	0.33	3.33	1.11	1638
2	18	18	20	70	Flange	1.00	1.11	1.11	756
3	28	10	10	35	Flange	2.80	0.36	1.00	256
4	18	18	40	140	Flange	1.00	2.22	2.22	1476
5	9	27	60	210	Flange	0.33	6.67	2.22	3258
6	28	10	10	35	Flange	2.80	0.36	1.00	256

Original Model

Flange Analysis (Ratio of Axial Forces) Center to Corner

	Model 1	Model 2	Model 3	Model 4	Model 5	Model 6
Bottom	0.442	0.130	0.003	0.285	0.620	0.003
Middle	1.667	2.570	0.022	1.993	1.132	0.022
Top	-0.270	-0.020	0.005	-0.418	-0.113	0.005

Web Analysis (Ratio of Slopes)

	Model 1	Model 2	Model 3	Model 4	Model 5	Model 6
Bottom	0.143	0.113	0.089	0.265	0.346	0.088
Middle	1.083	2.998	1.054	2.326	3.157	1.055
Top	-0.409	-0.282	-0.668	-0.463	-1.018	-0.668

STIFFENED GIRDERS (2x)

Flange Analysis (Ratio of Center to Corner Column)

	Model 1	Model 2	Model 3
Bottom	0.464		
Middle	1.573		
Top	-0.27		

Web Analysis (Stiffened Girders)

	Model 1
Bottom	0.152
Middle	1.094
Top	-0.458

STIFFENED GIRDERS (5x)

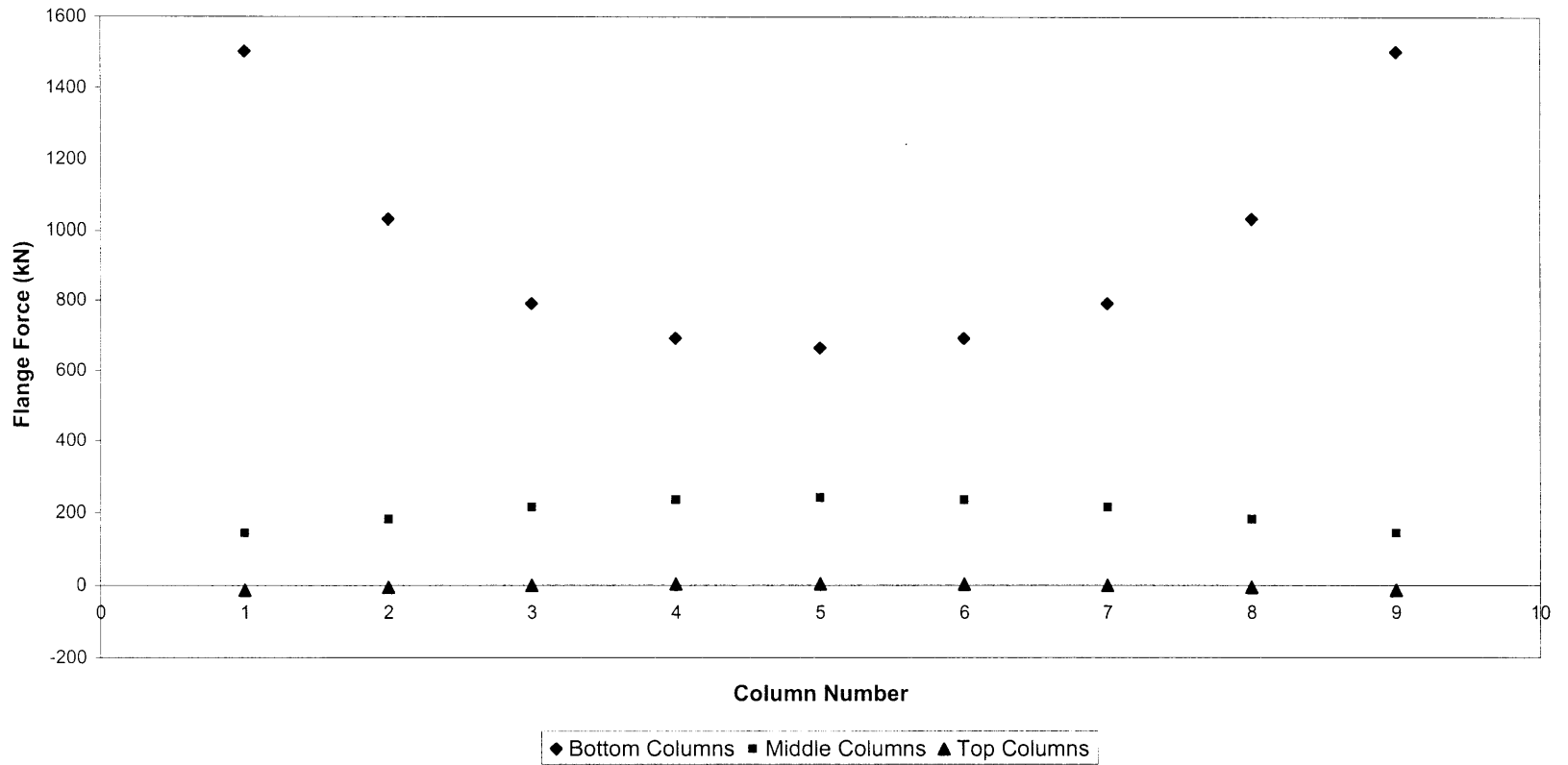
Flange Analysis (Ratio of Center to Corner Column)

	Model 1
Bottom	0.493
Middle	1.472
Top	-0.266

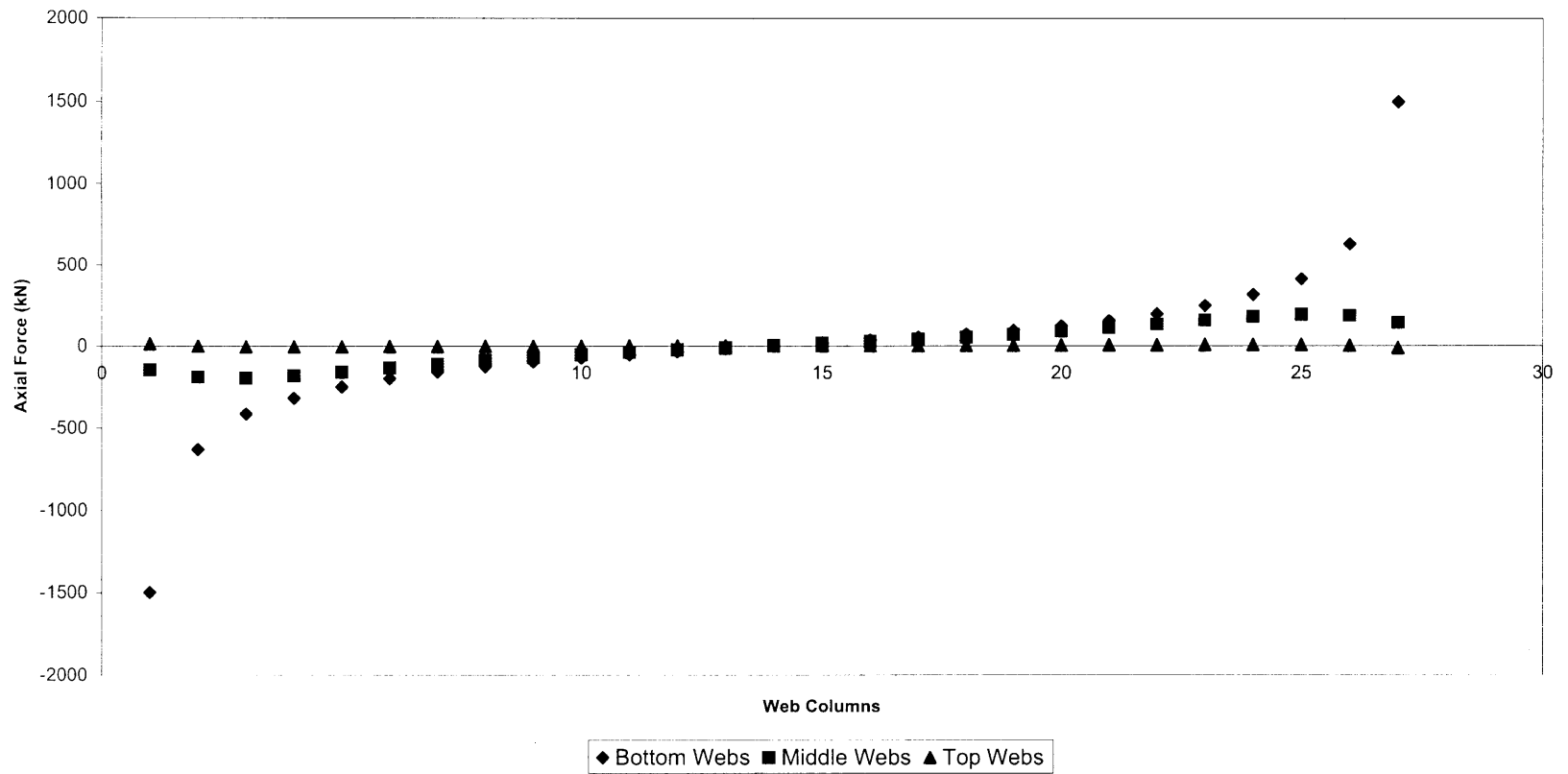
Web Analysis (Stiffened Girders)

	Model 1
Bottom	0.156
Middle	1.126
Top	-0.571

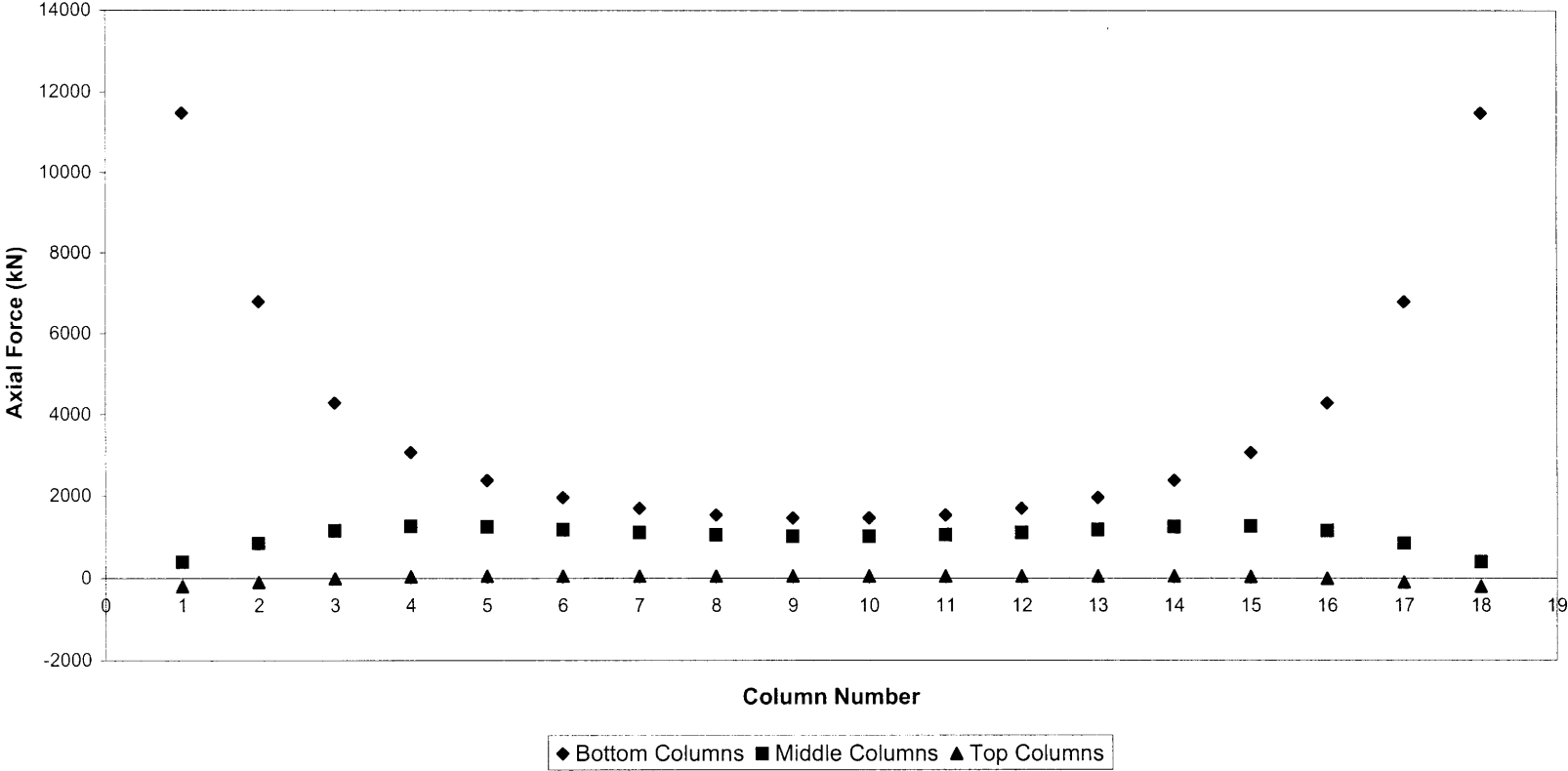
Axial Force Distribution (Flange) [F:W:H 1:3:3.33] Model 1



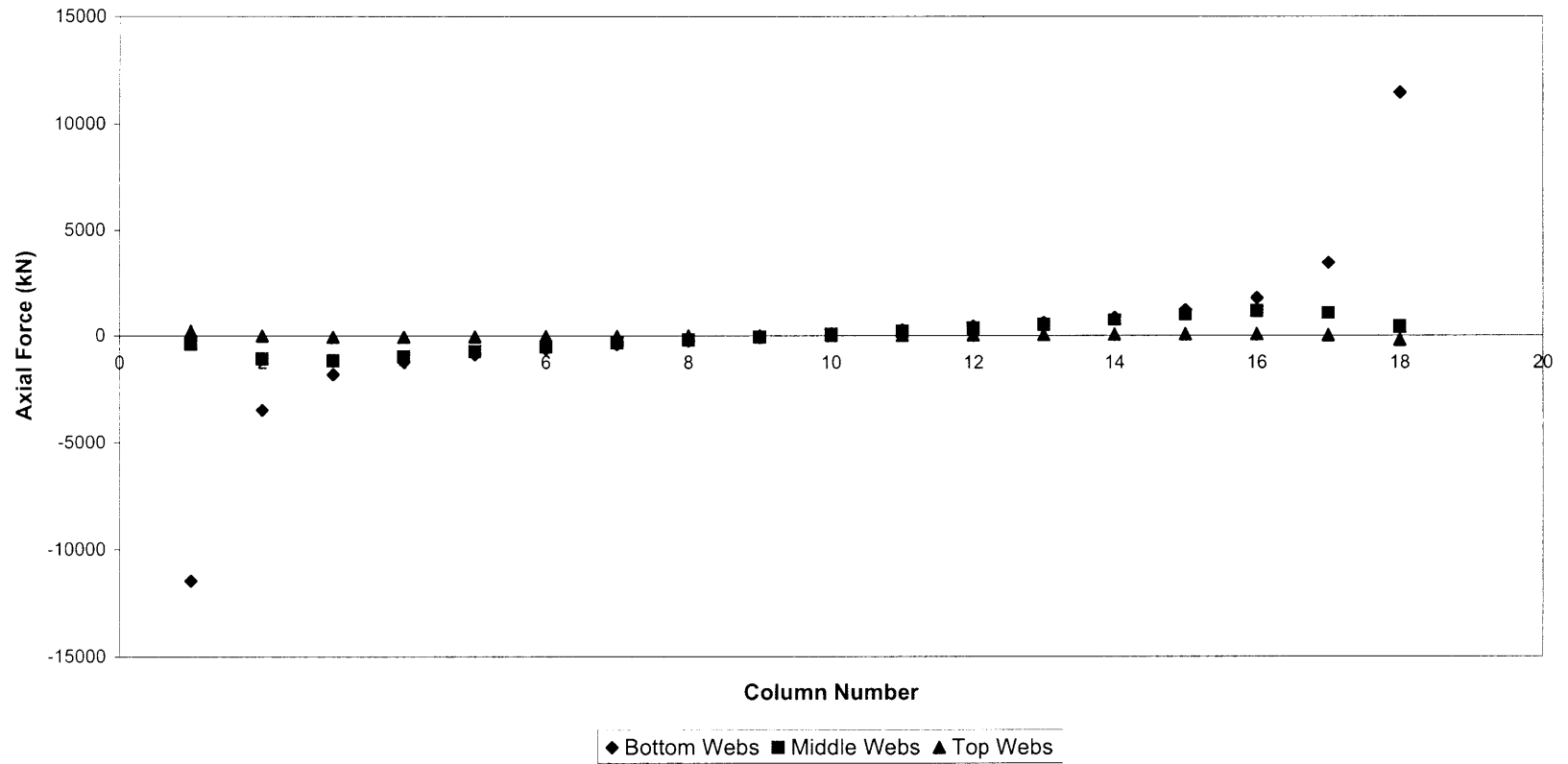
Axial Force Distribution (Web) [F:W:H 1:3:3.33] Model 1



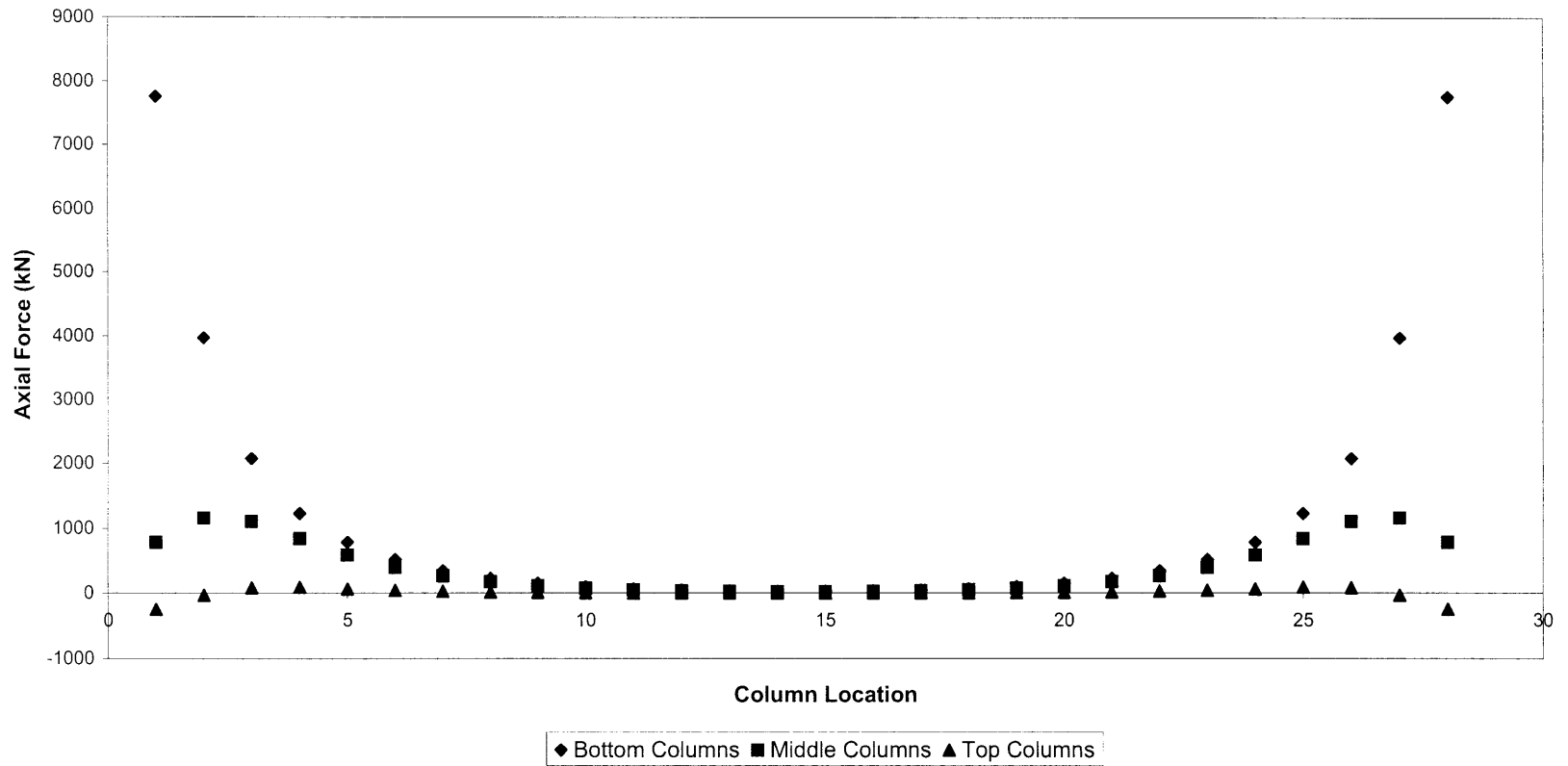
Axial Force Distribution (Flange) [F:W:H 1:1:1.11] Model 2



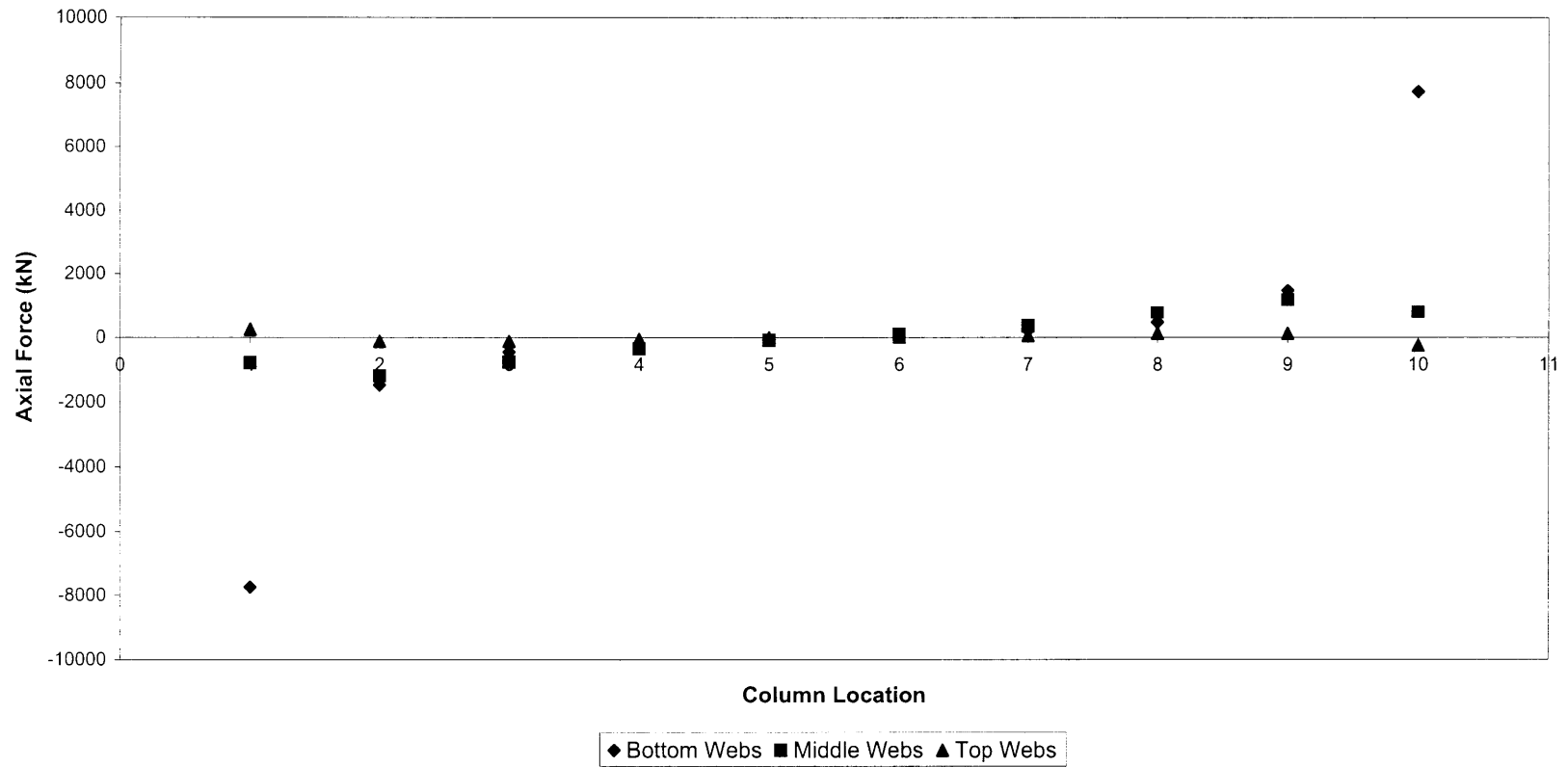
Axial Force Distribution (Web) [F:W:H 1:1:1.11] Model 2



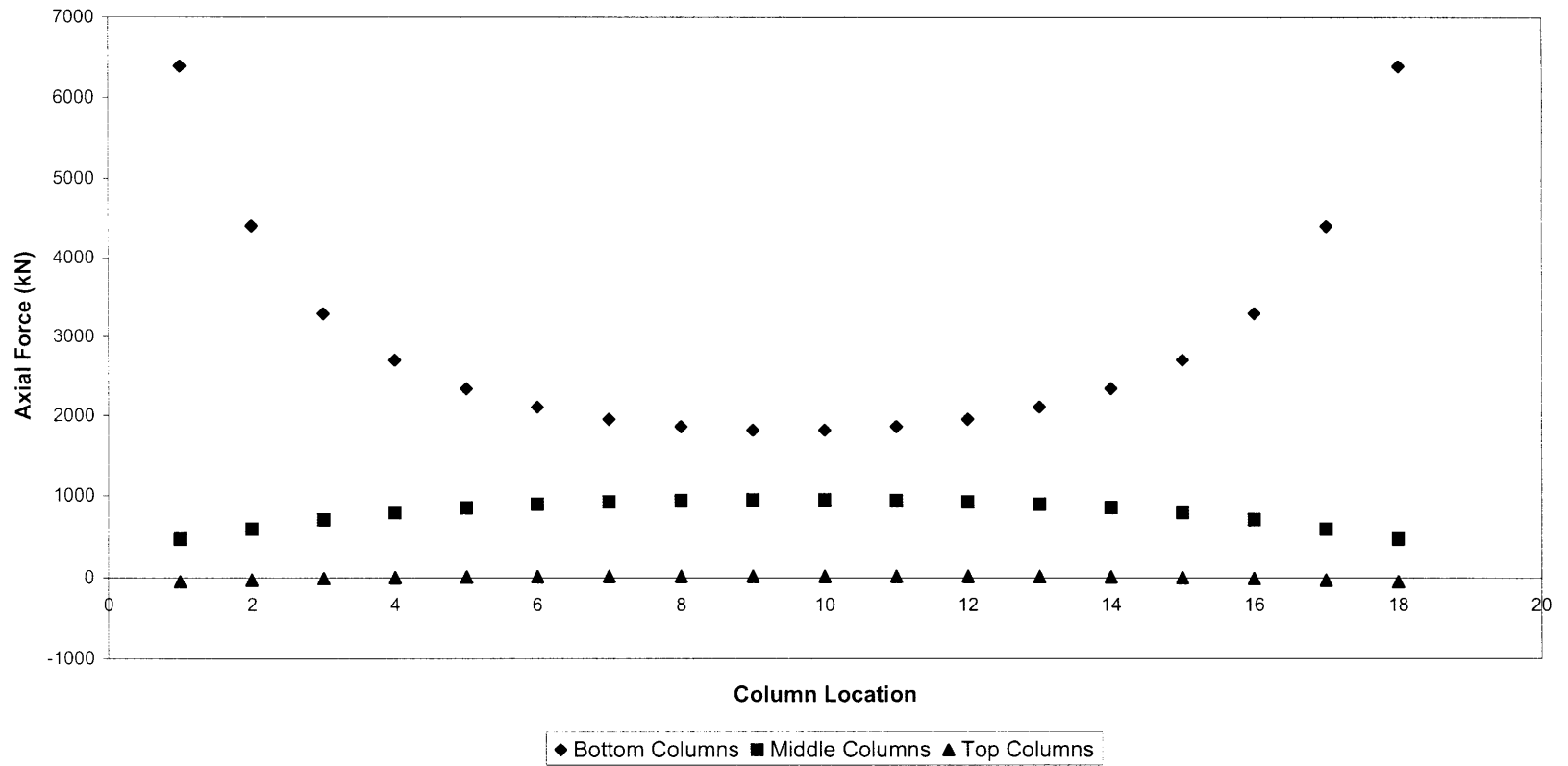
Axial Force Distribution (Flange) [F:W:H 2.8:1:1.1] Model 3



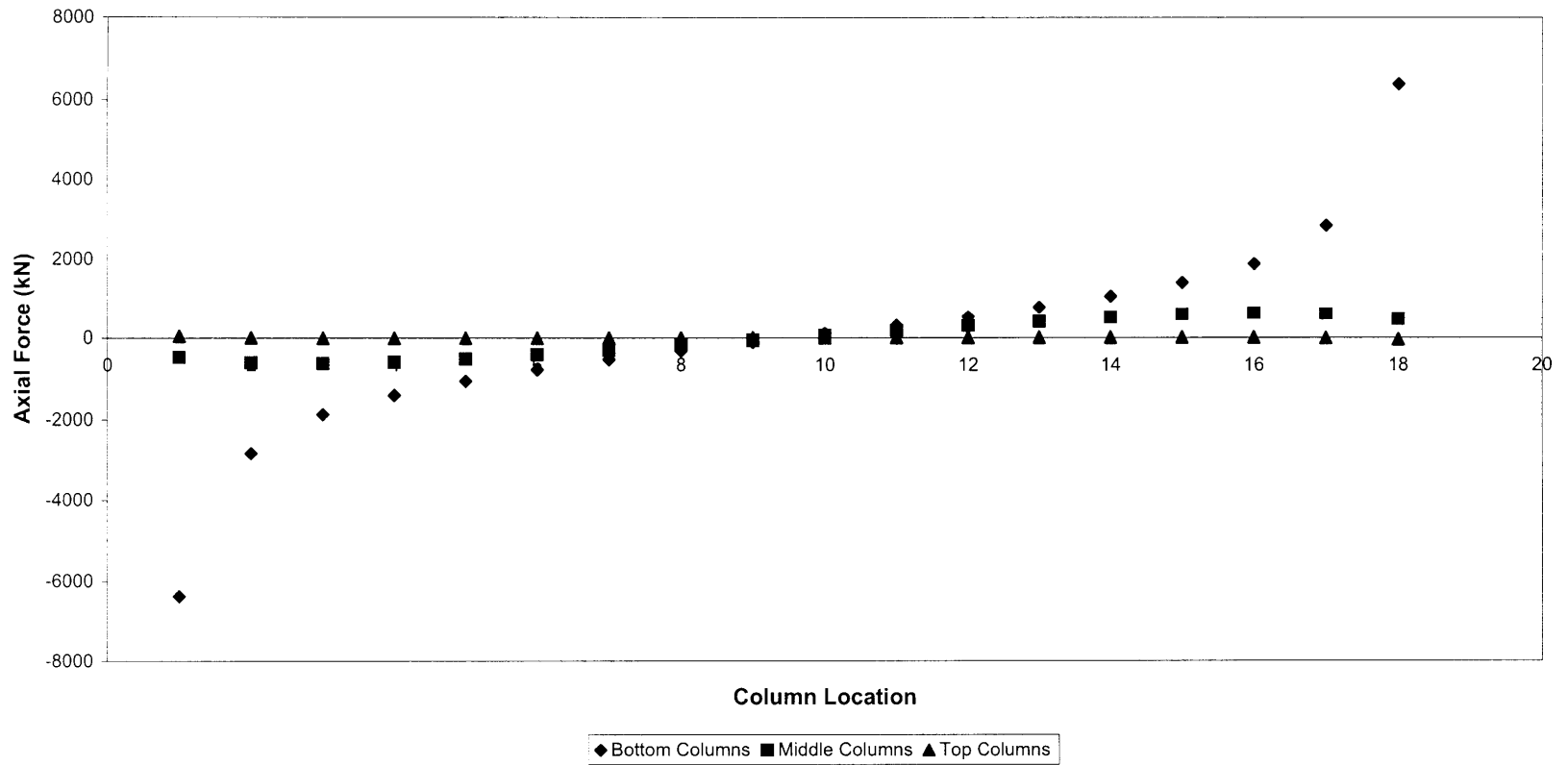
Axial Force Distribution (Web) [F:W:H 2.8:1:1.1] Model 3



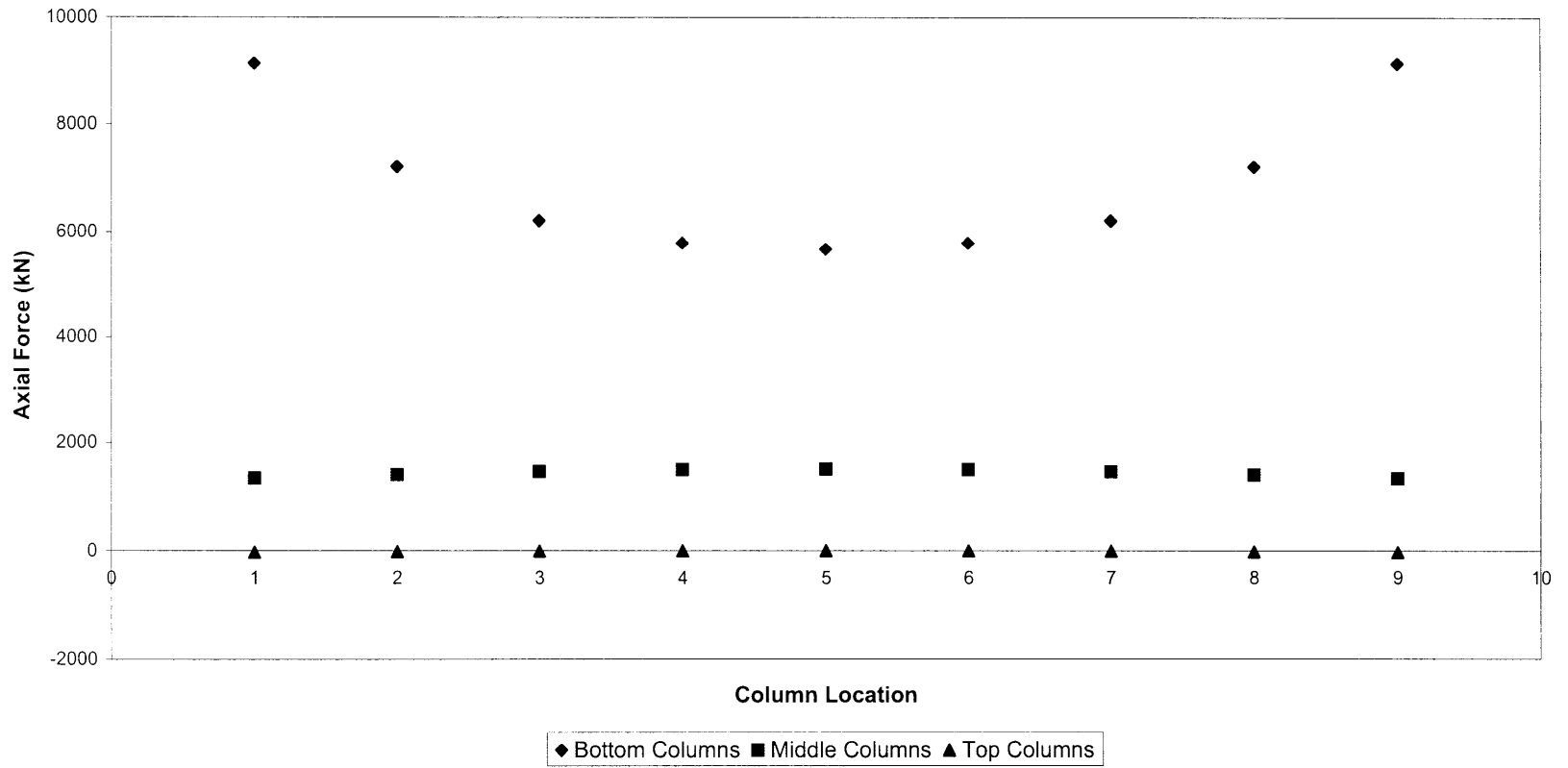
Axial Force Distribution (Flange) [F:W:H 1:1:2.22] Model 4



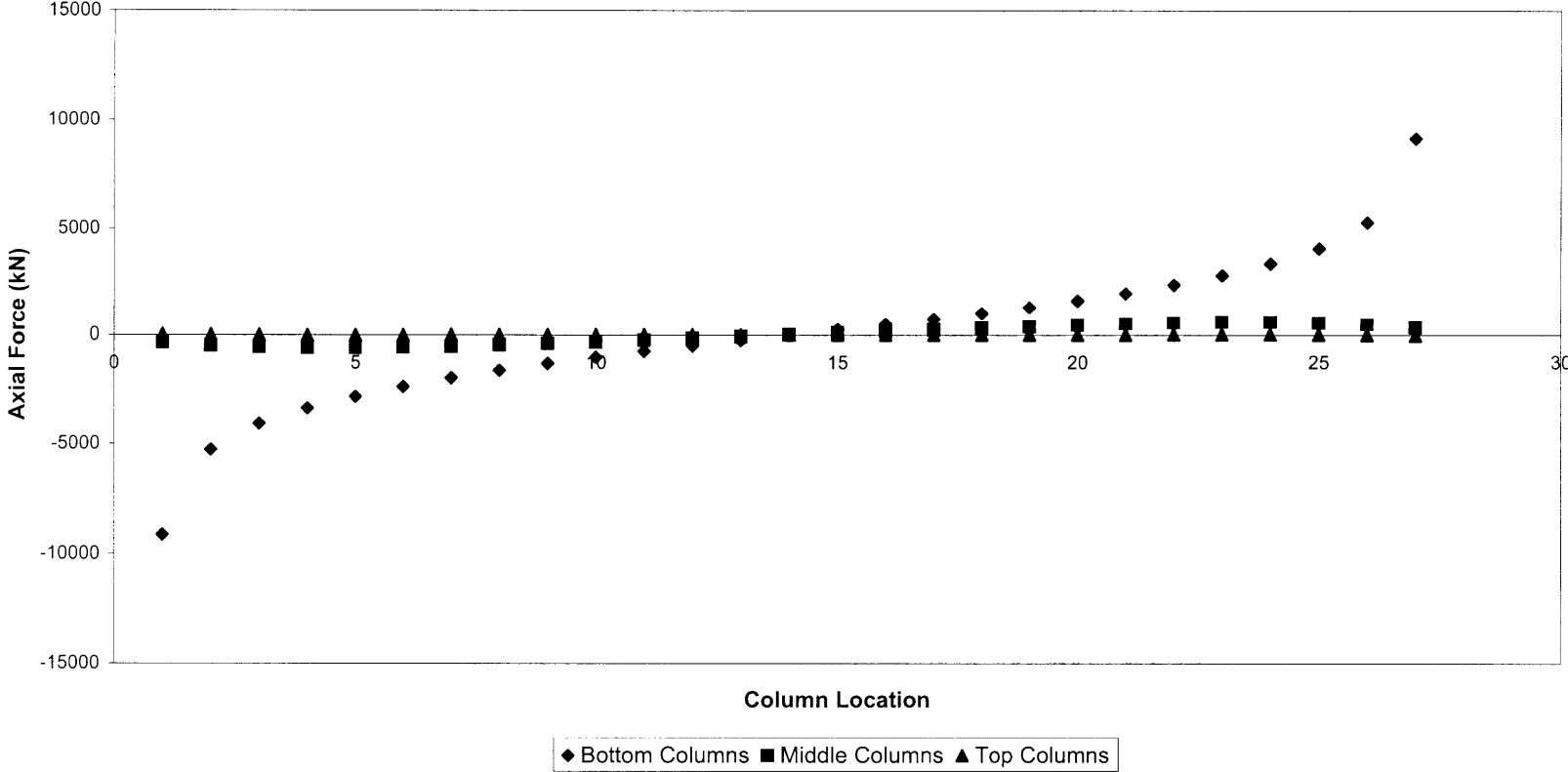
Axial Force Distribution (Web) [F:W:H 1:1:2.22] Model 4



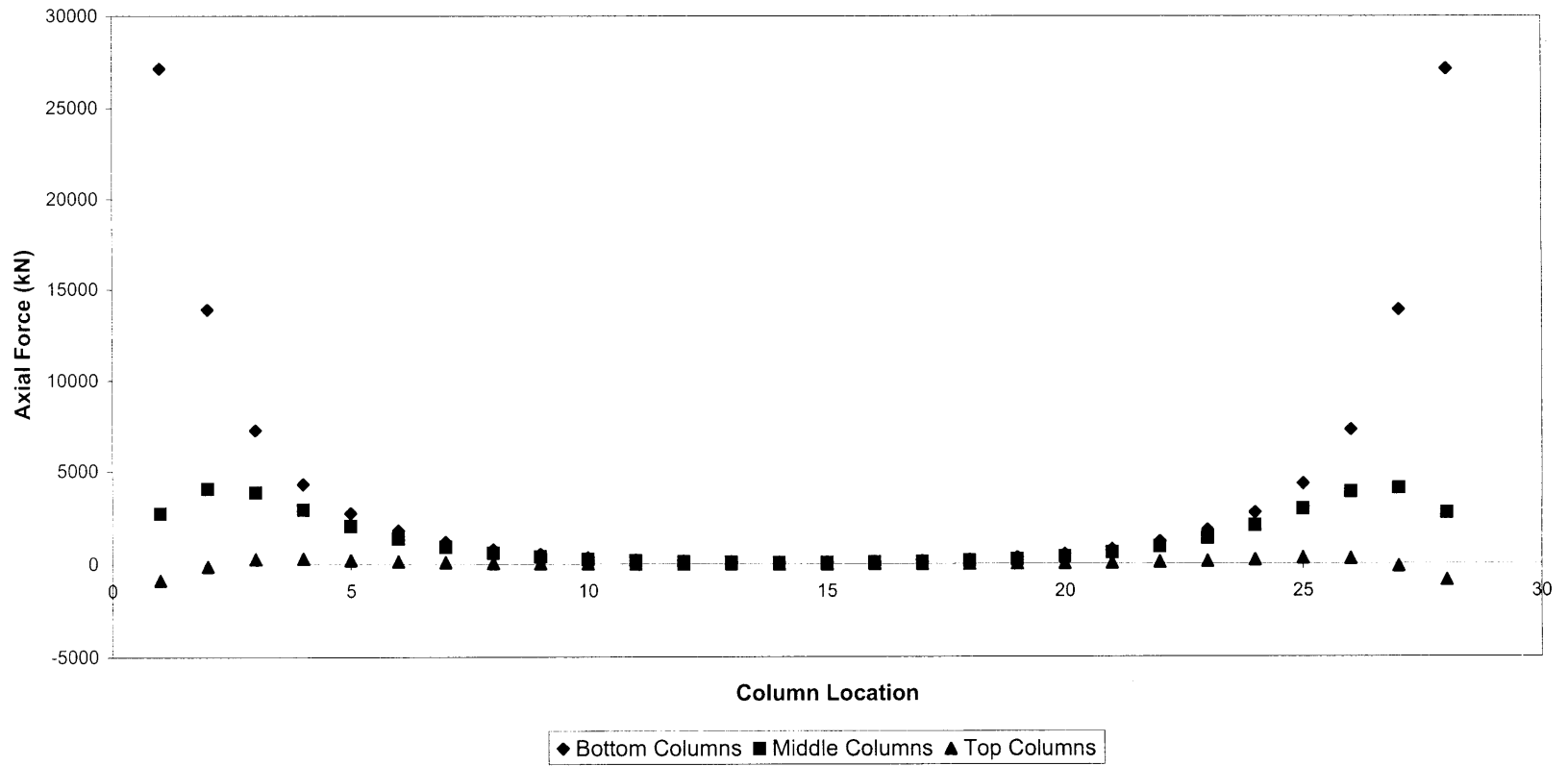
Axial Force Distribution (Flange) [F:W:H 1:3:6.67] Model 5



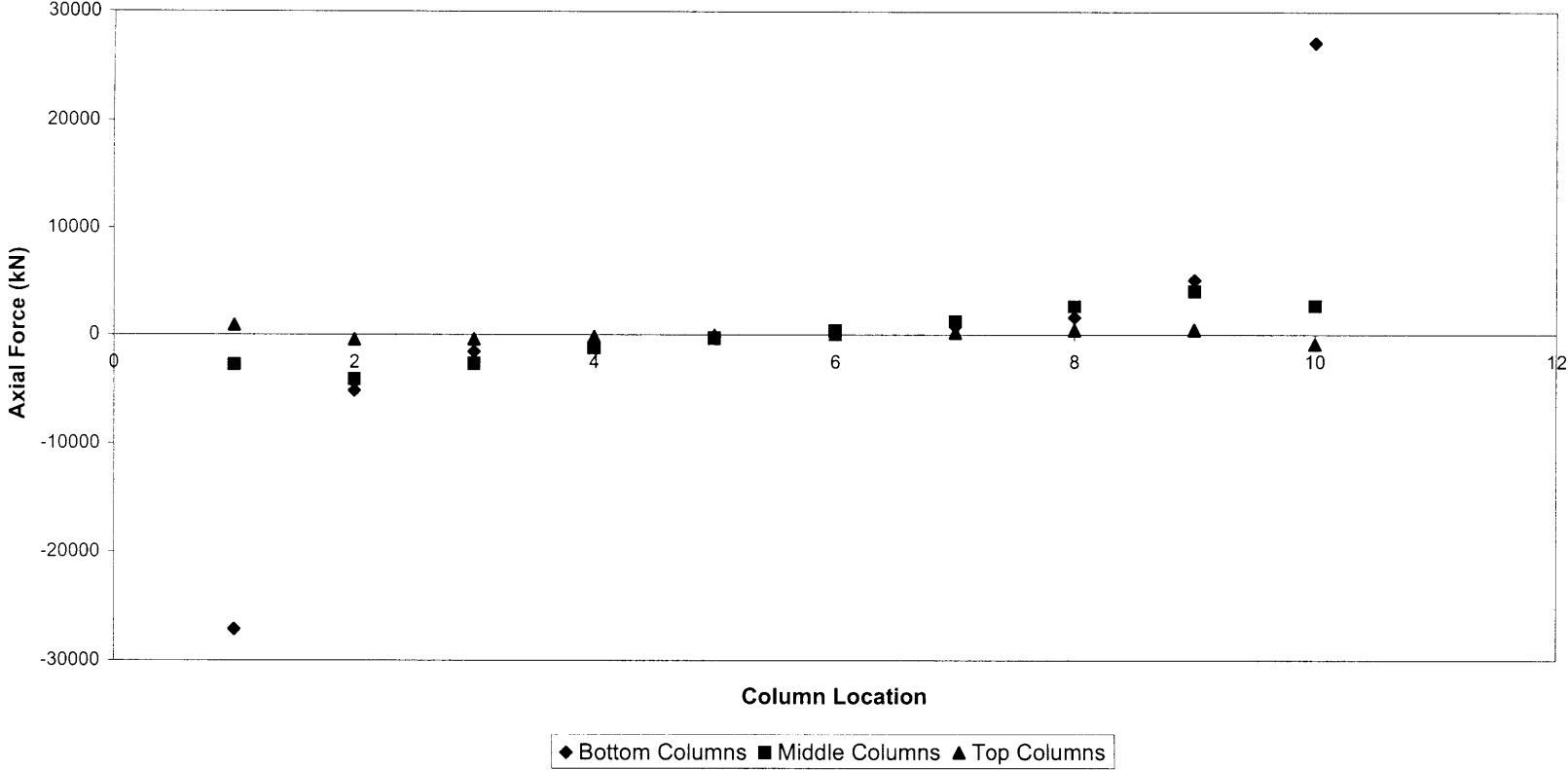
Axial Force Distribution (Web) [F:W:H 1:3:6.67] Model 5



Axial Force Distribution (Flange) [F:W:H 2.8:1:1] Model 6



Axial Force Distribution (Web) [F:W:H 2.8:1:1] Model 6



Results of Parametric Study

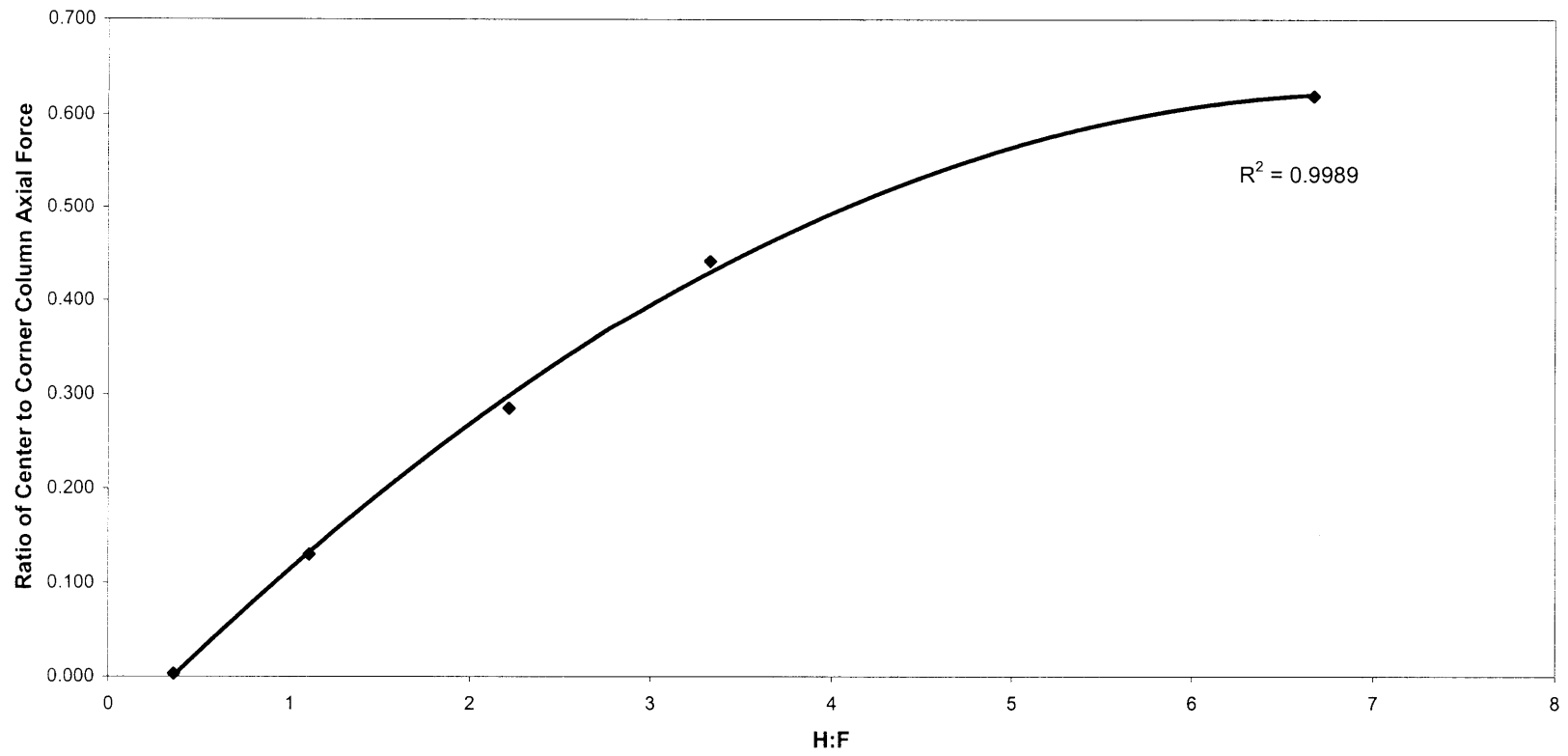
H/F	Flange Shear Lag
3.33	0.442
1.110	0.130
0.360	0.003
2.220	0.285
6.670	0.620
0.360	0.003

H/W	Web Shear Lag
1.111	0.143
1.111	0.113
1.000	0.089
2.222	0.265
2.222	0.346
1.000	0.088

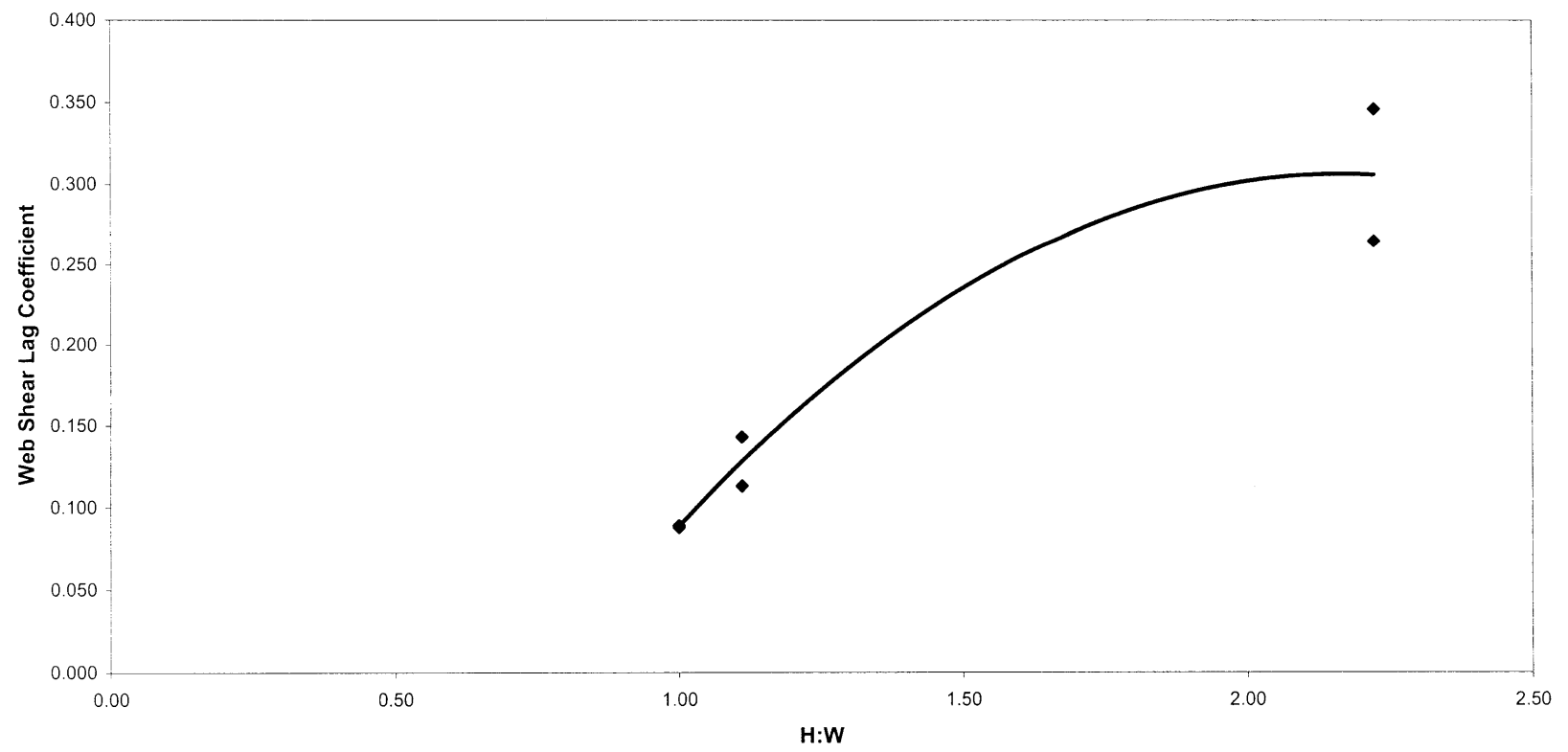
F/W	Flange Shear Lag
0.330	0.442
1.000	0.13
2.800	0.003
1.000	0.285
0.330	0.62
2.800	0.003

F/W	Web Shear Lag
0.330	0.143
1.000	0.113
1.000	0.265
0.330	0.346

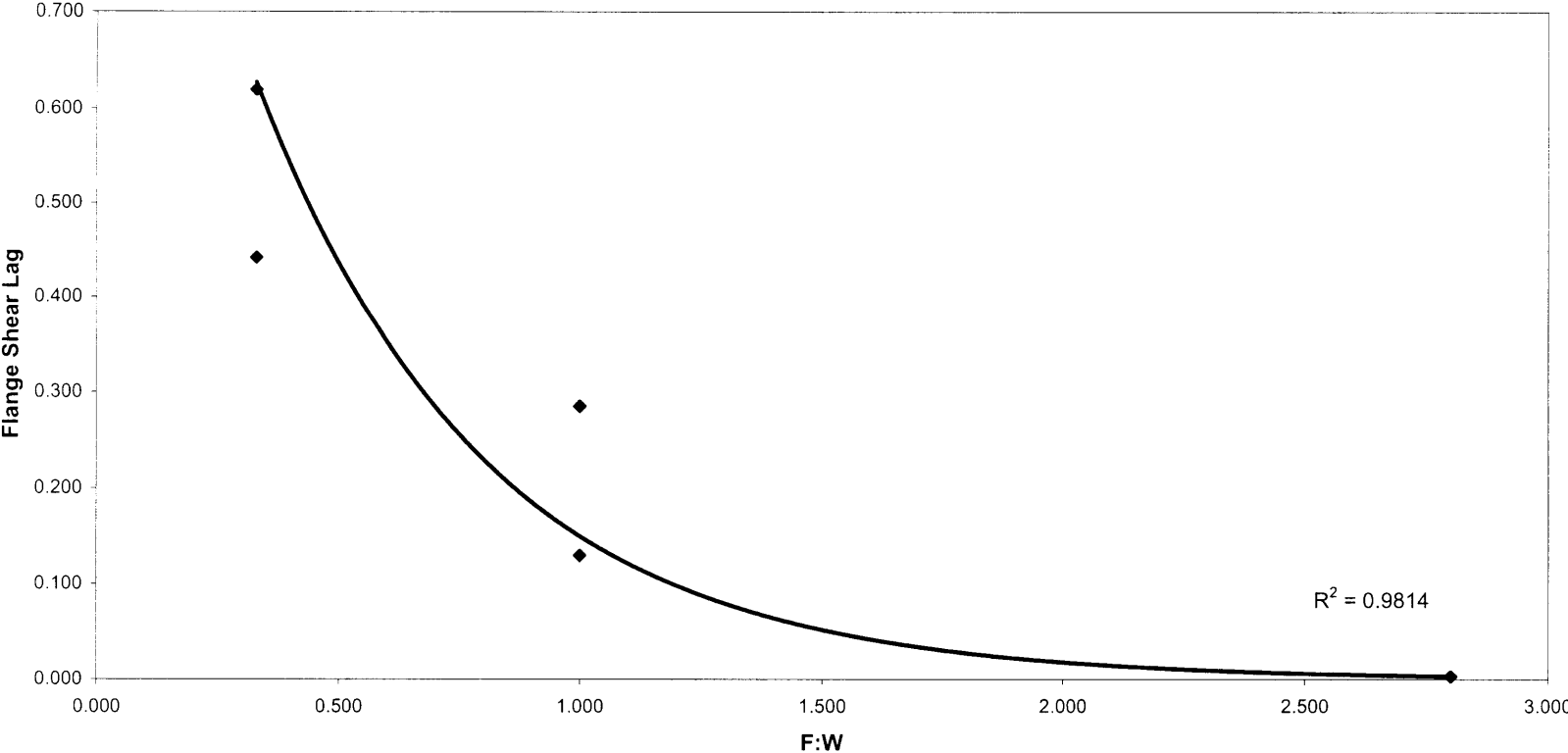
Variation of Flange Shear Lag with H:F Ratio



Variation of Web Shear Lag with H:W Ratio



Variation of Flange Shear Lag with F:W Ratio



Appendix G

Results of Parametric Study

40 Story

% allocated to brace	s
90	1.57
80	1.38
70	0.97
60	0.69
50	0.51
40	0.44
30	0.34
20	0.28

Area of Bracing	
D	0.1500
t	Area
0.0100	0.0044
0.0150	0.0064
0.0200	0.0082
0.0250	0.0098
0.0300	0.0113
0.0350	0.0126
0.0400	0.0138
0.0450	0.0148
0.0500	0.0157
0.0550	0.0164
0.0600	0.0170
0.0650	0.0174

20 Story

% allocated to brace	s
90	0.11
80	0.06
70	0.04
60	0.03
50	
40	
30	
20	

Area of Bracing	
D	0.1000
t	Area
0.0100	0.0028
0.0150	0.0040
0.0200	0.0050
0.0250	0.0059
0.0300	0.0066
0.0350	0.0071
0.0400	0.0075
0.0450	0.0078
0.0500	0.0079
0.0550	0.0078
0.0600	0.0075
0.0650	0.0071

Results of Parametric Study

30 Story

% allocated to brace	s
90	0.7
80	0.36
70	0.22
60	0.14
50	0.12
40	
30	
20	

30 Story s=.25

% allocated to brace	s
90	0.58
80	0.3
70	0.2
60	0.16
50	0.13
40	
30	
20	

Area of Bracing

D	Area
0.0100	0.0036
0.0150	0.0052
0.0200	0.0066
0.0250	0.0079
0.0300	0.0090
0.0350	0.0099
0.0400	0.0107
0.0450	0.0113
0.0500	0.0118
0.0550	0.0121
0.0600	0.0123
0.0650	0.0123

Model Parameters		
Uniform Load	26	kN/m
Base Shear	3640	kN
Base Moment		kN-m
no of columns	6	
no of stories	40	
allowable drift	1/500	
allowable top disp	0.28	
assumed s	1/2	
calculated gamma	1/750	
allowable disp (per story)	0.005	m
h	3.5	m
L _b	7	m
% allocated to Brace	90%	%
Stiffness Ratio	9.00	D _{truss} /D _{frame}
f	3	

40 story structure

aspect ratio 6.666666667

Brace Parameters		
A ^d	0.0174	m ²
A ^c	5.40E-02	m ²
Inertia of Braced Bay	4.76E+01	m ⁴
E	2.00E+08	kPA
theta	0.46	rad

area of diagonal
area of chord

Columns with 0.7m width

3 bay bracing scheme
mod of elasticity
diagonal angle

Frame Parameters		
I _c	4.196E-03	m ⁴
I _b	4.196E-03	m ⁴
r	2.00	

Required Shear Stiffness for Desired Distribution			
Required D _{truss}	2,457,000	kN/m	Required D _{frame} 273,000 kN/m

Actual Truss Shear Stiffness		
D _{truss}	2,490,085	kN/theta
Truss Bending Stiffness		
D _{bending}	2.65E+08	kN-m/theta

Actual Frame Shear Stiffness		
K _{interior}	469756	kN/theta
K _{corner}	93951	kN/theta
D _{frame (6 columns)}	563,708	kN/theta

Expected Results		
Total Shear Stiffness	3.05E+08	kN/theta
Calculated Gamma	1/839	theta
Calculated Shear Disp (x-dir)	0.083	m
Calculated Bending Disp (x-dir)	0.131	m
Total Displacement (x-dir)	0.21	m
s	1.57	

V/Dt
cantilever bending

Model Parameters	
Uniform Load	26 kN/m
Base Shear	3640 kN
Base Moment	kN-m
no of columns	6
no of stories	40
allowable drift	1/500
allowable top disp	0.28
assumed s	1/2
calculated gamma	1/750
allowable disp (per story)	0.005 m
h	3.5 m
L _b	7 m
% allocated to Brace	80% %
Stiffness Ratio	4.00 D _{truss} /D _{frame}
f	3

40 story structure

Brace Parameters	
A ^d	0.0148 m ²
A ^c	5.40E-02 m ²
Inertia of Braced Bay	4.76E+01 m ⁴
E	2.00E+08 kPA
theta	0.46 rad

area of diagonal
area of chord
Columns with 0.7m width
3 bay bracing scheme
mod of elasticity
diagonal angle

Frame Parameters	
I _c	4.196E-03 m ⁴
I _b	4.196E-03 m ⁴
r	2.00

Required Shear Stiffness for Desired Distribution			
Required D _{truss}	2,184,000	kN/m	Required D _{frame} 546,000 kN/m

Truss Shear Stiffness	
D _{truss}	2,118,004 kN/theta
Truss Bending Stiffness	
D _{bending}	2.65E+08 kN-m/theta

Frame Shear Stiffness	
K _{interior}	469756 kN/theta
K _{corner}	93951 kN/theta
D _{frame (6 columns)}	563,708 kN/theta

Expected Results	
Total Shear Stiffness	2.68E+08 kN/theta
Calculated Gamma	1/737 theta
Calculated Shear Disp (x-dir)	0.095 m
Calculated Bending Disp (x-dir)	0.131 m
Total Displacement (x-dir)	0.23 m
s	1.38

V/Dt
cantilever bending

Model Parameters		
Uniform Load	26	kN/m
Base Shear	3640	kN
Base Moment		kN-m
no of columns	6	
no of stories	40	
allowable drift	1/500	
allowable top disp	0.28	
assumed s	1/2	
calculated gamma	1/750	
allowable disp (per story)	0.005	m
h	3.5	m
L _b	7	m
% allocated to Brace	70%	%
Stiffness Ratio	2.33	D _{truss} /D _{frame}
f	3	

40 story structure

Brace Parameters		
A ^d	0.0138	m ²
A ^c	8.00E-02	m ²
Inertia of Braced Bay	7.06E+01	m ⁴
E	2.00E+08	kPA
theta	0.46	rad

area of diagonal
area of chord
Columns with 0.7m width
3 bay bracing scheme
mod of elasticity
diagonal angle

Frame Parameters		
I _c	6.03E-03	m ⁴
I _b	6.03E-03	m ⁴
r	2.00	

Required Shear Stiffness for Desired Distribution			
Required D _{truss}	1,911,000	kN/m	Required D _{frame} 819,000 kN/m

Truss Shear Stiffness		
D _{truss}	1,974,895	kN/theta
Truss Bending Stiffness		
D _{bending}	3.92E+08	kN-m/theta

Frame Shear Stiffness		
K _{interior}	674743	kN/theta
K _{corner}	134949	kN/theta
D _{frame (6 columns)}	809,691	kN/theta

Expected Results		
Total Shear Stiffness	2.78E+08	kN/theta
Calculated Gamma	1/765	theta
Calculated Shear Disp (x-dir)	0.092	m
Calculated Bending Disp (x-dir)	0.088	m
Total Displacement (x-dir)	0.18	m
s	0.97	

V/Dt
cantilever bending

Model Parameters		
Uniform Load	26	kN/m
Base Shear	3640	kN
Base Moment		kN-m
no of columns	6	
no of stories	40	
allowable drift	1/500	
allowable top disp	0.28	
assumed s	1/2	
calculated gamma	1/750	
allowable disp (per story)	0.005	m
h	3.5	m
L _b	7	m
% allocated to Brace	60%	%
Stiffness Ratio	1.50	D _{truss} /D _{frame}
f	3	

40 story structure

Brace Parameters		
A ^d	0.0113	m ²
A ^c	1.06E-01	m ²
Inertia of Braced Bay	9.35E+01	m ⁴
E	2.00E+08	kPA
theta	0.46	rad

area of diagonal
area of chord
Columns with 0.7m width
3 bay bracing scheme
mod of elasticity
diagonal angle

Frame Parameters		
I _c	7.70E-03	m ⁴
I _b	7.70E-03	m ⁴
r	2.00	

Required Shear Stiffness for Desired Distribution			
Required D _{truss}	1,638,000	kN/m	Required D _{frame} 1,092,000 kN/m

Truss Shear Stiffness		
D _{truss}	1,617,124	kN/theta
Truss Bending Stiffness		
D _{bending}	5.19E+08	kN-m/theta

Frame Shear Stiffness		
K _{interior}	861481	kN/theta
K _{corner}	172296	kN/theta
D _{frame (6 columns)}	1,033,777	kN/theta

Expected Results		
Total Shear Stiffness	2.55E+08	kN/theta
Calculated Gamma	1/728	theta
Calculated Shear Disp (x-dir)	0.096	m
Calculated Bending Disp (x-dir)	0.067	m
Total Displacement (x-dir)	0.16	m
s	0.69	

V/Dt
cantilever bending

Model Parameters		
Uniform Load	26	kN/m
Base Shear	3640	kN
Base Moment		kN-m
no of columns	6	
no of stories	40	
allowable drift	1/500	
allowable top disp	0.28	
assumed s	1/2	
calculated gamma	1/750	
allowable disp (per story)	0.005	m
h	3.5	m
L _b	7	m
% allocated to Brace	50%	%
Stiffness Ratio	1.00	D _{truss} /D _{frame}
f	3	

40 story structure

Brace Parameters		
A ^d	0.0098	m ²
A ^c	1.54E-01	m ²
Inertia of Braced Bay	1.36E+02	m ⁴
E	2.00E+08	kPA
theta	0.46	rad

area of diagonal
area of chord
Columns with 0.7m width
3 bay bracing scheme
mod of elasticity
diagonal angle

Frame Parameters		
I _c	1.06E-02	m ⁴
I _b	1.06E-02	m ⁴
r	2.00	

Required Shear Stiffness for Desired Distribution			
Required D _{truss}	1,365,000	kN/m	Required D _{frame} 1,365,000 kN/m

Truss Shear Stiffness		
D _{truss}	1,402,462	kN/theta
Truss Bending Stiffness		
D _{bending}	7.55E+08	kN-m/theta

Frame Shear Stiffness		
K _{interior}	1184466	kN/theta
K _{corner}	236893	kN/theta
D _{frame (6 columns)}	1,421,360	kN/theta

Expected Results		
Total Shear Stiffness	2.62E+08	kN/theta
Calculated Gamma	1/776	theta
Calculated Shear Disp (x-dir)	0.090	m
Calculated Bending Disp (x-dir)	0.046	m
Total Displacement (x-dir)	0.14	m
s	0.51	

V/Dt
cantilever bending

Model Parameters		
Uniform Load	26	kN/m
Base Shear	3640	kN
Base Moment		kN-m
no of columns	6	
no of stories	40	
allowable drift	1/500	
allowable top disp	0.28	
assumed s	1/2	
calculated gamma	1/750	
allowable disp (per story)	0.005	m
h	3.5	m
L _b	7	m
% allocated to Brace	40%	%
Stiffness Ratio	0.67	D _{truss} /D _{frame}
f	3	

40 story structure

Brace Parameters		
A ^d	0.0082	m ²
A ^c	1.76E-01	m ²
Inertia of Braced Bay	1.55E+02	m ⁴
E	2.00E+08	kPA
theta	0.46	rad

area of diagonal
area of chord
Columns with 0.7m width
3 bay bracing scheme
mod of elasticity
diagonal angle

Frame Parameters		
I _c	1.18E-02	m ⁴
I _b	1.18E-02	m ⁴
r	2.00	

Required Shear Stiffness for Desired Distribution			
Required D _{truss}	1,092,000	kN/m	Required D _{frame} 1,638,000 kN/m

Truss Shear Stiffness		
D _{truss}	1,173,488	kN/theta
Truss Bending Stiffness		
D _{bending}	8.62E+08	kN-m/theta

Frame Shear Stiffness		
K _{interior}	1322169	kN/theta
K _{corner}	264434	kN/theta
D _{frame (6 columns)}	1,586,603	kN/theta

Expected Results		
Total Shear Stiffness	2.76E+06	kN/theta
Calculated Gamma	1/758	theta
Calculated Shear Disp (x-dir)	0.092	m
Calculated Bending Disp (x-dir)	0.040	m
Total Displacement (x-dir)	0.13	m
s	0.44	

V/Dt
cantilever bending

Model Parameters		
Uniform Load	26	kN/m
Base Shear	3640	kN
Base Moment		kN-m
no of columns	6	
no of stories	40	
allowable drift	1/500	
allowable top disp	0.28	
assumed s	1/2	
calculated gamma	1/750	
allowable disp (per story)	0.005	m
h	3.5	m
L _b	7	m
% allocated to Brace	30%	%
Stiffness Ratio	0.43	D _{truss} /D _{frame}
f	3	

40 story structure

Brace Parameters		
A ^d	0.0064	m ²
A ^c	2.40E-01	m ²
Inertia of Braced Bay	2.12E+02	m ⁴
E	2.00E+08	kPA
theta	0.46	rad

area of diagonal
area of chord
Columns with 0.7m width
3 bay bracing scheme
mod of elasticity
diagonal angle

Frame Parameters		
I _c	1.48E-02	m ⁴
I _b	1.48E-02	m ⁴
r	2.00	

Required Shear Stiffness for Desired Distribution					
Required D _{truss}	819,000	kN/m	Required D _{frame}	1,911,000	kN/m

Truss Shear Stiffness		
D _{truss}	915,893	kN/theta
Truss Bending Stiffness		
D _{bending}	1.18E+09	kN-m/theta

Frame Shear Stiffness		
K _{interior}	1656910	kN/theta
K _{corner}	331382	kN/theta
D _{frame (6 columns)}	1,988,292	kN/theta

Expected Results		
Total Shear Stiffness	2.90E+08	kN/theta
Calculated Gamma	1/798	theta
Calculated Shear Disp (x-dir)	0.088	m
Calculated Bending Disp (x-dir)	0.029	m
Total Displacement (x-dir)	0.12	m
s	0.34	

V/Dt
cantilever bending

Model Parameters		
Uniform Load	26	kN/m
Base Shear	3640	kN
Base Moment		kN-m
no of columns	6	
no of stories	40	
allowable drift	1/500	
allowable top disp	0.28	
assumed s	1/2	
calculated gamma	1/750	
allowable disp (per story)	0.005	m
Required Dt	2730000	
h	3.5	m
L _b	7	m
% allocated to Brace	20%	%
Stiffness Ratio	0.25	D _{truss} /D _{frame}
f	3	

40 story structure

Brace Parameters		
A ^d	0.0044	m ²
A ^c	2.78E-01	m ²
Inertia of Braced Bay	2.45E+02	m ⁴
E	2.00E+08	kPA
theta	0.46	rad

area of diagonal
area of chord
3 bay bracing scheme
mod of elasticity
diagonal angle
Columns with 0.7m width

Frame Parameters		
I _c	1.63E-02	m ⁴
I _b	1.63E-02	m ⁴
r	2.00	

Total 2,730,000

Required Shear Stiffness for Desired Distribution			
Required D _{truss}	546,000	kN/m	Required D _{frame} 2,184,000 kN/m

Truss Shear Stiffness		
D _{truss}	629,677	kN/theta

Truss Bending Stiffness		
D _{bending}	1.36E+09	kN-m/theta

Frame Shear Stiffness		
k _{interior}	1822601	kN/theta
k _{corner}	364520	kN/theta
D _{frame (6 columns)}	2,187,121	kN/theta

Expected Results		
Total Shear Stiffness	2.82E+06	kN/theta
Calculated Gamma	1/774	theta
Calculated Shear Disp (x-dir)	0.090	m
Calculated Bending Disp (x-dir)	0.025	m
Total Displacement (x-dir)	0.12	m
s	0.28	

V/Dt
cantilever bending

Model Parameters		
Uniform Load	20	kN/m
Base Shear	1421	kN
Base Moment		kN-m
no of columns	6	
no of stories	20	
allowable drift	1/500	
allowable top disp	0.14	
assumed s	1/2	
calculated gamma	1/750	
allowable disp (per story)	0.005	m
Required Dt	1065750	
h	3.5	m
L _b	7	m
% allocated to Brace	90%	%
Stiffness Ratio	9.00	D _{truss} /D _{frame}
f	3	

40 story structure
aspect ratio 3.33333333

Brace Parameters		
A ^d	0.0066	m ²
A ^c	2.20E-02	m ²
Inertia of Braced Bay	1.94E+01	m ⁴
E	2.00E+08	kPA
theta	0.46	rad

area of diagonal
area of chord
3 bay bracing scheme
mod of elasticity
diagonal angle
Columns with 0.55m width

Frame Parameters		
I _c	1.05E-03	m ⁴
I _b	1.05E-03	m ⁴
r	2.00	

Total 1,065,750

Required Shear Stiffness for Desired Distribution			
Required D _{truss}	959,175	kN/m	Required D _{frame} 106,575 kN/m

Truss Shear Stiffness		
D _{truss}	944,515	kN/theta
Truss Bending Stiffness		
D _{bending}	1.08E+08	kN-m/theta

Frame Shear Stiffness		
k _{interior}	117551	kN/theta
k _{corner}	23510	kN/theta
D _{frame (6 columns)}	141,061	kN/theta

Expected Results		
Total Shear Stiffness	1.09E+08	kN/theta
Calculated Gamma	1/764	theta
Calculated Shear Disp (x-dir)	0.135	m
Calculated Bending Disp (x-dir)	0.015	m
Total Displacement (x-dir)	0.15	m
s	0.11	

V/Dt
cantilever bending

Model Parameters		
Uniform Load	20	kN/m
Base Shear	1421	kN
Base Moment		kN-m
no of columns	6	
no of stories	20	
allowable drift	1/500	
allowable top disp	0.14	
assumed s	1/2	
calculated gamma	1/750	
allowable disp (per story)	0.005	m
Required Dt	1065750	
h	3.5	m
L _b	7	m
% allocated to Brace	80%	%
Stiffness Ratio	4.00	D _{truss} /D _{frame}
f	3	

20 story structure
aspect ratio 3.33333333

Brace Parameters		
A ^d	0.0059	m ²
A ^c	4.20E-02	m ²
Inertia of Braced Bay	3.70E+01	m ⁴
E	2.00E+08	kPA
theta	0.46	rad

area of diagonal
area of chord
3 bay bracing scheme
mod of elasticity
diagonal angle
Columns with 0.55m width

Frame Parameters		
I _c	1.99E-03	m ⁴
I _b	1.99E-03	m ⁴
r	2.00	

Total 1,065,750

Required Shear Stiffness for Desired Distribution			
Required D _{truss}	852,600	kN/m	Required D _{frame} 213,150 kN/m

Truss Shear Stiffness		
D _{truss}	844,339	kN/theta

Truss Bending Stiffness		
D _{bending}	2.06E+08	kN-m/theta

Frame Shear Stiffness		
k _{interior}	222563	kN/theta
k _{corner}	44513	kN/theta
D _{frame (6 columns)}	267,076	kN/theta

Expected Results		
Total Shear Stiffness	1.11E+08	kN/theta
Calculated Gamma	1/782	theta
Calculated Shear Disp (x-dir)	0.132	m
Calculated Bending Disp (x-dir)	0.008	m
Total Displacement (x-dir)	0.14	m
s	0.06	

V/Dt
cantilever bending

Model Parameters		
Uniform Load	20	kN/m
Base Shear	1421	kN
Base Moment		kN-m
no of columns	6	
no of stories	20	
allowable drift	1/500	
allowable top disp	0.14	
assumed s	1/2	
calculated gamma	1/750	
allowable disp (per story)	0.005	m
Required Dt	1065750	
h	3.5	m
L _b	7	m
% allocated to Brace	70%	%
Stiffness Ratio	2.33	D _{truss} /D _{frame}
f	3	

20 story structure
aspect ratio 3.33333333

Brace Parameters		
A ^d	0.005	m ²
A ^c	6.20E-02	m ²
Inertia of Braced Bay	5.47E+01	m ⁴
E	2.00E+08	kPA
theta	0.46	rad

area of diagonal
area of chord
3 bay bracing scheme
mod of elasticity
diagonal angle
Columns with 0.55m width

Frame Parameters		
I _c	2.82E-03	m ⁴
I _b	2.82E-03	m ⁴
r	2.00	

Total 1,065,750

Required Shear Stiffness for Desired Distribution			
Required D _{truss}	746,025	kN/m	Required D _{frame} 319,725 kN/m

Truss Shear Stiffness		
D _{truss}	715,542	kN/theta
Truss Bending Stiffness		
D _{bending}	3.04E+08	kN-m/theta

Frame Shear Stiffness		
k _{interior}	315932	kN/theta
k _{corner}	63186	kN/theta
D _{frame (6 columns)}	379,119	kN/theta

Expected Results		
Total Shear Stiffness	1.09E+08	kN/theta
Calculated Gamma	1/770	theta
Calculated Shear Disp (x-dir)	0.134	m
Calculated Bending Disp (x-dir)	0.005	m
Total Displacement (x-dir)	0.14	m
s	0.04	

V/Dt
cantilever bending

Model Parameters		
Uniform Load	20	kN/m
Base Shear	1421	kN
Base Moment		kN-m
no of columns	6	
no of stories	20	
allowable drift	1/500	
allowable top disp	0.14	
assumed s	1/2	
calculated gamma	1/750	
allowable disp (per story)	0.005	m
Required Dt	1065750	
h	3.5	m
L _b	7	m
% allocated to Brace	60%	%
Stiffness Ratio	1.50	D _{truss} /D _{frame}
f	3	

20 story structure
aspect ratio 3.333333333

Brace Parameters		
A ^d	0.005	m ²
A ^c	8.20E-02	m ²
Inertia of Braced Bay	7.23E+01	m ⁴
E	2.00E+08	kPA
theta	0.46	rad

area of diagonal
area of chord
Columns with 0.55m width
3 bay bracing scheme
mod of elasticity
diagonal angle

Frame Parameters		
I _c	3.56E-03	m ⁴
I _b	3.56E-03	m ⁴
r	2.00	

Total 1,065,750

Required Shear Stiffness for Desired Distribution			
Required D _{truss}	639,450	kN/m	Required D _{frame} 426,300 kN/m

Truss Shear Stiffness		
D _{truss}	715,542	kN/theta

Truss Bending Stiffness		
D _{bending}	4.02E+08	kN-m/theta

Frame Shear Stiffness		
K _{interior}	398442	kN/theta
K _{corner}	79688	kN/theta
D _{frame (6 columns)}	478,130	kN/theta

Expected Results		
Total Shear Stiffness	1.19E+06	kN/theta
Calculated Gamma	1/840	theta
Calculated Shear Disp (x-dir)	0.123	m
Calculated Bending Disp (x-dir)	0.004	m
Total Displacement (x-dir)	0.13	m
s	0.03	

V/Dt
cantilever bending

Model Parameters		
Uniform Load	23	kN/m
Base Shear	2425	kN
Base Moment		kN-m
no of columns	6	
no of stories	30	
allowable drift	1/500	
allowable top disp	0.21	
assumed s	1/2	
calculated gamma	1/750	
allowable disp (per story)	0.005	m
Required Dt	1818750	
h	3.5	m
L _b	7	m
% allocated to Brace	90%	%
Stiffness Ratio	9.00	D _{truss} /D _{frame}
f	3	

30 story structure
aspect ratio 5

Brace Parameters		
A ^d	0.0113	m ²
A ^c	2.40E-02	m ²
Inertia of Braced Bay	2.12E+01	m ⁴
E	2.00E+08	kPA
theta	0.46	rad

area of diagonal
area of chord
3 bay bracing scheme
mod of elasticity
diagonal angle
Columns with 0.55m width

Frame Parameters		
I _c	1.37E-03	m ⁴
I _b	1.37E-03	m ⁴
r	2.00	

Total 1,818,750

Required Shear Stiffness for Desired Distribution			
Required D _{truss}	1,636,875	kN/m	Required D _{frame} 181,875 kN/m

Truss Shear Stiffness		
D _{truss}	1,617,124	kN/theta
Truss Bending Stiffness		
D _{bending}	1.18E+08	kN-m/theta

Frame Shear Stiffness		
k _{interior}	153376	kN/theta
k _{corner}	30675	kN/theta
D _{frame (6 columns)}	184,051	kN/theta

Expected Results		
Total Shear Stiffness	1.80E+08	kN/theta
Calculated Gamma	1/743	theta
Calculated Shear Disp (x-dir)	0.117	m
Calculated Bending Disp (x-dir)	0.083	m
Total Displacement (x-dir)	0.20	m
s	0.70	

V/Dt
cantilever bending

Model Parameters		
Uniform Load	23	kN/m
Base Shear	2425	kN
Base Moment		kN-m
no of columns	6	
no of stories	30	
allowable drift	1/500	
allowable top disp	0.21	
assumed s	1/2	
calculated gamma	1/750	
allowable disp (per story)	0.005	m
Required Dt	1818750	
h	3.5	m
L _b	7	m
% allocated to Brace	80%	%
Stiffness Ratio	4.00	D _{truss} /D _{frame}
f	3	

30 story structure
aspect ratio

5

Brace Parameters		
A ^d	0.0099	m ²
A ^c	4.60E-02	m ²
Inertia of Braced Bay	4.06E+01	m ⁴
E	2.00E+08	kPA
theta	0.46	rad

area of diagonal

Columns with 0.55m width

area of chord

3 bay bracing scheme

mod of elasticity

diagonal angle

Frame Parameters		
I _c	2.61E-03	m ⁴
I _b	2.61E-03	m ⁴
r	2.00	

Total 1,818,750

Required Shear Stiffness for Desired Distribution			
Required D _{truss}	1,455,000	kN/m	Required D _{frame} 363,750 kN/m

Truss Shear Stiffness		
D _{truss}	1,416,773	kN/theta
Truss Bending Stiffness		
D _{bending}	2.25E+08	kN-m/theta

Frame Shear Stiffness		
K _{interior}	291638	kN/theta
K _{corner}	58328	kN/theta
D _{frame (6 columns)}	349,966	kN/theta

Expected Results		
Total Shear Stiffness	1.77E+06	kN/theta
Calculated Gamma	1/729	theta
Calculated Shear Disp (x-dir)	0.120	m
Calculated Bending Disp (x-dir)	0.043	m
Total Displacement (x-dir)	0.16	m
s	0.36	

V/Dt

cantilever bending

Model Parameters		
Uniform Load	23	kN/m
Base Shear	2425	kN
Base Moment		kN-m
no of columns	6	
no of stories	30	
allowable drift	1/500	
allowable top disp	0.21	
assumed s	1/2	
calculated gamma	1/750	
allowable disp (per story)	0.005	m
Required Dt	1818750	
h	3.5	m
L _b	7	m
% allocated to Brace	70%	%
Stiffness Ratio	2.33	D _{truss} /D _{frame}
f	3	

30 story structure
aspect ratio 5

Brace Parameters		
A ^d	0.0079	m ²
A ^c	6.80E-02	m ²
Inertia of Braced Bay	6.00E+01	m ⁴
E	2.00E+08	kPA
theta	0.46	rad

area of diagonal
area of chord
3 bay bracing scheme
mod of elasticity
diagonal angle
Columns with 0.55m width

Frame Parameters		
I _c	3.71E-03	m ⁴
I _b	3.71E-03	m ⁴
r	2.00	

Total 1,818,750

Required Shear Stiffness for Desired Distribution			
Required D _{truss}	1,273,125	kN/m	Required D _{frame} 545,625 kN/m

Truss Shear Stiffness		
D _{truss}	1,130,556	kN/theta
Truss Bending Stiffness		
D _{bending}	3.33E+08	kN-m/theta

Frame Shear Stiffness		
k _{interior}	415795	kN/theta
k _{corner}	83159	kN/theta
D _{frame (6 columns)}	498,954	kN/theta

Expected Results		
Total Shear Stiffness	1.63E+08	kN/theta
Calculated Gamma	1/672	theta
Calculated Shear Disp (x-dir)	0.130	m
Calculated Bending Disp (x-dir)	0.029	m
Total Displacement (x-dir)	0.16	m
s	0.22	

V/Dt
cantilever bending

Model Parameters		
Uniform Load	23	kN/m
Base Shear	2425	kN
Base Moment		kN-m
no of columns	6	
no of stories	30	
allowable drift	1/500	
allowable top disp	0.21	
assumed s	1/2	
calculated gamma	1/750	
allowable disp (per story)	0.005	m
Required Dt	1818750	
h	3.5	m
L _b	7	m
% allocated to Brace	60%	%
Stiffness Ratio	1.50	D _{truss} /D _{frame}
f	3	

30 story structure
aspect ratio

5

Brace Parameters		
A ^d	0.0066	m ²
A ^c	1.10E-01	m ²
Inertia of Braced Bay	9.70E+01	m ⁴
E	2.00E+08	kPA
theta	0.46	rad

area of diagonal

Columns with 0.55m width

area of chord

3 bay bracing scheme

mod of elasticity

diagonal angle

Frame Parameters		
I _c	5.59E-03	m ⁴
I _b	5.59E-03	m ⁴
r	2.00	

Total 1,818,750

Required Shear Stiffness for Desired Distribution			
Required D _{truss}	1,091,250	kN/m	Required D _{frame} 727,500 kN/m

Truss Shear Stiffness		
D _{truss}	944,515	kN/theta

Truss Bending Stiffness		
D _{bending}	5.39E+08	kN-m/theta

Frame Shear Stiffness		
k _{interior}	626043	kN/theta
k _{corner}	125209	kN/theta
D _{frame (6 columns)}	751,252	kN/theta

Expected Results		
Total Shear Stiffness	1.70E+06	kN/theta
Calculated Gamma	1/699	theta
Calculated Shear Disp (x-dir)	0.125	m
Calculated Bending Disp (x-dir)	0.018	m
Total Displacement (x-dir)	0.14	m
s	0.14	

V/Dt

cantilever bending

Model Parameters		
Uniform Load	23	kN/m
Base Shear	2425	kN
Base Moment		kN-m
no of columns	6	
no of stories	30	
allowable drift	1/500	
allowable top disp	0.21	
assumed s	1/2	
calculated gamma	1/750	
allowable disp (per story)	0.005	m
Required Dt	1,818,750	
h	3.5	m
L _b	7	m
% allocated to Brace	50%	%
Stiffness Ratio	1.00	D _{truss} /D _{frame}
f	3	

30 story structure
aspect ratio 5

Brace Parameters		
A ^d	0.0066	m ²
A ^c	1.48E-01	m ²
Inertia of Braced Bay	1.31E+02	m ⁴
E	2.00E+08	kPA
theta	0.46	rad

area of diagonal
area of chord
3 bay bracing scheme
mod of elasticity
diagonal angle
Columns with 0.55m width

Frame Parameters		
I _c	7.07E-03	m ⁴
I _b	7.07E-03	m ⁴
r	2.00	

Total 1,818,750

Required Shear Stiffness for Desired Distribution			
Required D _{truss}	909,375	kN/m	Required D _{frame} 909,375 kN/m

Truss Shear Stiffness		
D _{truss}	944,515	kN/theta
Truss Bending Stiffness		
D _{bending}	7.25E+08	kN-m/theta

Frame Shear Stiffness		
k _{interior}	791398	kN/theta
k _{corner}	158280	kN/theta
D _{frame} (6 columns)	949,678	kN/theta

Expected Results		
Total Shear Stiffness	1.89E+08	kN/theta
Calculated Gamma	1/781	theta
Calculated Shear Disp (x-dir)	0.112	m
Calculated Bending Disp (x-dir)	0.013	m
Total Displacement (x-dir)	0.12	m
s	0.12	

V/Dt
cantilever bending

Model Parameters		
Uniform Load	23	kN/m
Base Shear	2425	kN
Base Moment		kN-m
no of columns	6	
no of stories	30	
allowable drift	1/500	
allowable top disp	0.21	
assumed s	1/4	
calculated gamma	1/625	
allowable disp (per story)	0.006	m
Required Dt	1515625	
h	3.5	m
L _b	7	m
% allocated to Brace	90%	%
Stiffness Ratio	9.00	D _{truss} /D _{frame}
f	3	

30 story structure
aspect ratio 5

Brace Parameters		
A ^d	0.009	m ²
A ^c	2.40E-02	m ²
Inertia of Braced Bay	2.12E+01	m ⁴
E	2.00E+08	kPA
theta	0.46	rad

area of diagonal
area of chord
Columns with 0.55m width
3 bay bracing scheme
mod of elasticity
diagonal angle

Frame Parameters		
I _c	1.37E-03	m ⁴
I _b	1.37E-03	m ⁴
r	2.00	

Total 1,515,625

Required Shear Stiffness for Desired Distribution			
Required D _{truss}	1,364,063	kN/m	Required D _{frame} 151,563 kN/m

Truss Shear Stiffness		
D _{truss}	1,287,975	kN/theta
Truss Bending Stiffness		
D _{bending}	1.18E+08	kN-m/theta

Frame Shear Stiffness		
K _{interior}	153376	kN/theta
K _{corner}	30675	kN/theta
D _{frame (6 columns)}	184,051	kN/theta

Expected Results		
Total Shear Stiffness	1.47E+06	kN/theta
Calculated Gamma	1/607	theta
Calculated Shear Disp (x-dir)	0.144	m
Calculated Bending Disp (x-dir)	0.083	m
Total Displacement (x-dir)	0.23	m
s	0.58	

V/Dt
cantilever bending

Model Parameters		
Uniform Load	23	kN/m
Base Shear	2425	kN
Base Moment		kN-m
no of columns	6	
no of stories	30	
allowable drift	1/500	
allowable top disp	0.21	
assumed s	1/4	
calculated gamma	1/625	
allowable disp (per story)	0.006	m
Required Dt	1515625	
h	3.5	m
L _b	7	m
% allocated to Brace	80%	%
Stiffness Ratio	4.00	D _{truss} /D _{frame}
f	3	

30 story structure
aspect ratio 5

Brace Parameters		
A ^d	0.0079	m ²
A ^c	4.60E-02	m ²
Inertia of Braced Bay	4.06E+01	m ⁴
E	2.00E+08	kPA
theta	0.46	rad

area of diagonal
area of chord
3 bay bracing scheme
mod of elasticity
diagonal angle
Columns with 0.55m width

Frame Parameters		
I _c	2.61E-03	m ⁴
I _b	2.61E-03	m ⁴
r	2.00	

Total 1,515,625

Required Shear Stiffness for Desired Distribution			
Required D _{truss}	1,212,500	kN/m	Required D _{frame} 303,125 kN/m

Truss Shear Stiffness		
D _{truss}	1,130,556	kN/theta
Truss Bending Stiffness		
D _{bending}	2.25E+08	kN-m/theta

Frame Shear Stiffness		
k _{interior}	291638	kN/theta
k _{corner}	58328	kN/theta
D _{frame (6 columns)}	349,966	kN/theta

Expected Results		
Total Shear Stiffness	1.48E+06	kN/theta
Calculated Gamma	1/611	theta
Calculated Shear Disp (x-dir)	0.143	m
Calculated Bending Disp (x-dir)	0.043	m
Total Displacement (x-dir)	0.19	m
s	0.30	

V/Dt
cantilever bending

Model Parameters		
Uniform Load	23	kN/m
Base Shear	2425	kN
Base Moment		kN-m
no of columns	6	
no of stories	30	
allowable drift	1/500	
allowable top disp	0.21	
assumed s	1/4	
calculated gamma	1/625	
allowable disp (per story)	0.006	m
Required Dt	1515625	
h	3.5	m
L _b	7	m
% allocated to Brace	70%	%
Stiffness Ratio	2.33	D _{truss} /D _{frame}
f	3	

30 story structure
aspect ratio

5

Brace Parameters		
A ^d	0.0066	m ²
A ^c	6.80E-02	m ²
Inertia of Braced Bay	6.00E+01	m ⁴
E	2.00E+08	kPA
theta	0.46	rad

area of diagonal
area of chord

Columns with 0.55m width

3 bay bracing scheme
mod of elasticity
diagonal angle

Frame Parameters		
I _c	3.71E-03	m ⁴
I _b	3.71E-03	m ⁴
r	2.00	

Total 1,515,625

Required Shear Stiffness for Desired Distribution			
Required D _{truss}	1,060,938	kN/m	Required D _{frame} 454,688 kN/m

Truss Shear Stiffness		
D _{truss}	944,515	kN/theta
Truss Bending Stiffness		
D _{bending}	3.33E+08	kN-m/theta

Frame Shear Stiffness		
k _{interior}	415795	kN/theta
k _{corner}	83159	kN/theta
D _{frame (6 columns)}	498,954	kN/theta

Expected Results		
Total Shear Stiffness	1.44E+06	kN/theta
Calculated Gamma	1/595	theta
Calculated Shear Disp (x-dir)	0.146	m
Calculated Bending Disp (x-dir)	0.029	m
Total Displacement (x-dir)	0.18	m
s	0.20	

V/Dt
cantilever bending

Model Parameters		
Uniform Load	23	kN/m
Base Shear	2425	kN
Base Moment		kN-m
no of columns	6	
no of stories	30	
allowable drift	1/500	
allowable top disp	0.21	
assumed s	1/4	
calculated gamma	1/625	
allowable disp (per story)	0.006	m
Required Dt	1515625	
h	3.5	m
L _b	7	m
% allocated to Brace	60%	%
Stiffness Ratio	1.50	D _{truss} /D _{frame}
f	3	

30 story structure
aspect ratio 5

Brace Parameters		
A ^d	0.0066	m ²
A ^c	9.00E-02	m ²
Inertia of Braced Bay	7.94E+01	m ⁴
E	2.00E+08	kPA
theta	0.46	rad

area of diagonal
area of chord
3 bay bracing scheme
mod of elasticity
diagonal angle
Columns with 0.55m width

Frame Parameters		
I _c	4.71E-03	m ⁴
I _b	4.71E-03	m ⁴
r	2.00	

Total 1,515,625

Required Shear Stiffness for Desired Distribution			
Required D _{truss}	909,375	kN/m	Required D _{frame} 606,250 kN/m

Truss Shear Stiffness		
D _{truss}	944,515	kN/theta
Truss Bending Stiffness		
D _{bending}	4.41E+08	kN-m/theta

Frame Shear Stiffness		
K _{interior}	526964	kN/theta
K _{corner}	105393	kN/theta
D _{frame (6 columns)}	632,357	kN/theta

Expected Results		
Total Shear Stiffness	1.58E+08	kN/theta
Calculated Gamma	1/650	theta
Calculated Shear Disp (x-dir)	0.134	m
Calculated Bending Disp (x-dir)	0.022	m
Total Displacement (x-dir)	0.16	m
s	0.16	

V/Dt
cantilever bending

Model Parameters		
Uniform Load	23	kN/m
Base Shear	2425	kN
Base Moment		kN-m
no of columns	6	
no of stories	30	
allowable drift	1/500	
allowable top disp	0.21	
assumed s	1/4	
calculated gamma	1/625	
allowable disp (per story)	0.006	m
Required Dt	1515625	
h	3.5	m
L _b	7	m
% allocated to Brace	50%	%
Stiffness Ratio	1.00	D _{truss} /D _{frame}
f	3	

30 story structure
aspect ratio

5

Brace Parameters		
A ^d	0.0052	m ²
A ^c	1.10E-01	m ²
Inertia of Braced Bay	9.70E+01	m ⁴
E	2.00E+08	kPA
theta	0.46	rad

area of diagonal
area of chord

Columns with 0.55m width

3 bay bracing scheme
mod of elasticity
diagonal angle

Frame Parameters		
I _c	5.59E-03	m ⁴
I _b	5.59E-03	m ⁴
r	2.00	

Total 1,515,625

Required Shear Stiffness for Desired Distribution			
Required D _{truss}	757,813	kN/m	Required D _{frame} 757,813 kN/m

Truss Shear Stiffness		
D _{truss}	744,163	kN/theta

Truss Bending Stiffness		
D _{bending}	5.39E+08	kN-m/theta

Frame Shear Stiffness		
k _{interior}	626043	kN/theta
k _{corner}	125209	kN/theta
D _{frame (6 columns)}	751,252	kN/theta

Expected Results		
Total Shear Stiffness	1.50E+06	kN/theta
Calculated Gamma	1/617	theta
Calculated Shear Disp (x-dir)	0.141	m
Calculated Bending Disp (x-dir)	0.018	m
Total Displacement (x-dir)	0.16	m
s	0.13	

V/Dt

cantilever bending